

Numerical Prediction of Burn Rates of Periodic and Disordered Heterogeneous Combustion

A Thesis submitted to University of Hyderabad for the
award of the degree of

Doctor of Philosophy

in Physics

by

Naine Tarun Bharat (10ACPP18)



ACRHEM, School of Physics

University of Hyderabad, Hyderabad 500046

Telangana, India.

June 2016



Declaration

I, **Naine Tarun Bharat**, hereby declare that the work presented in this thesis entitled “**Numerical Prediction of Burn Rates of Periodic and Disordered Heterogeneous Combustion**” has been carried out by me under the supervision of **Dr. G. Manoj Kumar**, Assistant Professor, ACRHEM, School of Physics, University of Hyderabad, Hyderabad, India, as per the Ph.D ordinances of the University, which is also free from plagiarism. I declare, to the best of my knowledge, that no part of this thesis has been submitted for the award of a research degree of any other University. I hereby agree that my thesis can be deposited in Shodhganga/INFLIBNET.

A report on plagiarism statistics from the University Librarian is enclosed.

Date:

(**Naine Tarun Bharat**)
Reg. No: 10ACPP18



**University of Hyderabad, Central University (P.O.),
Gachibowli, Hyderabad-500 046, India**

Certificate

This is to certify that the thesis entitled 'Numerical Prediction of Burn Rates of Periodic and Disordered Heterogeneous Combustion' being submitted to the University of Hyderabad by **Naine Tarun Bharat** (Reg. No: 10ACPP18), for the award of **Doctor of Philosophy in Physics**, is a bonafide work carried out by him under my supervision and guidance which is a plagiarism-free thesis.

The thesis has not been submitted previously in part or in full to this or any other University or Institution for the award of any degree or diploma.

Dr. G. Manoj Kumar
Thesis Supervisor
(ACRHEM)

Head of the Department/ Center
(ACRHEM)

Dean
(School of Physics)

To My Parents

A word of Gratitude

I dedicate this thesis to my parents, without whose constant moral support and encouragement, this day would not have been possible. At the outset, I would like to thank all those who have directly or indirectly helped me at various stages of my stay at the university.

First and foremost I would like to thank my thesis supervisor Dr. G. Manoj Kumar for his valuable guidance, scholarly inputs and consistent encouragement received throughout the research work. This thesis would not have been possible without his support. I cannot thank him enough and I am grateful to him forever.

I extend my gratitude to Prof. S.A. Rashkovskiy, Russian Academy of Sciences, Russia, for the valuable academic discussions and suggestions.

I would like to thank my DC members Dr. P. Prem Kiran and Dr. G. Vaitheeswaran for their valuable suggestions during the meetings. I also thank Prof. K.P.N Murthy, Dr.A.K. Chaudhary and Dr. S. Venu Gopal Rao for their support.

I am so delighted to express my deep gratitude to the former directors Prof. S. P. Tewari and present director Dr. K.Venkateswara Rao for providing needful facilities.

I wish to thank the Dean, School of Physics.

I wish to thank all my seniors and colleagues from ACRHEM for their support.

I feel it is a pleasant duty to express my regards to non-teaching staff of ACRHEM, School of Physics, workshop, IGM Library and University of Hyderabad administration.

I would like to acknowledge the funding agency Defense Research Development Organization (DRDO) India for sponsoring state of the art, through which this entire work was possible. I also acknowledge DRDO for providing me fellowship throughout this period.

My special thanks to my teacher's Ravinder sir, Rama Krishna sir, Pratap sir, Ashok sir, Sowjanya madam and Prof. Satyanarayan who has been the inspiration behind my interest to learn Physics.

(Naine Tarun Bharat)

Table of Contents

List of Figures

List of Tables

Nomenclature

Chapter 1

Introduction and Motivation	1-13
1.1 Introduction	1
1.2 Heterogeneous Combustion Modeling	2
1.3 Disorderiness in internal Microstructure	3
1.4 Description of model	4
1.5 Organization of thesis	6
1.6 References	9

Chapter 2

Dynamical and statistical behavior of discrete combustion waves in One-dimension: A theoretical and numerical study.	15-60
2.1 Introduction	15
2.2 Model of the system	
2.2.1 Discrete combustion waves	18
2.2.2 System structure	21
2.3 Numerical Results	22-56
Section I Identical Heat release	
2.3.1 Gamma Distribution	25-37
2.3.1.1 Characterization of system structure	25
2.3.1.2 Burning Front Propagation	27
2.3.1.3 Theoretical considerations	31
2.3.1.4 Self-similarity in burning front propagation	34
2.3.1.5 Standard deviation of burning time	35
2.3.2 Normal Distribution	37-40
2.3.2.1 Theoretical Analysis for Burn Rates	38
2.3.3 Comparison with Experimental Data	40-51
2.3.3.1 Ti-Si system	40
2.3.3.2 Relay-race mode vs. quasi-homogeneous mode	44
2.3.3.3 CMDB Propellants	47
2.3.3.4 Thermite systems	49
2.3.3.5 Quasi-Arrhenius' macrokinetics	51
Section II Disordered Heat release	52
2.3.4 Comparison with Thermite systems	54
2.4 Conclusion	56
2.5 References	57

Chapter 3

Correlation between Discrete Probability and Reaction Front Propagation Rate in Heterogeneous mixtures **61-74**

3.1 Introduction	61
3.2 Motivation	63
3.3 Statistics of ignition times	64
3.4 Results	67
3.4.1 Theoretical Considerations	72
3.5 Conclusions	73
3.6 References	74

Chapter 4

Role of Heat Loss on the propagation limits of reaction front of heterogeneous mixtures **75-94**

4.1 Introduction	75
4.2 Modeling	
4.2.1 System definition and assumptions	77
4.2.2 Theoretical analysis of Periodic system	78
4.3 Results	
4.3.1 Numerical Calculation of Burn rates of Periodic system	80
4.3.2 Combustion limits	81
4.3.3 Disordered System	83
4.3.4 Combustible limits of Disordered system	86
4.3.5 Burn rate	88
4.4 Conclusion	92
4.5 References	92

Chapter 5

Two Dimensional Modeling of Heterogeneous Combustion Process by Slice Reconfiguration Scheme **95-123**

5.1 Introduction	95
5.2 Modeling	98
5.2.1 Theoretical analysis of Periodic system	100
5.2.2 Realization of Periodic (Ordered) system	101
5.2.3 Periodic Boundary Condition	103
5.2.4 Algorithm	104
5.2.5 Faster Computation by Using MPI	104
5.2.6 Slice reconfiguration scheme	107
5.3 Results	
5.3.1 Periodic system	108
5.3.2 Disordered system	111
5.3.4 Burn rates	118
5.4 Conclusion	119
5.5 References	120

Chapter 6
Conclusion and Future scope

125-127

List of Publications

Awards

List of Figures

Figure 2.1 Probability Density Function for different Distributions.	22
Figure 2.2 Ignition time profile for different distributions. (1)Normal (2) Beta (3) Uniform (4) Gamma ($a=0.7$).	23
Figure 2.3 Comparison plot for maximum ignition delay times of adjacent cells.	24
Figure 2.4. Distribution of the distances between neighboring hot spots. The polygonal lines are the histogram of specific realization, smooth lines are theoretical probability density Eq. (3). a) $a=0.7$; b) $a=1$; c) $a=5$; d) $a=20$	26
Figure 2.5. Pair distribution function for cells in the system for different values of the shaping parameter: a) $a=0.7$; b) $a=1$; c) $a=5$; d) $a=20$	27
Figure 2.6. a) $a=0.7$; b) $a=1$; c) $a=5$; d) $a=15$. Propagation diagrams of discrete burning front for different ignition temperatures ε . The ignition temperatures are indicated over each line.	28
Figure 2.7. Correlation of time between ignition of neighbor heat sources and distance between them for $a=1$ (Top) and $a=15$ (bottom). Dots are results of numerical solution of Eq. (3), solid lines are correlation Eqs. (12), (10) for $\varphi = 1$: line 1 - $\varepsilon=0.05$, line 2 - $\varepsilon=0.4$	31
Figure 2.8. Dependence of burning rate on ignition temperature ε for different values of shaping parameter a . Markers are the results of direct numerical solution of Eq. (3); lines are the theoretical expression Eqs. (15), (10) with $\varphi = 1$	33
Figure 2.9. Dependencies $\eta(x)$ for $a = 1$ and $\varepsilon = 0.05 \dots 0.4$ with step 0.05.	35
Figure 2.10. Dependence of relative standard deviation of burning time on number of particles for different ignition temperatures ε . $a=1$ (left), $a=15$ (right). Markers are direct calculations; lines are theoretical dependence (22).	37
Figure 2.11. Comparison plot for normalized burn rate and non dimensional ignition temperature ε for different values of σ . Markers are the calculated results of Eq. (1),(2); lines are obtained by the theoretical expression Eqs. (24), (25) with $\varphi = 1$	40
Figure 2.12 . Burning temperature T_B (squares: scale in K, on the left) and burning rate r (bullets: scale in mm/s, on the right) as a function of the stoichiometry x of the initial sample. Markers are data of [9], solid line $r(x)$ is the theoretical dependence (26), (27) for gamma distribution. Inserting shows the dependence of shaping parameter a on the stoichiometry x used in calculation; dashed lines are the combustion limits.	42
Figure 2.13. (a) Left shows comparison of experimental and theoretical non dimensional burn rates on stoichiometry x [9] and parameter σ . (b) Shows the dependence of shaping	

parameter σ on the stoichiometry x used in calculation; dashed lines are the combustion limits. 44

Figure 2.14. Higher Ignition time profile for different Normal distributions.1=0.42(ϵ), 2=0.44(ϵ), 3=0.46(ϵ), 4=0.48(ϵ).46

Figure 2.15. (a) Plot for burning rate versus burn temperature for CMDB propellants with and without binding agent, based on data of work [10]. (b) Comparison plot for experimental and theoretical dependencies $\omega(\epsilon)$. Symbols are treated experimental data [10]; solid lines 1-4 are the theoretical dependence, lines 2&3 represents normal distributed system: 2) $\sigma=0.2886$: 3) $\sigma=0.408$; lines 1&4 represents gamma distributed system:1) $a=12$; 4) $a=6$48

Figure 2.16. (a) Correlation of burning rate and burning temperature for several thermite systems, based on data of work [47]. The arrows shows the critical points, which correspond to beginning of oscillatory combustion modes. (b) Comparing of experimental and theoretical dependencies $\omega(\epsilon)$. Dots are the treated experimental data [47] :solid lines 1-2 are the theoretical dependence for identical heat release , for normal distribution: lines 2 correspond to calculations for $\sigma=0.98$ and line 1 correspond to gamma $a=0.7$50

Figure 2.17. Comparison of Ignition time profiles for Identical heat release (1,2,3) and disordered heat release (1(a),2(a),3(a)) (q_j).1=0.15(ϵ),2=0.25(ϵ),3=0.35(ϵ).53

Figure 2.18. Comparison of Percentage of burn rates for identical (Boxes) and disordered (Circles) heat release.54

Figure 2.19. (a) Correlation of burning rate and burning temperature for thermite systems having lower combustion limits, based on data of work [47]. The arrows shows the critical points, which correspond to beginning of oscillatory combustion modes. (b) Comparing of experimental and theoretical dependencies $\omega(\epsilon)$. Symbols are the treated experimental data [47] :solid lines are the theoretical dependence for randomized heat release and normal distribution with microstructure described by line 1 $\sigma=0.05$ and by line 2 $\sigma=0.40$55

Figure 3.1. Function $\mu(N)$ for different values of parameters a and ϵ . Lines 1 and 3 - $\epsilon=0.05$, lines 2 and 4 - $\epsilon=0.4$; lines 1 and 2 - $a=1$, lines 3 and 4 - $a=15$66

Figure 3.2. Probability distribution function for gamma distribution of the distances between neighboring hot spots (cells) with different values of shaping parameter. Straight lines for lower and upper limits represent the schematic representation of novel method. (a) $a=1$ (b) $a=20$68

Figure 3.3 Plot for chisquare values at different values of lower limit on ignition temperature.69

Figure 3.4 Functional dependence of lower limit on ignition temperature. Circles represent the numerical values obtained through methodology and solid line represents the trend line.69

Figure 3.5 Comparison of the burn-rates obtained by the proposed method represented by 'o' with the numerically calculated values from [16] represented by solid line. Solid line is

compared and validated with experimental results in [16]. (a) $\epsilon=0.10$, (b) $\epsilon=0.20$ (c) $\epsilon=0.30$ (d) $\epsilon=0.40$70

Figure 4.1 Plot between Non-dimensional Ignition temperature and Burn rate calculated using theoretical equation (3) for different values of β . The circles in the figure show the maximal value of ignition temperature that can be obtained using theoretical equation (3).79

Figure 4.2. Comparison Plot between burn rates (ω) for different values of β . Circles obtained by Eq. (1) and solid lines by Eq.(3).81

Figure 4.3 Plot between temperature of a unburnt particle and time calculated using numerical equation (1) for different values of β . Dots in figure represent the numerical combustion limit.82

Figure 4.4. Ignition time profiles for $\beta=0.0001$ of a different systems. (a) $a=1$; (b) $a=10$; (c) $a=20$; (d) is periodic.84

Figure 4.5. Ignition time profiles for $\beta=0.01$ of a systems described by different positioning of reaction cells. (a) $a=1$; (b) $a=10$; (c) $a=20$; (d) is periodic.85

Figure 4.6. Distribution of delay in ignition times for different systems. (a) $a=1$ & $\beta=0.0001$; (b) $a=20$ & $\beta=0.0001$; (c) $a=1$ & $\beta=0.01$ and (d) $a=20$ & $\beta=0.01$86

Figure 4.7 Temperature profile for unburnt particle of a disordered system. (a) $\epsilon=0.37$ for 1183 particle (b) $\epsilon=0.14\epsilon=0.47$ for 3101 particle (d) $\epsilon=0.36$ for 1304 particle.87

Figure 4.8. Plot for comparison of Burn rates of different systems calculated using Eq.(1) and Eq. (2). 89

Figure 4.9 Plot for comparison of Burning rates and burning temperature for thermite mixture[12].90

Figure 4.10. Comparison plot between experimental and develop model results for burn rates and combustible limits. Solid lines are obtained from develop model and symbols are representation of experimental [9].91

Figure 5.1. Comparison plot for burn rates of an ordered system obtained theoretically using eq.(7) for different values of θ101

Figure 5.2. Plot for microstructure of the ordered system modeled on a two dimensional plane.’*’ represents the burnt particles and ‘o’ is for unburnt particles. Left represents for $\theta=1$ right $\theta=5$102

Figure 5.3. Schematic plot for the system incorporating periodic boundary. 1 Periodic boundary ($N_y=0$); 2 Periodic boundary ($N_y=1$).	103
Figure 5.4 Temperature profile for unburnt cells.	108
Figure 5.5. Comparison plot for burn rates of an ordered system obtained theoretically and numerically for different values of θ . Solid lines are theoretical burn rates and symbols represent numerical burn rates Δ -MPI and X- MPI and slice reconfiguration scheme.	109
Figure 5.6 Ignition time profiles of a periodic system.(a) $\theta=1$ (isotropic), (b) $\theta=7$ (anisotropic).	110
Figure 5.7. Plot for microstructure of the disordered system ($\theta=1$) modeled on a two dimensional plane.*' represents the burnt particles and 'o' is for unburnt particles.	111
Figure 5.8 Ignition time profile for Isotropic and Anisotropic ($\theta=2$). 1 Ordered 2 random systems.....	112
Figure 5.9. Snapshot of burnt region for an Isotropic system at different ignition temperatures (ε). (a) $t=19$ and $\varepsilon=0.46$; (b) $t=25$ and $\varepsilon=0.46$; (c) $t=27$ and $\varepsilon=0.47$; (d) $t=33$ and $\varepsilon=0.47$	114
Figure 5.10. Snapshot of burnt region for Non Isotropic ($\theta=2$) system at different ignition temperatures (ε). (a) $t=0.7$ and $\varepsilon=0.10$; (b) $t=2.2$ and $\varepsilon=0.10$; (c) $t=28$ and $\varepsilon=0.478$; (d) $t=34$ and $\varepsilon=0.478$	115
Figure 5.11. Snapshot of burnt region for Non Isotropic ($\theta=5$) system at different ignition temperatures (ε). (a) $t=0.7$ and $\varepsilon=0.10$; (b) $t=2.1$ and $\varepsilon=0.10$; (c) $t=36$ and $\varepsilon=0.49$; (d) $t=41$ and $\varepsilon=0.49$	116
Figure 5.12 Snapshot of burnt region for Non Isotropic ($\theta=7$) system at different ignition temperatures (ε). (a) $t=0.9$ and $\varepsilon=0.10$; (b) $t=2.4$ and $\varepsilon=0.10$; (c) $t=17$ and $\varepsilon=0.50$; (d) $t=25$ and $\varepsilon=0.50$	117
Figure 5.13 Comparison plots of burn rates calculated for ordered and random systems	119

List of Tables

Table 2.1 Probability density function for different random distributions	21
Table 4.1 Theoretical and numerical combustible limits.....	82
Table 4.2. Numerical combustible limits of disordered system.....	88
Table 5.1 List of Optimized dimensions(x,y) and periodic boundary.....	110
Table 5.2 Comparison of computational time between both methods for ignition temperatures (ϵ)=0.25 & 0.35.....	118
Table 5.3 Performance weight for number of nodes by slice reconfiguration scheme.....	118

NOMENCLATURE

Symbol	Physical Significance (Non-Dimensional)
$t = t(\kappa/l_0^2)$	Ignition time
$x = x/l_0$	Position of particle(Point heat source)
$\varepsilon = \frac{T_{ign} - T_{in}}{T_{ad} - T_{in}}$	Ignition temperature
$q_i = Q_i/Q_0$	Heat release
$T_{ad} = T_{in} + \frac{Q_0}{\rho c l_0}$	Adiabatic temperature
$\omega = (x_k - x_i)/(t_k - t_i)$	Burn rate
ll	Lower limit
ul	Upper limit
$\beta = \frac{kt}{\rho c}$	Heat parameter
θ	Linear parameter along y-direction

CHAPTER 1

Introduction and Motivation

1.1 Introduction

Combustion is an exothermic reaction [1-3] between reactants, that usually release heat energy and produce products in the form of soot and smoke. Combustion is generally classified as Premixed or non premixed combustion, laminar or turbulent, Subsonic or supersonic and Homogeneous or heterogeneous. The homogeneous or heterogeneous combustion is significant classification of combustion process based on the nature of reactants and propagation of combustion wave. Combustion wave represents a self-organized system where a chemical reaction, localized in the reaction front, propagates throughout the reaction medium converting initial reactants into final products [1-3]. Homogeneous combustion [3], observed in diesel engine, fuel and oxidizer are mixed perfectly to a point of auto ignition. The steady state combustion represents an important class of homogeneous process, where invariable space distributions of temperature, concentrations, density, etc., propagate with constant velocity through the reactive medium. In heterogeneous combustion the chemical reaction exists in more than one physical state. The propagation of thermal wave is complicated by the heterogeneous structure of the system and results in micro oscillations. The phenomenon of heterogeneous combustion [4-13] is observed in a variety of processes including combustion synthesis of materials [14-17], burning of solid propellants [18-20], coal and biomass [21-22], forest fires [23-25], reaction propagation in fluidized beds [26-28] and in clouds of solid particles or spray combustion, gasless combustion [29-30]. Gasless combustion waves commonly occur in heterogeneous mixtures of powder reactants such as $Ta+xC$, $Ni +xAl$, $Ti +xSi$ [31]. Here locally initiated exothermic reaction can propagate through the mixture in the form of bright glowing combustion front, without notable gasification. The absence of gaseous flame and solid state of the combustion products allows terming the process as solid-flame combustion or gasless [32-35]. Self-sustained combustion can be realized within some concentration limits for a given binary mixture [36-38] of condensed heterogeneous mixtures. Since the combustion products consist of valued refractory compounds, gasless combustion makes a basis of combustion synthesis technology [14-17], the so-called self-propagating high-temperature synthesis (SHS). The SHS is most energy saving, cost effective method of obtaining inorganic compounds and it is mainly observed in combustion of heterogeneous mixtures.

1.2 Heterogeneous combustion Modeling

Some of the significant physical parameters of actual combustion process [41-52] include complexities in internal microstructure, distribution of heat sources, heat release, heat loss or gain, propagation of combustion wave specifically in multi dimensional systems etc... These parameters play a crucial role in actual combustion process. While many researchers have contributed to experimental investigations [31, 39-50] of quantification of dynamic combustion parameters (burn rate, flame structure...) of combustion process over the years, a very few works [33-36, 48-51] are devoted to modeling of heterogeneous combustion that includes systematic study for the effects of various physical parameters. Experimental investigation of combustion phenomenon has its own disadvantages such as expensive, safety measures, time consuming and difficult to track the profile of combustion wave. Modeling and simulation can overcome the difficulties of experimental investigations, has inherent safety and wide operational features that make them attractive choices for a broad range of applications, including combustion of coal, solid propellants, aerosols, thermite mixtures etc. These advances are possible by theoretical foundation; the strong interplay between theory, experiment, computation; and unified description of the roles of combustion mechanics and kinetics. Detailed fundamental understanding of the combustion process should serve as a strong foundation for the prediction of heterogeneous mixtures burning behavior in the more complicated non-steady situations like instability [41-45], flame quenching [46-59] and ignition performance. These combustion characteristics can be traced from the knowledge of the internal microstructure and propagation of combustion wave.

The combustion of heterogeneous mixture is a very complex process [39-50] and the influences of physical parameters in disordered system are not carried exhaustively. The role of significant physical parameters and reaction kinetics of the combustion wave can be obtained through mathematical modeling and numerical simulation. The effects of physical parameters in actual combustion process are analyzed from the available experimental data [31, 39-50]. These effects are systematically incorporated into combustion wave propagation theory and a physical model is developed. Thus combustion wave characteristics are predicted for entire range of heterogeneous mixtures. Results obtained from the numerical calculations of developed model are validated with experimental data. Inferences drawn after comparison of results from experimental and developed model are useful in distinguishing the role of physical parameters played during combustion process. This combination of developing physical model, diagnosing the combustion wave propagation and interpreting

data obtained from developed model is the approach followed in investigating the characteristics of combustion wave.

1.3 Disorderness in internal microstructure

Combustible mixtures are characterized by large scale of heterogeneity of the distribution of combustible particles [51-52]. In addition the heterogeneous media also involves boundary regions between particles. The combustible particles and voids between them typically have different physical and chemical properties [51-52, 56-59]. Internal structure of heterogeneous mixtures is one of the factors that affect thermal wave characteristics [39-52, 56-61]. The role of sample structure and consumption of reactant in combustion process were adequately demonstrated by the experimental studies using high resolution micro video recorder [39-45]. Such experimental studies have shown that the self-propagating thermal (combustion) front becomes complex waves at macro scales. In these situations the internal microstructure of the actual solid combustible system in most of the cases is a priori unknown and is practically difficult, expensive to determine. The mathematical model shown in this thesis considers different ranges of internal microstructure characterized by disordered spatial distribution of the particles. The concept of randomizing the distribution of combustible particles of heterogeneous mixtures accounts for the loss of continuity of thermal wave when the characteristic thickness of thermal wave becomes comparable with the size of combustible particles. The scope of internal microstructure characteristics that have the potential to significantly affect the combustion of heterogeneous mixtures is wide and varied. This is because of the complexities associated [31-50] with physical and chemical processes that interact and participate during combustion process.

Heterogeneous combustion is complicated by internal micro structure and the consumption of reaction cells of the system even at stationary mode of combustion. Such complications results in micro-oscillations of combustion wave. This phenomenon of combustion wave under critical condition of operation leads to combustion limit [39-50]. The structure of heterogeneous mixture and consumption of reactants are the major factors affecting the dynamical combustion properties. The experiments [45-50] have detected the mechanism modes of combustion which is either quasi-homogeneous or relay- race. The mechanisms of initiation, ignition, burning and performance of heterogeneous mixtures are dominated by the nature of heterogeneities [31-50]. The ignition behavior, performance and reaction zone characteristics of heterogeneous mixtures with voids, internal microstructure and other discontinuities are very different and neglected by classical flame theories. The

knowledge gained from the classic theoretical and experimental studies [31, 39-50] of the combustion process in the past allowed progress towards the better understanding of heterogeneous combustion process. The continuous wave solution cannot be applied for describing the combustion process of such heterogeneous mixtures. However the combustion front in such media propagates in a wave like manner and the combustion velocity is considered as an average parameter. Hence homogenous approach can now be applied for describing the heterogeneous combustion process if and only if the combustible particles are of point size and the size of combustible particles is less than the thickness of combustion front.

Present thesis is focused on the development, simulation and validation of mathematical model of a heterogeneous combustion process that incorporates various physical parameters such as disordered internal micro structure, heat release and heat loss of heterogeneous mixtures. The role and significance of physical parameters is established and the numerical results calculated from mathematical model are analyzed in detail in the chapters.

1.4 Description of Model

The internal microstructure of the combustible system is modeled by distributing immobile reaction cells (point heat sources) on one, two dimensional chain. Periodic or different random distributions are used for positioning neighboring cells. The medium filling the space between the reaction cells are characterized by thermal conductivity κ , linear mass density ρ and specific heat c . Heat transfer between reaction cells is carried through these medium. The cells are characterized by an ignition temperature T_{ign} . When the temperature of an unburnt cell reaches the value T_{ign} , the ignition and instantaneous burning away of the cell occurs with release of heat. The combustion front propagates from left to right direction i.e from burnt cells to unburnt cells. The model under consideration simplifies the reaction kinetics of actual heterogeneous combustion process. The parameters of the model such as ignition temperature signify the characteristic features of the reactants. If this model is regarded to actual combustion of heterogeneous mixtures, the sense of ignition temperature becomes apparent with respect to combustible limits and quantity of inert diluent.

The analysis for heat equation is conveniently carried out in non-dimensional variables (shown in chapters 2, 4 and 5) and the governing equation is obtained. In non-dimensional variables the one dimensional governing equation between ignition temperature and time is given by

$$2\sqrt{\pi\varepsilon} = \sum_{i=-\infty}^{k-1} \frac{1}{\sqrt{t_k - t_i}} \exp\left(-\frac{(x_k - x_i)^2}{4(t_k - t_i)}\right)$$

Where ε is ignition temperature, x is position and t is the ignition time of the reaction cell. For a given ignition temperature, the governing equation enables the finding of ignition moment of k^{th} cell, t_k , if all t_i (for $i < k$) are known. The system under consideration is single-parametric: all solutions for this system depend on the system structure and on the single parameter ε - the non-dimensional ignition temperature of the sources.

Using the one dimensional governing equation for specific system, it is possible to find the burning rate both of the one dimensional system as whole and in its different parts. For example, a mean burning rate (ω) for the section between the cells i and $k > i$ is equal to

$$\omega = (x_k - x_i)/(t_k - t_i)$$

In particular for a periodic system, consisting of identical heat source, the analytic solution for burn rate is known [34,51]. Nevertheless, for the calculation of non-steady burning rate, which always takes place in disordered systems and even in periodic systems at initial period of combustion immediately after initiation of the system and also beyond the stability threshold [34,51], it is necessary to solve the governing equation. The exothermic reaction is commonly initiated by heating one end of the sample. From a theoretical point of view, this is equivalent to setting the temperature at one of the boundaries, say $x=0$, to a specific value $T_i > T_{ign}$, and the rest of the sample at the ambient temperature T_{in} at $t=0$. In order to achieve a stable ignition of the sample (combustible system) in numerical calculations, it is considered, as an initial conditions, that the few of first heat sources are inflamed compulsorily and consistently with time intervals $\tau = 0$; after that the system was left to itself, and the process developed in accordance to governing equation. For a given ε , t_k was varied in small steps until the summation in governing equation reached the values of ε . After cross checking the numerical results of a periodic system obtained from governing equation with results of analytic solution, the numerical results for disordered system are calculated.

The developed model at first stage (one dimensional) is simulated for different disordered distributions of positioning neighboring reaction cells to account for randomness in internal microstructure. In successive stages the model is incorporated with additional physical parameters such as randomizing the distribution of heat releases and heat loss of cells. After successful mathematical modeling of one dimensional combustion process, the model is extended to two dimensional to account for the structure of reaction front.

The exercise of numerical simulation of the heterogeneous combustion process requires huge computing time on a desktop computer. For example burn rate of an ignition temperature obtained from numerical simulation is the result of 40 sets of random distributions. Computation time can even extend up to multiple months for two dimensional modeling. Desktop computers with MATLAB cannot serve the purpose. Proper utilization of multiple processors that perform sharing and parallel operation at a time can be the best option. OPENMPI and MPI [62] are a few of parallel computing systems. C programming language is the best available platform for task parallelism. MPI stands for message passing interface; here many calculations are performed simultaneously by sharing and synchronizing the data between the processors. Master processor initiates the slave processors by distributing the data. After the calculations are performed by slave processors, the master gathers the computed data from slave. During this operation, the slaves have to wait for further instruction from master. Development of super computer with features of parallel computing allowed scientists and engineers for mathematical modeling of combustion process [62]. High performance parallel computing machine embedded with 128*8 processors is utilized for numerical calculation.

After successful comparison of numerical results with available experimental data the model is thus established and validated. Thus models developed are simulated for wide range of operating conditions, and results obtained are compared with established theories. At this stage the developed model now can be used as a tool box for predicting and analyzing the combustion process. This toolbox reduces the experimental costs and difficulties. Numerous numerical experiments can be performed with help of developed toolbox. The numerical model developed for modeling the performance of heterogeneous combustion process is described along with their application to scientific and engineering problems in the chapters.

1.5 Organization of the thesis

The thesis is divided into four working chapters 2, 3, 4, 5 and chapter 6 for conclusion. Chapters 2, 3 and 4 emphasizes about the numerical simulations, technique, analysis and validation of results for one dimensional system. Chapter 5 concentrates on the numerical simulation of two dimensional modeling.

Chapter 2 studies the role of disorderness of internal microstructure in the combustion of heterogeneous mixtures. The nature of distribution of particles in heterogeneous mixtures is apriori unknown and plays a crucial role in the combustion process. One dimensional

modeling of heterogeneous mixtures is categorized into ordered and disordered system to perform numerical experiments for propagation of combustion front. Different random distributions (uniform, beta, normal and gamma) are employed for distributing the point heat sources in a disordered system. Two cases, identical and random, for the nature of distribution of heat release of point source in a system are considered. The numerical results show that the random structure of microheterogeneous system plays a crucial role in the combustion front propagation. Particularly the normal and gamma distribution of arranging neighboring reaction cells with identical heat releases can be the powerful methodology in describing the combustion process of actual heterogeneous systems. Wide ranges of behavior of actual heterogeneous mixtures are reproduced by varying the shaping (a) or standard deviation (σ) parameter of the model. As the degree of randomness increases the combustion front propagates with stops. Propagation of combustion front in a disordered system at higher ignition temperatures has been observed to be in relay race mode. Burn rate of a heterogeneous system sensitively depends on internal microstructure of system. Successful comparison of the experimental data (burning of CMDDB propellants, thermite and powder mixtures) with numerical results obtained with model is performed in this chapter. Different combustion limit for different thermite systems observed during experiments are the consequences of randomized heat release. Experimental data for thermite systems that have lower inflammability limits are analyzed in the view of randomizing heat releases of cells. The model developed in the view of randomizing heat release reproduces the experimental burn rates and experimental combustion limit.

Chapter 3 proposes a novel approach for correlation between the burn rates and discrete probability of neighboring reaction cells of one dimensional disordered system. Role of internal microstructure disorderness, with identical heat release, in modeling heterogeneous system is clearly established in the chapter 2. However the computation time for simulating the combustion process of a disordered system is huge and increases with increase in ignition temperature. Numerical technique that cuts down the computational time based on the knowledge gained from numerous numerical experiments is proposed in this chapter. In the proposed approach, it is shown that the burn rates of a disordered (gamma, normal distribution) system can be obtained directly from the selective cumulative count of a distribution function that describes the distribution of the spacing of the reaction cells. Cumulative count from a lower to upper limit yields the normalized burn rate of a disordered system. With the upper limit fixed, the lower limit depends on the non-dimensional ignition

temperature. This approach is validated and augurs well with numerical results for gamma and normal distribution of spacing neighbor cells over entire range of shaping and standard deviation parameters. Additionally, this approach also facilitates the prediction of burning limits of heterogeneous mixtures.

Chapter 4 studies the role of heat loss in combustion process. Heat energy released by the combustion of particle results in retarding the exothermic reaction process due to ambient conditions. Heterogeneous mixture like thermite mixtures that involve heat loss are considered in this chapter. A one dimensional model is proposed that substantively explains the characteristic features of thermite mixture. Reaction cells in disordered system are arranged by probability density function of gamma distribution. Wide ranges of disordered system are obtained by changing the shaping parameter (a) of gamma distribution. Numerical results suggest that the heat loss in the actual system does not affect the burn rate although plays a vital role in deciding the combustion limit. Heat loss in the system leads to decrease in thermal runaway and retards ignition process affecting the combustion limit. Numerical results with effect of disorderness in microstructure and heat loss are discussed.

Chapter 5 studies about the two dimensional heterogeneous combustion process. The computation time for a two dimensional system with optimized periodic boundary conditions is of the order of weeks on a desktop computer. Hence to reduce the computation time, the parallel computing facility is utilized for running the indigenous code. This code parallelizes the task of calculation of temperature of unburnt particles at each step of time. The computational time after implementing parallel computing is reduced to hours. Analyses of the temperature profile of unburnt particles suggest that the unburnt particles can be categorized as conjunction of hot and cool cells. Slice reconfiguration scheme, considers around 20% unburnt cells for each iteration, is proposed for further reduction of computation time that instead considers only hot reaction cells. This method achieves a multi fold improvement in computation time instead of considering total reaction cells, without loss of any accuracy. Results show that reaction rate sensitively depends on internal microstructure and expansion parameter of the system. Fingering like instability patterns that are encountered during experiments are obtained with the developed two dimensional model.

Chapter 6 concludes the results of thesis, and presents a brief description of future perspectives. Three dimensional modeling which is more close to actual system and results in

this direction can lead us to better prediction of actual combustion process. Progress in three dimensional modeling is only possible with step by implementation of all physical parameters as described in previous chapters 2, 4 and 5. An In house c code with parallel computing for three dimensional model of combustion process has been built. To obtain the optimization of parameters (l_x, l_y, l_z, N_y, N_z (periodic boundaries)) the c code consumes around couple of months of computation time on work station. The three dimensional work is carried out in future work.

1.6 References

- [1] Zeldovich YB, Frank-Kamenetskii DA. Theory of the thermal flame propagation. Zh Fiz Khim 1938;12(1):100–5.
- [2] Levashov EA, Bogatov YV, Milovidov AA. Macrokinetics and mechanism of a self-propagating high-temperature synthesis process in titanium-carbon-based systems. Fiz Goren Vzryva 1991;27(1): 88–93.
- [3] Merzhanov AG, Rogachev AS. Structural macrokinetics of SHS processes. Pure Appl Chem 1992;64(7):941–53.
- [4] Hwang, S., Mukasyan, A.S., Rogachev, A.S., Varma, A., 1998. Combustion wave microstructures in gas–solid system: experiments and theory. Combustion Science and Technology 123, 165.
- [5] Hwang, S., Mukasyan, A.S., Varma, A., 1998. Mechanism of combustion wave propagation in heterogeneous reaction systems. Combustion Flame 115, 354.
- [6] Merzhanov, A.G., Rogachev, A.S., 2000. Discrete heat waves in active heterogeneous media: basic principles and introduction to the theory. Russian Journal of Physical Chemistry 74, S20.
- [7] Mukasyan, A.S., Hwang, S., Sytshev, A.E., Rogachev, A.S., Merzhanov, A.G., Varma, A., 1996. Combustion wave microstructure in heterogeneous gasless systems. Combustion Science and Technology 115, 335.
- [8] Mukasyan, A.S., Rogachev, A.S., Varma, A., 2000. Microstructural mechanisms of combustion in heterogeneous reaction media. Proceedings Combustion Institute 28, 1413.
- [9] Rogachev, A.S., Shugaev, V.A., Kachelmyer, C.R., Varma, A., 1994. Mechanisms of structure formation during combustion synthesis of materials. Chemical Engineering Science 49, 4949.
- [10] Varma, A., Rogachev, A.S., Mukasyan, A.S., Hwang, S., 1998a. Combustion synthesis of advanced materials: principles and applications. Advances in Chemical Engineering 24, 79.

-
- [11] Varma, A., Rogachev, A.S., Mukasyan, A.S., Hwang, S., 1998b. Complex behavior of self-propagating reaction waves in heterogeneous media. *Proceedings of the National Academy of Sciences* 95, 11053.
- [12] Mallard E, Le Chatelier HL. *Combustion des Melanges Gazeux Explosifs. Annales des Mones Annales des Mines* 1883;4(208): 274–381.
- [13] Mason EW, Wheller RVJ. The uniform movement during the propagation flame. *Chem Soc* 1917;CXI:1044–58.
- [14] Merzhanov AG, Mukasyan AS, Rogachev AS, Sytchev AE, Varma A. Microstructure of combustion wave in heterogeneous gasless systems. *Combust Explos Shock Wave* 1996;32(6):334–47.
- [15] Varma A, Rogachev AS, Mukasyan AS, Hwang S. Complex behavior of self-propagating reaction waves in heterogeneous media. *Proc Natl Acad Sci USA* 1998;95:11053–8.
- [16] Frolov YV, Pivkina AN, Aleshin VV. Structure of HCS and its influence on combustion wave. *Int J Self-Propagat High-Temp Synth* 2001;10(1):31–54.
- [17] Zhang JY, Fu ZY, Wang WM, Zhang QJ. A marco-homogenous and micro-heterogeneous model for self-propagating high temperature synthesis. *Mater Sci For* 2005;475(4):475–9.
- [18] Pivkin NM, Pelych J. High-frequency instability of combustion in solid rocket motors. *Propulsion Power* 1995;11(4):651–6.
- [19] Smirnov VN, Petulov VY, Chuiko SV, Sokolovskii FS, Nechai GV. Specific low-frequency instability of combustion for a microheterogeneous charge in a rocket chamber. *Khim Fiz* 1998;17(8): 121–30.
- [20] Grabski R, Frank M. Theoretical investigation of flame structures. *Int Ann Conf ICT* 1991;122. 113/1–8.
- [21] Suzuki A, Yamamoto T, Aoki H, Miura T. Percolation model for simulation of coal combustion process. *Proc Combust Inst* 2002; 29:459–66.
- [22] Miccio F. Modeling percolative fragmentation during conversion of entrained char particles. *Korean J Chem Eng* 2004;21(2):404–11.
- [23] Favier C. Percolation model of fire dynamic. *Phys Lett A* 2004;330: 396–401.
- [24] Viegas DG. *Philos Trans R Soc Lond A* 1998;356:2907.

- [25] Gardner RH, Romme WH, Turner MG. Predicting forest fire effects at landscape scales. In: Mladenoff DJ, Baker WL, editors. *Spatial modeling of forest landscapes: approaches and applications*. Cambridge: Cambridge University Press; 1999. p. 163–85.
- [26] Scala F, Salatino P, Chirone R. Fluidized bed combustion of biomass char of *Robinia pseudoacacia*. *Energy Fuels* 2000;14(4): 781–90.
- [27] Molerus O. Appropriately defined dimensionless groups for the description of flow phenomena in dispersed systems. *Chem Eng Sci* 1998;53(4):753–9.
- [28] Marban G, Pis JJ. Fuertes AB Characterizing fuels for atmospheric fluidized bed combustion. *Combust Flame* 1995;103(1/2):41–58.
- [29] Kauffman CW, Nicholls JA. Shock-wave ignition of liquid fuel drops. *AIAA J* 1971;9(5):880–5.
- [30] Fedorov AV. Mathematical modeling of the ignition of a cloud of microdrops of a hydrocarbon fuel. *Fiz Goren Vzryva* 2002;38(5):97–100.
- [31] Dvoryankin A. V., Strunina A. G., and Merzhanov A. G. Stability of combustion in thermite systems, *Comb. Expl. Shock Waves*, 21, No. 4, 421–424 (1985).
- [32] A.S. Mukasyan, A.S. Rogachev, Discrete reaction waves: Gasless combustion of solid powder mixtures. *Progress in Energy and Combustion Science* 34, 377–416 (2008).
- [33] A.S. Rogachev, Microheterogeneous mechanism of gasless combustion. *Comb. Expl. Shock Waves*, 39, 150–158 (2003).
- [34] S.A. Rashkovskii, Hot-spot combustion of heterogeneous condensed mixtures. Thermal percolation. *Comb. Expl. Shock Waves*, 41, 35–46 (2005).
- [35] S.A. Rashkovskiy, Simulation of Gasless Combustion of Mechanically Activated Solid Powder Mixtures. *Advances in Science and Technology*, Vol. 63, P. 213-221 (2010).
- [36] P. S. Grinchuk and O. S. Rabinovich. Effect of random internal structure on combustion of binary powder mixtures. *Physical Review E* 71, 026116 (2005).
- [37] F.-D. Tang, A.J. Higgins, S. Goroshin. Effect of discreteness on heterogeneous flames: Propagation limits in regular and random particle arrays. *Combustion Theory and Modelling*. Vol. 13, No. 2, 319–341 (2009).
- [38] A. S. Rogachev, F. Baras, Dynamical and statistical properties of high-temperature self-propagating fronts: An experimental study. *Physical Review E* 79, 026214 (2009).
- [39] Spalding, D.B., A Theory of Inflammability Limits and Flame-Quenching, *Proc. Roy. Soc., Ser. A*, vol. 240, no. 1220, pp. 83–100 (1957).

-
- [40] Lina hu, Claude-Michel Brauner, Jie Shen and Gregory I. Sivashinsky, Modeling and Simulation of Fingering pattern formation in a Combustion model, *Mathematical Models and Methods in Applied Sciences* Vol. 25, No. 4 (2015) 685–720.
- [41] Jackson R. Mayo and Alan R. Kerstein, Fronts in randomly advected and heterogeneous media and nonuniversality of Burgers turbulence: Theory and numerics, *Physical Review E* **78**, 056307(2008).
- [42] Hiroshi Gotoda, Yuta Shinoda, Masaki Kobayashi and Yuta Okuno, Detection and control of combustion instability based on the concept of dynamical system theory, *Physical Review E* **89**, 022910 (2014).
- [43] M. Myllys, J. Maunuksela, J. Merikoski, J. Timonen, V. K. Horvath, M. Ha and M. den Nijs, Effect of a columnar defect on the shape of slow-combustion fronts, *Physical Review E* **68**, 051103 (2003).
- [44] V. V. Bychkov and M. A. Liberman, Stability of Solid Propellant Combustion, *Physical Review Letters* 73,14 (1994).
- [45] J. Maunuksela, M. Myllys, O.-P. Kähkönen, J. Timonen, N. Provatas, M. J. Alava and T. Ala-Nissila, Kinetic Roughening in Slow Combustion of Paper, *Physical Review Letters* 79, 8 (1997).
- [46] Ory Zik, Zeev Olami and Elisha Moses, Fingering Instability in Combustion, *Physical Review Letters* 81, 18 (1998).
- [47] J. Merikoski, J. Maunuksela, M. Myllys, J. Timonen and M. J. Alava, Temporal and Spatial Persistence of Combustion Fronts in Paper, *Physical Review Letters* 90, 2 (2003).
- [48] I. Idris and V. N. Biktashev, Analytical Approach to Initiation of Propagating Fronts, *Physical Review Letters* 101, 244101 (2008).
- [49] G. R. Ruetsch, L Vervisch and A. Linan, Effects of heat release on triple flames, *Phys. Fluids* 7 (6), June 1995.
- [50] P. S. Grinchuk, O. S. Rabinovich, A. S. Rogachev and N. A. Kochetov, Fast and Slow Modes of the Propagation of the Combustion Front in Heterogeneous Systems, *JETP Letters*, Vol. 84, No. 1, pp. 11–15, 2006.
- [51] S.A. Rashkovskiy, G.M. Kumar, S.P. Tewari, One-dimensional discrete combustion wave in periodic and random systems. *Combustion Science and Technology*, 182: 1009–1028, (2010).
- [52] N. Tarun Bharath, S. A. Rashkovskiy, S. P. Tewari and G .M. Kumar, Dynamical and statistical behavior of discrete combustion waves: A theoretical and numerical study, *Phys. Rev. E* 87,042804 (2013).

- [53] Naine Tarun Bharath, Manoj Kumar Gundawar, Effects of Disordered Microstructure and Heat release on Propagation of Combustion Front, Cogent engineering (2016).
- [54] D. A. Frank-Kamenetskii, *Diffusion and Heat Transfer in Chemical Kinetics* (Plenum Press, New York, 1969).
- [55] A. D. Polyanin, *Handbook of Linear Partial Differential Equations for Engineers and Scientists*, (Chapman & Hall/CRC Press, Boca Raton–London, 2002).
- [56] Zel'dovich, Ya.B., Theory of Flame Propagation in Gases, *Zh. Eksp. Teor. Fiz.*, vol. 11, no. 1, pp. 159–168 (1941).
- [57] Zeldovich, Y.B., Barenblatt, G.I., Librovich, V.B., and Makhviladze, G.M. The Mathematical Theory of Combustion and Explosions, (Plenum Press, New York and London 1985).
- [58] L. D. Landau and E. M. Lifshitz, *Statistical physics part 1*, (3ed., Pergamon, 1980)
- [59] C.W. Gardiner. Handbook of Stochastic Methods for Physics, Chemistry and the Natural Sciences, Springer Series in Synergetics, Volume 13, (2nd, Springer-Verlag, Berlin Heidelberg, New York, Tokyo, 1985)
- [60] S. A. Rashkovskii, Structure of heterogeneous condensed mixtures, *Combust. Expl. Shock Waves*, 35, No. 5, 523–531 (1999).
- [61] S. A. Rashkovskii, Role of the structure of heterogeneous condensed mixtures in the formation of agglomerates, *Combust. Expl. Shock Waves*, 38, No. 4, 435–445 (2002).
- [62] Chao-Tung Yang , Chih-Lin Huang, Cheng-Fang Lin, Hybrid CUDA, OpenMP, and MPI parallel programming on multicore GPU clusters, *Computer Physics Communications* 182 (2011) 266–269.

CHAPTER 2

Dynamical and statistical behavior of discrete combustion waves in One-dimension: A theoretical and numerical study

Present chapter illustrates theoretical and numerical study of combustion waves in a discrete one-dimensional disordered system. Internal microstructure of a combustible system is discretized and modeled with different random distributions. Also two cases for the nature of distribution of heat releases of reaction cells are taken into account, one with identical heat release and the other with randomized heat release. To study and analyze combustion waves for identical heat release, various random distributions like uniform, beta, gamma and normal have been considered for distributing neighboring reaction cells. The results show that the random structure of microheterogeneous system plays a crucial role in the dynamical and statistical behavior of the system. This is a consequence of nonlinear interaction of the random structure of the system with the thermal wave. Particularly the normal and gamma distribution of arranging neighboring reaction cells can be the powerful methodology in describing the combustion process of wide ranges of actual heterogeneous systems. The burning rate of powder system sensitively depends on its internal structure. The Arrhenius' macrokinetics at combustion of disperse systems can take place even in absence of Arrhenius' microkinetics; it can have purely thermal nature and be related to their heterogeneity and to existence of threshold temperature. It is also observed that combustion of disperse systems always occurs in microheterogeneous mode according to the relay-race mechanism. Different combustion limit for different thermite systems observed during experiments are the consequences of randomized heat release. Experimental data for Thermite systems that have lower inflammability limits are analyzed in the view of randomizing heat releases of cells. The model developed in the view of randomizing heat release reproduces the experimental burn rates and experimental combustion limit.

2.1 Introduction

A combustion wave represents a self-organized process in which a chemical reaction, localized in a relatively narrow layer (so called reaction front), propagates throughout the reaction media, converting initial reactants into combustion products. Depending on the nature of reaction media, the process can be either homogeneous, or heterogeneous, in case of medium consisting of several phases. The phenomenon of heterogeneous combustion is observed in a variety of processes including combustion synthesis of materials [1–9], burning of solid propellants [10–14], coals and biomass [15–17], forest fires [18–20], reaction

propagation in fluidized beds [21–23] and in clouds of solid particles or spray combustion [24–27]. Gasless combustion waves commonly occur in heterogeneous mixtures of powder reactants such as $Ta+xC$, $Ni+xAl$, $Ti+xSi$, CMDB propellants and thermite mixtures etc [1–9]. Locally initiated exothermic reaction can propagate through the mixture in the form of bright glowing combustion front, without notable gasification. The absence of gaseous flame and solid state of the combustion products allow us to term the process as solid-flame combustion [28]. Self-sustained combustion can be realized within some concentration limits for a given binary mixture. Since the combustion products consist of valued refractory compounds, gasless combustion makes a basis of combustion synthesis technology [1–9, 28], the so-called self-propagating high-temperature synthesis (SHS). The structure of heterogeneous condensed mixtures is one of the major factors affecting the combustion wave characteristics as well as the properties of the products. An important role of the sample structure in such processes became especially evident after experimental studies using *in situ* high-resolution microscopic video recording [5–9]. Such microscopic studies have shown that at small time scales the behavior of self-propagating high-temperature reaction waves can become complex [5–9]. High-speed microscopic video recording has revealed [5–9] a micro-heterogeneous mechanism of steady-state combustion in this system: the combustion front was found to consist of microscopic hot spots caused by flash burning of individual particles in the mixture.

It is well-known [29,30], that in homogeneous systems under certain conditions a stationary process of combustion can be replaced by a more complex, oscillating, modes of combustion, and under certain other conditions the combustion becomes impossible. This is connected with the non-linearity of the system considered, in which instability occurs under certain conditions: the system undergoes a Hopf bifurcation, resulting in a combustion front that moves with a pulsating speed. In homogeneous systems, this instability has a thermal nature. Such a behavior is characterized for a wide class of nonlinear phenomena from physics to life sciences [31]. Under certain conditions, it is associated with the development of complex behaviors such as multiple states, abrupt transitions, periodic or chaotic oscillations, waves, and spatial patterns [32–33]. In the case of combustion of heterogeneous systems, a propagation of thermal wave is complicated by the heterogeneous structure of the system. These results in micro-oscillations of combustion wave even at stable stationary modes. The extensive investigations in the field of heterogeneous combustion have been carried out in the last decade; however most of the works are devoted to experimental

investigation of different aspects of combustion of heterogeneous systems. Only very few reports are devoted to theoretical analysis of combustion of heterogeneous systems [34-39] and there were only a few attempts in the literature to take into account the system randomness and its effect on the combustion of heterogeneous systems. A random process of propagation of combustion wave in a heterogeneous system, stimulated by interaction of combustion wave with a random structure of the system, has, first of all, a fundamental interest since it is the simple example of such kind of processes.

The present chapter investigates the above mentioned problems. In this chapter, the dynamical, structural and statistical properties of combustion of one-dimensional disordered heterogeneous system are studied with significance to different random distributions employed for positioning neighboring reaction cells and their heat releases. The methodology, resembles to Monte Carlo simulation, will enable to perceive the affect of minute changes in microstructure on dynamic combustion parameters such as stability of reaction front, ignition delay times and average burn rate. Such minute aspects are controlled by discrete model and are illustrated with significant change in parameters such as scale and shaping parameter of distribution. The affect of randomizing heat releases on combustion process is given very little importance and almost times neglected in earlier literatures. Such situations commonly arise for improper mixing of heterogeneous mixtures, changing the diluter and percentage of diluter. Two different cases of reactant consumption are considered, in present chapter, by identical distribution of heat release or by randomizing the heat release. The use of different random distribution (Normal, beta, gamma and uniform) for the distances between the adjacent cells allows studying wide variations in the structure of the system, ranging from clusters to completely disordered systems and furthering up to regular periodic systems. The novel approach shall optimistically list the priority of distributions in modeling a discrete combustion process. The possible limits of a combustion process are studied for normal distribution. The discrete model is now validated and compared with experimental results performed on combustion of CMDDB propellants, Ti-Si system and different thermite systems. The above work is performed for identical heat release. Most works on combustion modeling have reported that the effect of random heat release in combustion process [52-53] is negligible and considered the heat release to be identical for all the cells. Section II studies the systematic affect of heat consumption of reaction cells on combustion process. The model of discrete combustion waves (percolate

combustion) [35, 38] which has very interesting behavior, similar to behavior of combustion of actual heterogeneous systems is considered here.

2.2 Model of the system

2.2.1 Discrete combustion waves

The traditional description of solid-phase combustion is based on the heat equation with a source term representing an exothermic reaction [40]. In experimental situations, the reacting sample usually has a cylindrical geometry and in many circumstances the variation of the temperature field along the transversal direction is small and can be ignored. Upon neglecting transversal heat losses, the one-dimensional macroscopic equation can be used for description of the evolution of the temperature of such a system. A one dimensional system, consisting of reaction cells (particles) – the point heat sources, distributed along an axis x , similar to earlier reports on combustion of system with periodic and uniform random distribution have been considered here [35,38]. As the distribution of adjacent reaction cells in actual system is a priori unknown, and the systematic effect of these distributions on combustion wave is not investigated until now. In this chapter, different random distributions among the distances between the adjacent cells have been introduced. The medium filling the space between the reaction cells is characterized by thermal conductivity κ , density ρ and heat capacity c . The cells are considered to be immobile and are characterized by an ignition temperature T_{ign} . When the temperature of an unburnt cell reaches the value T_{ign} , the ignition and instantaneous burning away of the cell occurs with release of heat. The model under consideration simplifies essentially the kinetics of an actual combustion process and reduces it to two parameters: ignition temperature T_{ign} and nature of distribution of heat release Q_i . If the model, considered in this chapter, as applied to gasless combustion of heterogeneous systems [1-9,28], the sense of ignition temperature becomes apparent. The gasless combustion systems represent a mixture of powders, each of which is chemically inert by itself. However, as a result of interaction, they are capable of releasing a big amount of heat which is enough for self-sustained combustion. The initial particles of powder components constituting the systems of gasless combustion are in the solid state. In this state they are unable to enter into chemical reaction with each other because the reaction can proceed only after mixing of components. Thus, the melting of components is a necessary condition for beginning of chemical reaction in such systems. Experimental data [5-9] shows that chemical reaction between the components starts practically immediately

after appearance of liquid phase in the system and burn-out time for active particles is always essentially less (at least on order) than characteristic time of heating of the particles from initial temperature up to ignition temperature. This allows, considering the process of burn-out of active elements (reaction cells) of the system as instantaneous and the instant of reaching of some threshold temperature T_{ign} , at which a liquid phase (e.g. molten materials or eutectic) appears in the system, can be considered as an instant of ignition of the cells. The problem under consideration is described by one dimensional equation of thermal conductivity with delta sources which has solution

$$T(t, x) = T_{in} + \sum_{i(t)} \Delta T_i(t - t_i, x - x_i) \quad (1)$$

$$\Delta T_i(t, x) = (Q_i / c\rho) \frac{1}{2\sqrt{\pi \kappa t}} \exp\left(-\frac{x^2}{4\kappa t}\right)$$

where T_{in} is the initial temperature of the system; t_i is the instant of ignition of i -th cell, located at x_i . For a system of identical heat sources $Q_i = Q_0$. The analysis is conveniently carried out in non-dimensional variables [38], by defining the ignition time for burning cell $t = t_i(k/l_o^2)$, distance of unburnt particle $x = x_i/l_o$, Ignition temperature $\varepsilon = \frac{T_{ign} - T_{in}}{T_{ad} - T_{in}}$ and

heat release in combustion $q_i = Q_i/Q_0$, $T_{ad} = T_{in} + \frac{Q_0}{\rho c l_0}$ is so-called adiabatic temperature or burning temperature of the system; $l_0 = \lim_{N \rightarrow \infty} ((x_N - x_0)/N)$ is the mean distance

between neighboring heat sources in the system. In non-dimensional variables the governing equation between ignition temperature and time is given by [35,38]

$$2\sqrt{\pi\varepsilon} = \sum_{i=-\infty}^{k-1} \frac{1}{\sqrt{t_k - t_i}} \exp\left(-\frac{(x_k - x_i)^2}{4(t_k - t_i)}\right) \quad (2)$$

For a given ignition temperature, this relationship enables the finding of ignition moment of k^{th} cell, t_k , if all t_i (for $i < k$) are known. In general Eq. (2) has a set of solutions; however the ignition moment t_k corresponds only to the minimal solution of all such possibilities. Thus, Eq. (2) allows calculation of the sequence of the times of ignition of all heat sources in the

system, and, thereby, to determine the dynamics of combustion. Note that the system under consideration is single-parametric: all solutions for this system depend on the system structure and on the single parameter ε - the non-dimensional ignition temperature of the sources. Using the solution of Eq. (2) for specific system, it is possible to find the burning rate both of the system as whole and in its different parts. For example, a mean burning rate for the section between the cells i and $k > i$ is equal to

$$\omega = (x_k - x_i)/(t_k - t_i) \quad (3)$$

In particular, for periodic system, consisting of identical hot-spots(heat source), the steady-state burning rate Eq. (3) will be the same for all i and k , and Eq. (2) becomes [35]:

$$\varepsilon = \varepsilon_p(\omega) \quad (4)$$

where the function is introduced as

$$\varepsilon_p(\omega) = \frac{\sqrt{\omega}}{2\sqrt{\pi}} \sum_{k=1}^{\infty} \frac{1}{\sqrt{k}} \exp(-\omega k/4) \quad (5)$$

For the calculation of non-steady burning rate, which always takes place in disordered systems and even in periodic systems at initial period of combustion immediately after initiation of the system and also beyond the stability threshold [35], it is necessary to solve the non-linear algebraic Eq. (2). The exothermic reaction is commonly initiated by heating one end of the cylindrical sample. From a theoretical point of view, this is equivalent to setting the temperature at one of the boundaries, say $x=0$, to a specific value $T_i > T_{ign}$, and the rest of the sample at the ambient temperature T_{in} at $t=0$.

In order to achieve a stable ignition of the sample (combustible system) in numerical calculations, it is considered, as an initial conditions, that the 1000 of first heat sources are inflamed compulsorily and consistently with time intervals $\tau = 0$; after that the system was left to itself, and the process developed in accordance to Eq. (2). For a given ε , t_k was varied in small steps until the summation in Eq. (2) reached the values of ε . Basically, once the reaction is initiated, one observes the formation of a heat front that, after a short delay, starts to propagate with a constant speed up to the vicinity of the outer boundary, $x=L$. However, under some particular circumstances, this “stationary regime” may become unstable. The system under consideration is non-linear one and it posses the complex and interesting behavior depending on its structure and ignition temperature ε [35, 38].

2.2.2 System structure

Spacing of unburnt reaction cells in periodic system is done by regular spacing at a distance of unity. Random system that involves distribution of positioning unburnt cells is achieved by probability density function of various random distributions namely uniform, normal, gamma and beta with a mean of unity. The Probability density function for different distributions are listed in Table 2.1. A gamma distribution with shaping parameter $a=0.7$ and normal distribution with $\sigma=0.05$ are also considered for comparison. Total reaction cells in the model are considered as concatenation of 1000 burnt and 2500 unburnt cells.

These probability density functions of different random distributions are employed in positioning adjacent reaction cells. Thus modeled systems are numerically simulated using eqn. (2). While performing numerical simulations two cases of distribution of heat release (q_i) are considered: 1) Identical heat release and 2) Disordered heat release.

S.no.	Distribution	Probability Density Function P(L)	Parameters	Mean=1
1.	Normal	$= \frac{1}{\sigma\sqrt{2\pi}} e^{-\frac{(L-\mu)^2}{2\sigma^2}}$	σ, μ	μ
2.	Uniform	$= \frac{(L-a)}{(b-a)}$	a, b	$\frac{a+b}{2}$
3.	Beta	$= \frac{1}{B(a,b)} L^{(a-1)} (1-L)^{(b-1)}$	a, b	$\frac{a}{a+b}$
4.	Gamma	$= \frac{a^a}{\Gamma(a)} L^{a-1} \exp(-aL)$	a	$a^*(1/a)$

Table 2.1 Probability density function for different random distributions.

Figure 2.1 shows the probability density functions for spacing unburnt cells. The average spacing of particles is always maintained to be unity to facilitate a direct comparison of the results with a periodic system [1].

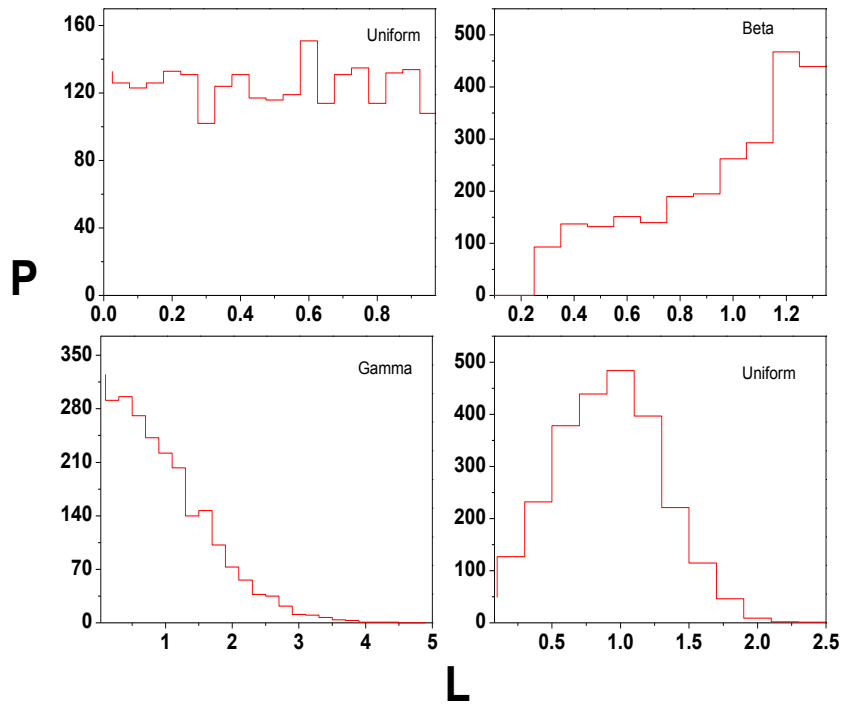


Figure 2.1 Probability Density Function for different Distributions

2.3 Numerical Results

Section I Identical Heat release

Combustion of the systems with two different structures has been considered in [35,38]: (i) with periodic spacing of the reaction cells and (ii) with random distribution of the reaction cells along the axis x . Ignition time profiles are obtained by using Eq. (2) for different distributions (shown in figure 2.1) of positioning neighboring reaction cells at different ignition temperatures ε . Note, identical distribution of heat release at all reaction cells is considered here. Figure 2.2 shows the ignition time profiles at different ignition temperatures of a combustible system described by different probability density functions employed for positioning neighboring reaction cells as shown in Figure 2.1. $\sigma=0.05$ for normal distribution and $a=0.7$ for gamma distribution are considered for comparison. Ignition time profiles depend both on the classification of distribution and ignition temperatures.

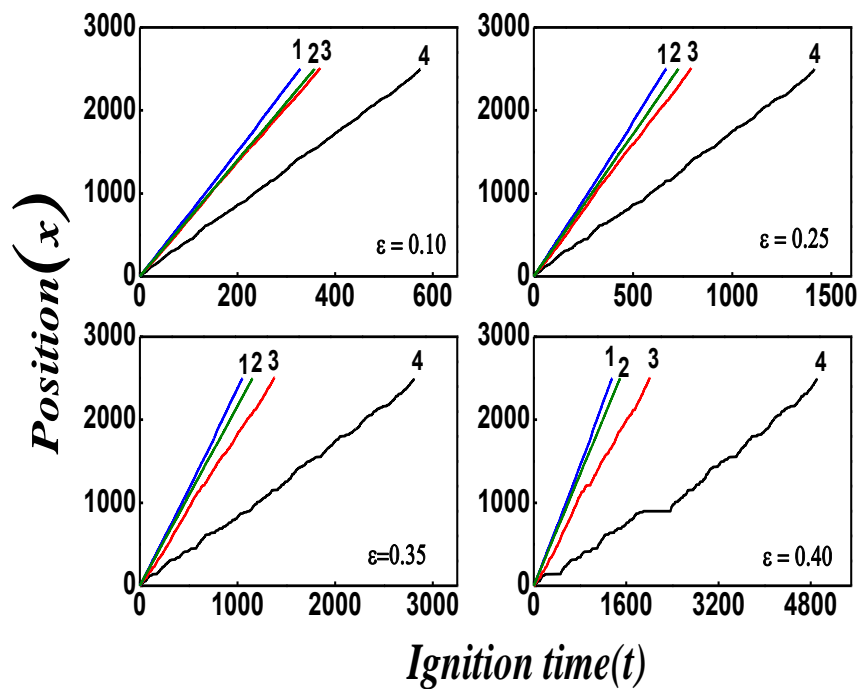


Figure 2.2 Ignition time profile for different distributions. (1)Normal (2) Beta (3) Uniform (4) Gamma ($a=0.7$).

The randomness in microstructure of a system also has critical influence on the ignition time profiles. The ignition time profiles are linear for both normal distribution and beta distribution of neighboring reaction cells and is identical to the periodic system. This can be inferred from figure 2.1, where it can be seen for a beta distribution about 70 percent of the cells spacing's are in the range of 0.8 to 1.2 and 100 percent for the normal distribution. The particles in spite of their random spacing, bear a close resemblance to a periodic system with unit spacing and hence a linear relation. However, the combustion front, for gamma distribution of neighboring reaction cells with shaping parameter $a=0.7$, is noticeable with more stops as the ignition temperature increases. Also a similar affect can be seen for a normal distributed system with higher values of σ , which will be shown in next section. Instability in combustion or reaction front stops is more prominent at higher ignition temperatures and higher degree of randomness in microstructure of the system.

At higher ignition temperatures, though the quantity of heat energy obtained from the burnt cells is same as compared to a corresponding periodic system, the front sees stops in the propagation of reaction front as a result of the randomness of neighboring reaction cells. With an increase in degree of randomness of positioning neighboring reaction cells, the

obtained heat energy has to overcome the disordered microstructure of system, particularly those points on the chain where the neighbor-cell spacing is very large. This can be quantified by observing the maximum ignition delay times of a system. The combustion stops in reaction front propagation are result of increased ignition delay times. Delays in ignition times are due to increase in induction periods between active cells and ignition temperature of a developed system.

Figure 2.3 shows plot between ignition temperature and maximum ignition delay times of a system. These maximum ignition delay times are obtained from the correlation analysis between adjacent reaction cells and their ignition delay times. From the correlation analysis it is observed that the variance of the ignition delay times increases with increase in degree of randomness in microstructure and ignition temperature.

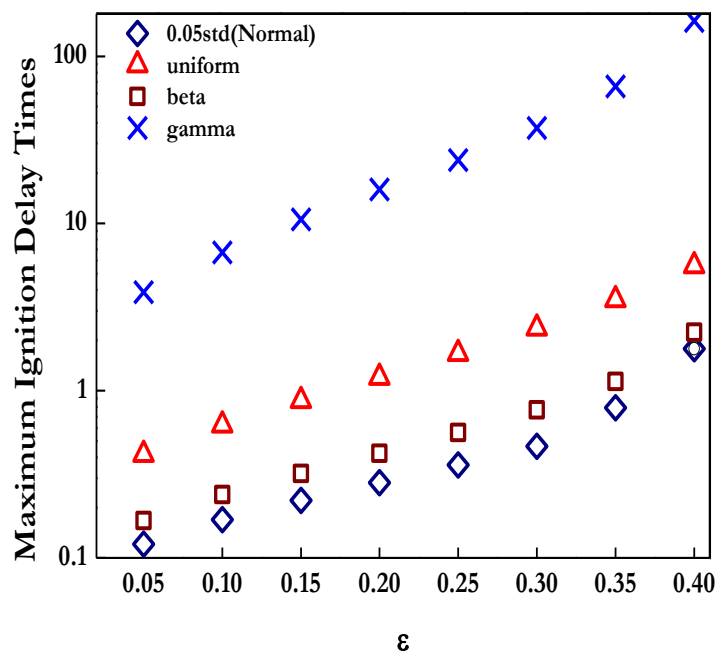


Figure 2.3 Comparison plot for maximum ignition delay times of adjacent cells.

From Figure 2.3 it is observed that maximum delay in ignition times of a system is proportional to degree of randomness in microstructure and ignition temperature of the system. The maximum delay in ignition times at particular ignition temperature shows the trend periodic < normal ($\sigma=0.05$) < beta < uniform < gamma ($a=0.7$). The maximum

ignition delay times also plays the crucial role in deciding the stability of reaction front and thus burn rates.

As the nature of distribution of reaction cells in actual systems is apriori unknown and it is of academic interest to find out the appropriate distribution. At the same time, the analysis of experimental data [9,47] shows, that the structure of actual system changes with a change in concentrations of powder components; this results in changing in burning rate of the system even if all other parameters remain constant (e.g. at the constant burning temperature). For this reason it is interesting to investigate the model system with wide variations in structure which allows studying the effect of system structure on its combustion. For Beta and uniform distributions, it is observed that there is no change in shape of distribution and consequently there is no effect on burn rates. Burn rates are calculated using eqn.(3) are shown in subsequent sections. Gamma and normal distribution of neighboring reaction cells have an advantage of variation in shaping and standard deviation parameter. Hence the numerical calculations for the discrete model developed in the view of normal and gamma distribution of neighboring cells have been carried out. Gamma or normal distribution has additional advantage of shaping parameter without change in mean.

2.3.1 Gamma Distribution

2.3.1.1 Characterization of system structure

A one-dimensional system in which the distances L between neighboring reaction cells are random ones adhering to the gamma distribution is

$$p(L) = \frac{a^a}{\Gamma(a)} L^{a-1} \exp(-aL) \quad (6)$$

where a is a shaping parameter has been considered in this study. The mean distance between cells is always equal to unity in non-dimensional variables. The parameter a in the Eq. (6) allows varying the system structure in the wide ranges and investigating the effect of the structure on propagation of combustion wave. Probability density for gamma distribution, calculated by using expression Eq. (6) and obtained numerically by Monte Carlo method is shown in Figure 2.4.

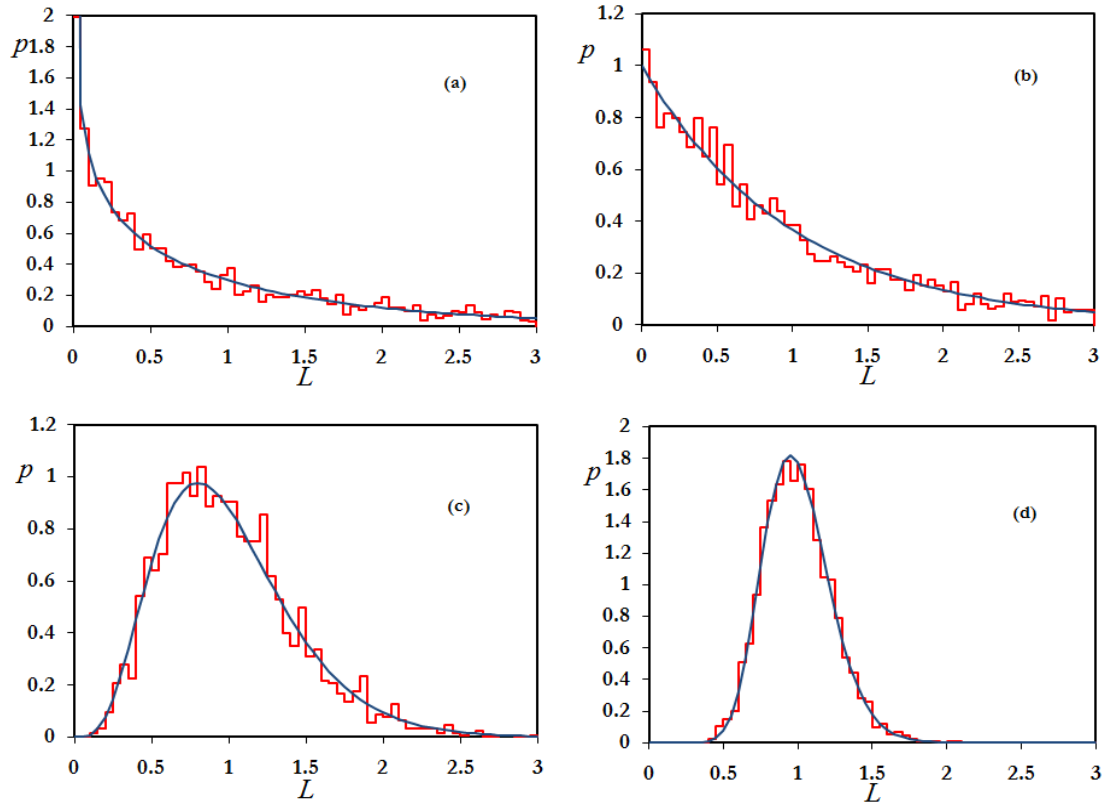


Figure 2.4. Distribution of the distances between neighboring hot spots. The polygonal lines are the histogram of specific realization, smooth lines are theoretical probability density Eq. (3). a) $a=0.7$; b) $a=1$; c) $a=5$; d) $a=20$.

One of the most important characteristic of random structure is a pair distribution function $g(r)$, which is defined for one-dimensional system as follows

$$g(r) = \frac{N(r, dr)}{2\langle n \rangle dr} \quad (7)$$

where $N(r, dr)$ is the number of reaction cells on the segment $[r, r + dr]$, located on the distance r from given cell, averaged throughout the cells of the system; $\langle n \rangle$ is the mean density of reaction cells on the axis x ; in non-dimensional variables $\langle n \rangle = 1$. The pair distribution function (7) is shown in figure 2.5, calculated for different values of shaping parameter a . From Figure 2.4 and 2.5 it can be seen that the formation of long-range order in the system occurs with an increase in parameter a in the range $a > 1$ and at $a = \infty$ the system becomes a periodic one. On the contrary, the probability of very closely spaced reaction cells increases for $a < 1$. Clusterization of the reaction cells occurs in the system for $a < 1$: the cells are collected in dense groups (clusters). The distance between cells in the cluster can be very small ($r \ll 1$), resulting in the practically simultaneous ignition of all cells in the cluster. This means that cluster can participate in combustion as a unified reaction cell

with a bigger heat release, which is equal to sum of heat released by all elementary reaction cells incorporated into the cluster. It is necessary to note that the number of elementary reaction cells in the cluster will be random and the total heat release is quantized: $q_i n$, where q_i (identical for all cells) is the heat release of single elementary reaction cell, $n = 1, 2, \dots$ is the random integer, equal to number of elementary reaction cells incorporated in the cluster. Thus, the system with gamma distribution of distances between neighboring reaction cells allows modeling the systems with wide-range variations in its structure: from clusters ($a < 1$) to completely disordered ($a = 1$) and further up to regular periodic systems ($a \rightarrow \infty$).

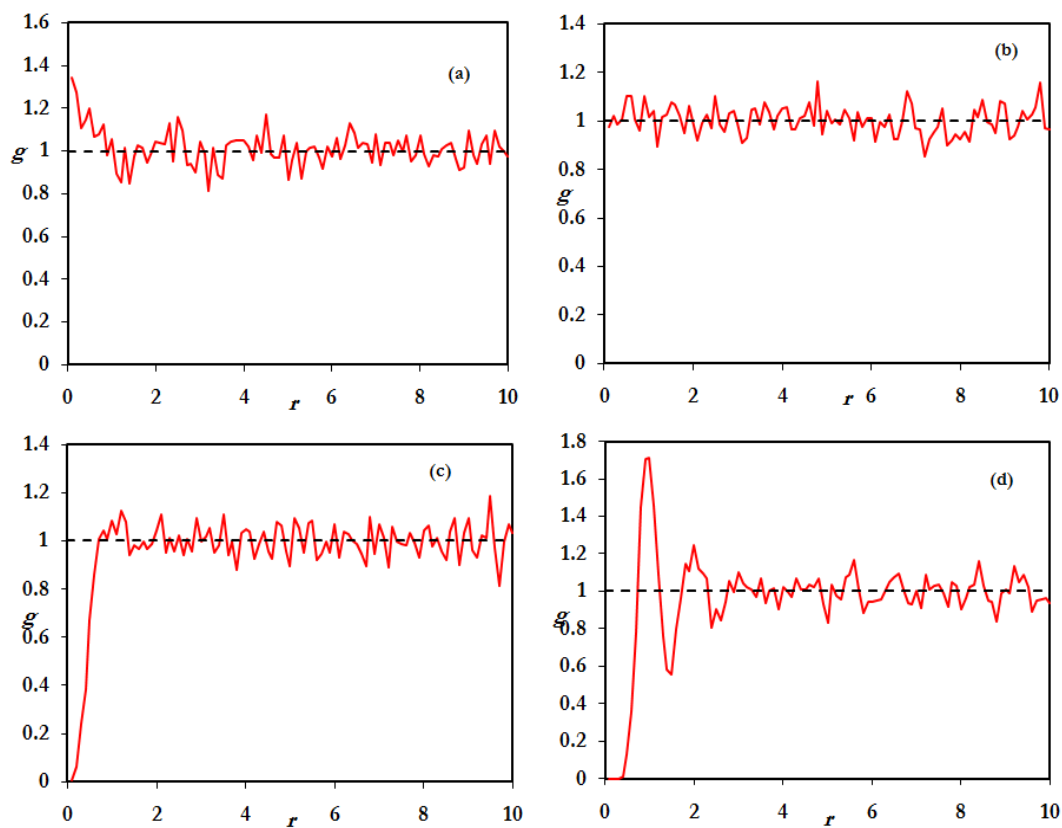


Figure 2.5. Pair distribution function for cells in the system for different values of the shaping parameter: a) $a=0.7$; b) $a=1$; c) $a=5$; d) $a=20$.

2.3.1.2 Burning Front Propagation

Propagation diagrams of discrete burning front, obtained by solution of Eq. (2) for different values of shaping parameter a and different ignition temperatures ε are shown in Figure 2.6. All lines in Figure 2.6 for single parameter a , but for different values ε correspond to the same realization of random structure of the system. Combustion occurs in form of

consequent jumps: relatively long periods of front stopping (induction periods) are followed by fast burning-out of some part of the sample with practically constant burning rate, and followed by a new induction period again. Duration of induction periods and periods of “continuous” combustion are random and it is connected with the random structure of the system [5-9]. In experiments [9], the change of mixture parameters and in concentrations of powder components (e.g. a changing in stoichiometric coefficient x in mixture $Ti + xSi$) results in either regularization or stochastization of combustion process. The former resulting from the fluctuations of duration of induction periods decrease and process becomes more stable, and the latter when combustion becomes more random one with long and random induction periods.

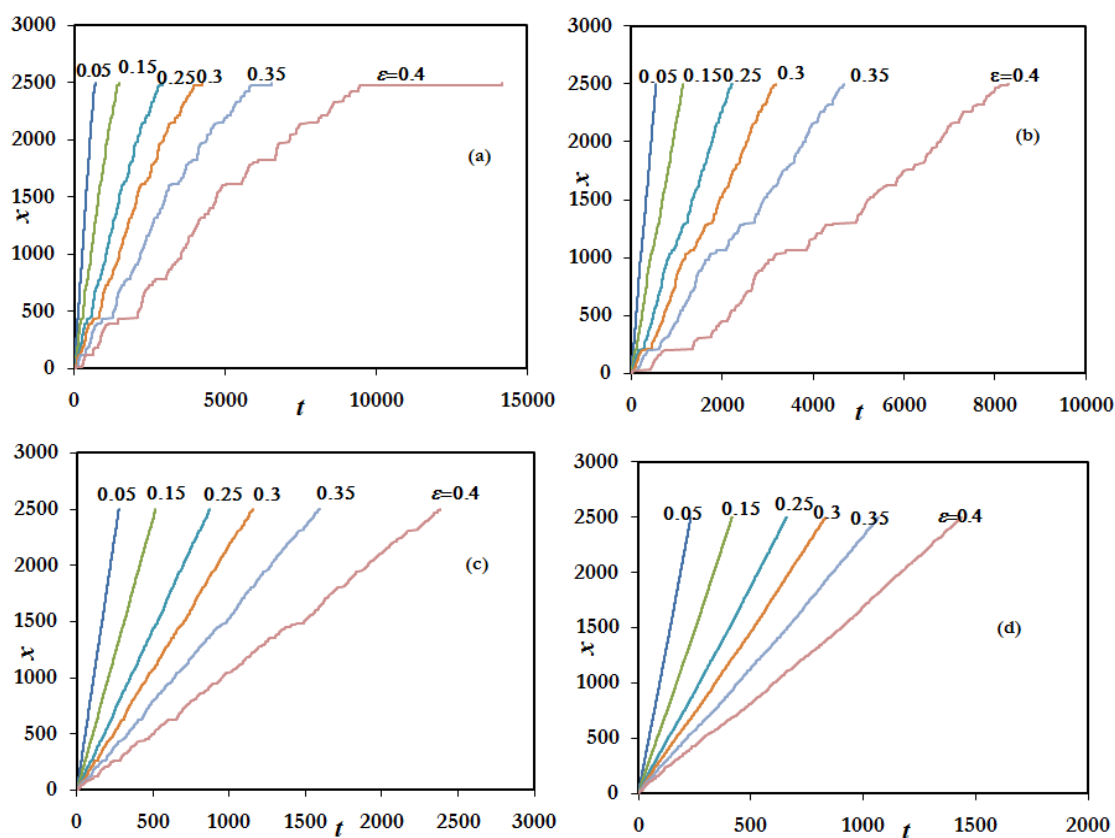


Figure 2.6. a) $a=0.7$; b) $a=1$; c) $a=5$; d) $a=15$. Propagation diagrams of discrete burning front for different ignition temperatures ε . The ignition temperatures are indicated over each line.

A similar behavior of burning front is observed in the model under consideration. It follows from figure 2.6 that a stability of combustion process decreases with a decrease in parameter a : the lesser the more pronounced a discrete and random nature of the process. For the same values of parameter a , the process is more regular at smaller ε ; the more ε the more random is the process, the stronger effect of fluctuation of random structure of the system on the

burning front propagation. Calculations show that for $\varepsilon > 0.45$ it is impossible to have a stable combustion process for any initial conditions: the system is extinguished after burning-out of some number of reaction cells. Theoretically, this appears as follows: due to system's random structure there are always neighboring pairs of reaction cells with extremely long distance between them. The induction period for these pairs is also extremely long. The ignition delay time increases with increase in non-dimensional ignition temperature ε for all pairs of reaction cells but more rapidly for pairs with long distances. This is clearly seen in figure 2.6 (especially in figure. 2.6 (a) and (b)). At $\varepsilon \sim 0.45$ the induction period for one of the pairs of hot-spots having a long distance becomes so much bigger that the temperature field in the system has enough time to level off due to thermal conductivity. As a result, the temperature of the next unburned hot-spot does not reach the ignition temperature and its ignition does not occur. This immediately results in stopping of combustion of the system as whole.

The theory of inflammability limits was developed by Zel'dovich [42] and Spalding [43] for steady propagation of flat premixed gas flames. According to this theory, an inflammability limit is a direct result of heat losses. Roughly speaking, propagation of combustion wave becomes impossible when the rate of heat losses into ambient environment grows faster than the rate of heat release from exothermic combustion reaction. Dilution of initial mixture with an inert compound as well as deviation from optimal (Stoichiometric) ratio decreases the heat release, therefore, an inflammability limit can be reached in this way. This approach does not look such evident in the case when heat losses from the sample surface are negligible compared to heat release inside the sample (e.g., in case of large samples). The classical theory suggests that, in the latter case, the inflammability limit is determined by radiative heat losses [44]. This cannot be directly applied to gasless mixtures because they are opaque and, therefore, radiation cannot escape from the inner regions of the sample. The model under consideration shows that inflammability limit can be reached due to changing of kinetic parameters of the system (e.g. the ignition temperature) even at absence of heat losses. The analysis of figure 2.6 shows that decrease in non-dimensional ignition temperature of hot-spots ε and increase in shaping parameter a results in regularization of combustion process. On the contrary, an increase in non-dimensional ignition temperature ε and decrease in shaping parameter a results in stochastization of combustion process with strong induction periods corresponding to the horizontal segments in figure 2.6. Because the combustion of the system under consideration represents the

sequence of ignition of discrete hot-spots, the burning rate is actually determined by the sum of ignition delay periods between neighboring hot-spots. Therefore it is of interest to analyze a correlation of the ignition delay time between neighboring hot-spots and distances between them. From the definition of non-dimensional steady-state burning rate for periodic system it can be written as

$$\tau = \omega_p^{-1} L^2 \quad (8)$$

where τ is the time interval between ignition of neighboring sources; L is the non-dimensional distance between neighboring sources; $\omega_p(\varepsilon)$ is the non-dimensional burning rate for periodic system with unit distances between neighboring sources [35,38]. Figure 2.7 shows the correlations between τ and L , obtained in calculations of combustion of disordered system with gamma-distribution eqn.(6) for different values of shaping parameters a and non-dimensional ignition temperature ε .

A treatment of the results of calculations (Figure 2.7) shows, that upper and lower boundaries of interval of tolerance can be described by expression

$$\tau = b^\pm(\varepsilon, a) L^m \quad (9)$$

where $m(\varepsilon, a)$ and $b^\pm(\varepsilon, a)$ are the parameters which depend on ε and a ; parameters $b^\pm(\varepsilon, a)$ characterize the upper and lower boundaries of interval of tolerance. As mentioned above, for $a \rightarrow \infty$ the system under consideration turns into a periodic system for which in accordance with Eq.(9) $m = 2$.

Correlation analysis of results of numerical calculations of Eq. (2) for system under consideration in wide-range of parameters $a \in [0.7...20]$ and $\varepsilon \leq 0.45$ results in following expression for the power $m(\varepsilon, a)$:

$$m = 2 + 0.2 \exp\left(3.18\varepsilon^{0.66} + (0.1 + 0.029 \ln \varepsilon)a - (0.0012 + 0.003\varepsilon)a^2\right) \quad (10)$$

having the correct limit $m \rightarrow 2$ as $a \rightarrow \infty$ and for $\varepsilon \rightarrow 0$.

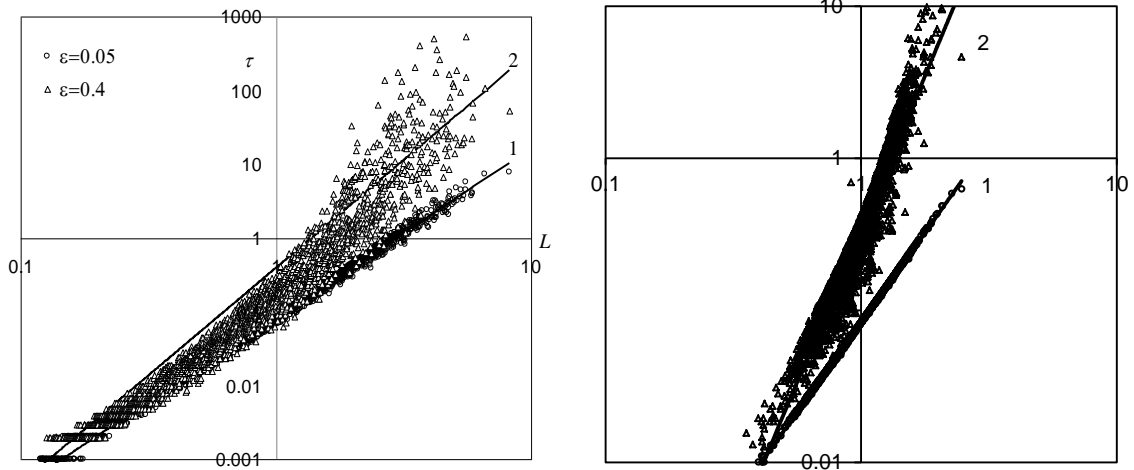


Figure 2.7. Correlation of time between ignition of neighbor heat sources and distance between them for $a=1$ (left) and $a=15$ (right). Dots are results of numerical solution of Eq. (3), solid lines are correlation Eqs. (12), (10) for $\varphi = 1$: line 1 - $\varepsilon = 0.05$, line 2 - $\varepsilon = 0.4$.

Note that in limiting range $a \in [0.7...20]$ one can use the more simple expression

$$m = 2.2 - 0.01a + 2.23a^{0.27} \varepsilon \quad (11)$$

which has the same degree of accuracy but has not the correct limit $m \rightarrow 2$ at $a \rightarrow \infty$ and $\varepsilon \rightarrow 0$. The calculations show (figure 2.7) that a line

$$\tau = \varphi \omega_p^{-1} L^m \quad (12)$$

can be used for fitting of correlation under consideration, where φ is the fitting parameter of order of unit.

2.3.1.3 Theoretical considerations

In this section a theoretical dependence for normalized burn rates is obtained for comparing numerical results. Correlation Eq. (12) allows finding a theoretical dependence of burning rate of the system under consideration on the parameters a and ε . Average burning rate of disordered system is calculated for the time intervals between ignition of neighboring sources and the distances between them are related by Eq.(12). Consider some time interval, during which some number of heat sources $N \gg 1$ are burned away. Duration of this time interval is

$$t_N = \sum_{i=1}^N \tau_i$$

Taking into account the Eq. (12), it is obtained as

$$t_N = \varphi \omega_p^{-1} \sum_{i=1}^N L_i^m$$

or

$$t_N = \varphi \omega_p^{-1} N \langle L^m \rangle \quad (13)$$

Where

$$\langle L^m \rangle = \frac{1}{N} \sum_{i=1}^N L_i^m$$

is the mean value of the parameter L^m . Because

$$\langle L^m \rangle = \int_0^{\infty} L^m P(L) dL$$

one can easily obtain while taking into account Eq. (6)

$$\langle L^m \rangle = \frac{\Gamma(a+m)}{a^m \Gamma(a)} \quad (14)$$

where

$$\Gamma(m+1) = \int_0^{\infty} z^m e^{-z} dz$$

is the gamma-function.

Mean burning rate of the system under consideration as a whole

$$\omega_r = \frac{N}{t_N}$$

or with taking into account Eq. (13)

$$\omega_r = \omega_p(\varepsilon) \frac{1}{\varphi \langle L^m \rangle}$$

Taking into account Eq. (14), it is obtained as

$$\omega_r / \omega_p = \frac{1}{\varphi} a^m \frac{\Gamma(a)}{\Gamma(a+m)} \quad (15)$$

In the limit $a \rightarrow \infty$ the system becomes periodic; this means that $\omega_r \rightarrow \omega_p(\varepsilon)$, moreover in accordance to Eqs. (8), (9) $m \rightarrow 2$ in this limit. Taking into account this result

$\lim_{a \rightarrow \infty} \frac{a^m \Gamma(a)}{\Gamma(a+m)} = 1$ is obtained; thus one concludes that $\varphi \rightarrow 1$ in this limit. Figure 2.8 shows

both the burning rates, obtained by direct numerical solution of Eq. (3) and the theoretical

dependencies, calculated by using Eqs.(10), (15) with $\varphi = 1$. It can be observed that theoretical dependence Eqs.(15) and (10) with $\varphi = 1$ correctly describes the results of direct numerical simulations in the whole range of parameters a and ε . For this reason, the dependence Eq. (12) with the condition $\varphi = 1$ will be used in further analysis of combustion process in the system under consideration. Equation (11) generalizes the results [38] on the case of arbitrary value of shaping parameter a . In particular,

$$\lim_{\varepsilon \rightarrow 0} \left\{ \omega_r(\varepsilon, a) / \omega_p(\varepsilon) \right\} = \frac{a}{a+1} \quad (16)$$

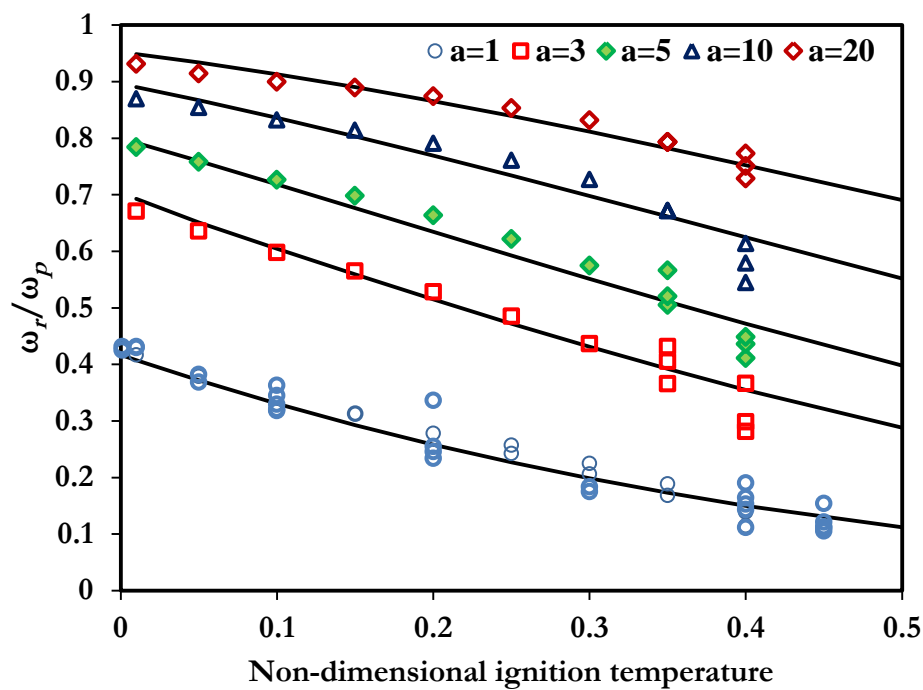


Figure 2.8. Dependence of burning rate on ignition temperature ε for different values of shaping parameter a . Markers are the results of direct numerical solution of Eq. (3); lines are the theoretical expression Eqs. (15), (10) with $\varphi = 1$.

Thus, the burning rate of a disordered system is always less than a burning rate of the periodic system with the same adiabatic burning temperature and the same ignition temperature T_{ign} . The mathematical models with periodic structures are used very often for simulation of the real heterogeneous systems [8,34,35]; in doing so, the periodic models have the same average characteristics as those for the real systems. It is usually assumed that mean burning rate obtained in simulations of such periodic model should be equal to a mean burning rate of real disordered system. The results above show that this is not the case: a real

system (e.g. aerosol, SHS-system, composite solid propellant etc.), which has a disordered structure, cannot be substituted by a periodic system in simulations because their burning rate can differ by many times.

2.3.1.4 Self-similarity in burning front propagation

Analysis of the dependences of ignition time of hot-spots on their coordinates $t(x)$ for the same random realization of the system structure but for different ε (figure 2.6) shows that they share a number of traits with each other. It is seen from figure 2.6, that the same features of function $t(x)$ present on dependences $t(x)$ for all ε : at the same points x on all curves there are the similar heterogeneity; they differ by only a scale, which increases with ε . Thus, dependences $t(x)$, corresponding to different ε , reproduce the same features of combustion wave propagation, reflecting the peculiarities in internal structure of the system. The scale of these peculiarities on the curves $t(x)$ is different for different ε : the less the ε the less manifestation of the system structure in the process of propagation of combustion wave and on the contrary, the more the ε the stronger manifestation of peculiarities of the system structure in combustion. This is a result of non-linearity of the system which amplifies the fluctuations of combustion process induced by random structure of the system. For analysis of these features, the dependencies $t(x)$ were processed in coordinates

$$\eta(x_i) = \frac{1}{A} (t(x_i) - (x_i + x_0) / \omega_r)$$

where ω_r is the burning rate of the system at given (ε, a) ; parameters $A(\varepsilon)$ and $x_0(\varepsilon)$ were selected to give the best match of dependences $\eta(x)$ at all ε for given structure of the system. The results of such calculations for $a = 1$ are shown in figure 2.9. Similar dependences $\eta(x)$ take place also for other values of parameter a . It can be seen that in the whole range of ε almost identical dependence $\eta(x)$ are obtained, differences exist only in fine details. Deviation from unified dependence in the initial period is connected, apparently, with the transient process, however, one can see even in this period all the dependencies $\eta(x)$ have the same features and repeat each other. Thus, one can say that propagation of combustion front over a given system of hot-spots is described by unified dependence for all ε :

$$t(x_i) = (x_i + x_0) / \omega_r + A \eta(x_i) \quad (17)$$

reproducing all main features in behavior of combustion front; in doing so the function $\eta(x)$ does not depend on ε and it is determined only by the system structure, i.e. by distribution of reaction cells in the system

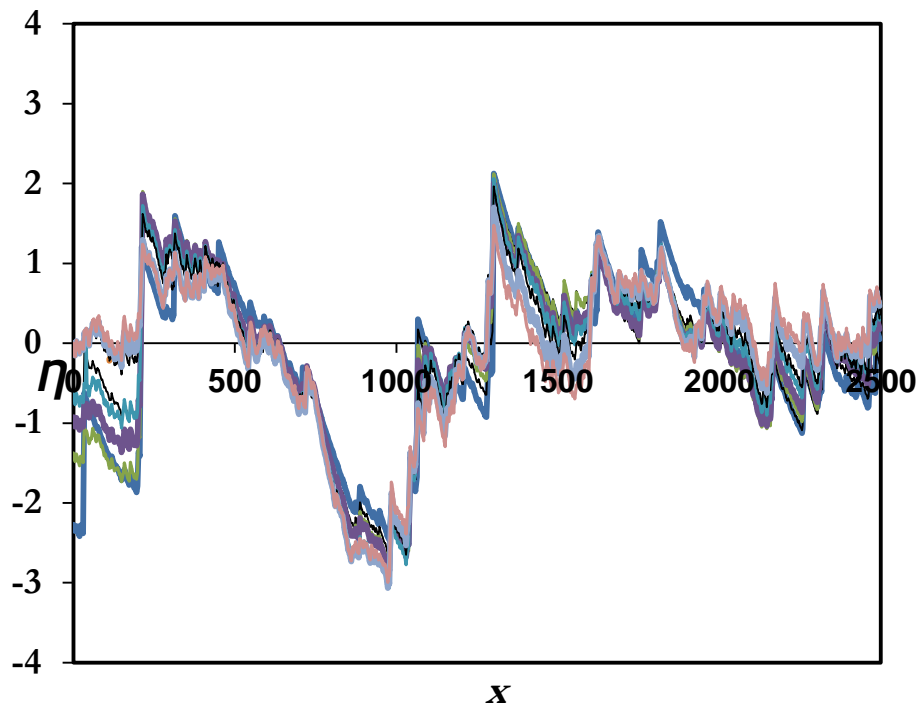


Figure 2.9. Dependencies $\eta(x)$ for $\alpha = 1$ and $\varepsilon = 0.05 \dots 0.4$ with step 0.05.

. This means that function $\eta(x)$ is different for different random realizations of the system structure. This allows one to say that propagation of combustion front in one-dimensional system with random distribution of hot-spots is self-similar and function $\eta(x)$ is some structure function which characterizes mainly the structure of the system and weakly depending on its kinetic characteristics, in particular on ε . This means that function $\eta(x)$ will be the same both at relatively big values of ε and at $\varepsilon \ll 1$.

2.3.1.5 Standard deviation of burning time

Experimental data on combustion of powder mixtures [5-9] show that process of propagation of discrete combustion wave in actual systems is random and it is accompanied with essential fluctuations of both instantaneous and local parameters of combustion wave and burning rate of the system as a whole. The results of modeling confirm these facts (Figure 2.6 and 2.7). Fluctuations observed in calculations are connected with both random structure of the system and non-linearity of the system as a whole: the non-linearity of the

system in combination with its random structure at certain conditions can amplify a non-uniformity of combustion process up to its total termination. These results in dependence of the parameters of combustion wave (primarily the burning rate of the system) on specific realization of random structure of the system and have the essential fluctuation from experiment to experiment. The fluctuation of burning rate of the system is estimated as a whole. Consider the burning time of the system, consisting of N reaction cells

$$t_N = \sum_{i=1}^N \tau_i$$

The ignition delay times τ_i depend on location of hot-spots in the system and for system under consideration they are the random. The discrete random process L_i , $i = \dots, 1, 2, 3, \dots$, by definition, is markovian one. Standard deviation of the system's burning time is calculated based on the assumption that discrete random process τ_i is also markovian, that is, the ignition delay times τ_i relating to different hot-spots are the statistically independent random quantities. In this case the burning time of the system consisting of N hot-spots has the mean value

$$\langle t_N \rangle = N \langle \tau \rangle \quad (18)$$

and standard deviation

$$\sigma_t = \sqrt{\langle t_N^2 \rangle - \langle t_N \rangle^2} = \sqrt{N} \sqrt{\langle \tau^2 \rangle - \langle \tau \rangle^2} \quad (19)$$

The relative standard deviation of the system's burning time together with Eq. (18) is

$$\frac{\sigma_t}{\langle t_N \rangle} = \frac{1}{\sqrt{N}} \sqrt{\frac{\langle \tau^2 \rangle}{\langle \tau \rangle^2} - 1} \quad (20)$$

Using the correlation Eq. (12) with $\varphi = 1$, it can be written as

$$\langle \tau \rangle = \omega_p^{-1} \langle L^m \rangle, \quad \langle \tau^2 \rangle = \omega_p^{-2} \langle L^{2m} \rangle \quad (21)$$

where $\langle L^m \rangle$ is determined by the expression Eq. (14) for any m . Using Eqs. (21) and (14), for relative standard deviation of the system's burning time one obtains the expression

$$\frac{\sigma_t}{\langle t_N \rangle} = \frac{1}{\sqrt{N}} \sqrt{\frac{\Gamma(a)\Gamma(a+2m)}{\Gamma^2(a+m)} - 1} \quad (22)$$

where the parameter m is determined by the correlation Eq. (10). Figure 2.10 shows the calculated dependencies of relative standard deviation on the number of hot-spots in the

system for different values of ignition temperature ε for $a=1$ and $a=15$. The markers in figure 2.10 indicate the results of direct calculations using the dependences $x(t)$ obtained by solution of the Eq. (2). In the latter case, the time of burn-out of different segments with N hot-spots for the same sample were analyzed. These segments were considered as separate samples (different realizations of the random structure), consisting of N hot-spots. Such an analysis was carried out for different random realizations of the system for the same value of parameter a , in so doing the parameter a was varied in the range $[0.7 \dots 20]$.

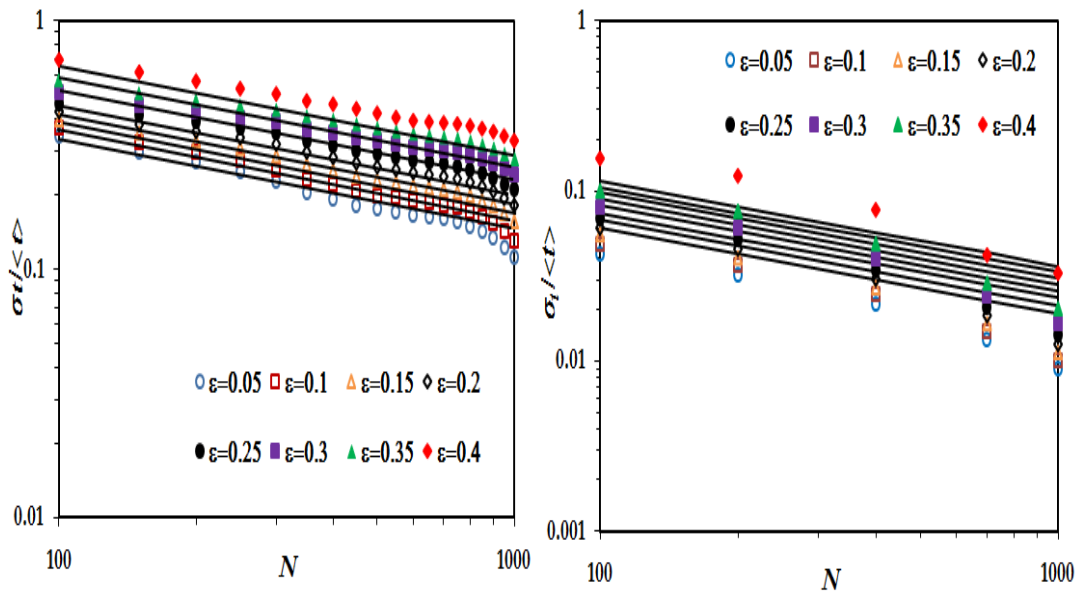


Figure 2.10. Dependence of relative standard deviation of burning time on number of particles for different ignition temperatures ε . $a=1$ (top), $a=15$ (bottom). Markers are direct calculations; lines are theoretical dependence (22).

As a consequence of this analysis, the mean value and standard deviation of the burning time were determined. The relative standard deviation of burning rate approximately equals to relative standard deviation of burning time for the same sample. Dependence of fluctuations of burning time on number of hot-spots in the system Eq. (22) is the standard one for Markov random processes [45].

2.3.2 Normal Distribution

Normal distribution also offers several advantages - its fixed shape and positioning adjacent cells with controlled deviation from mean, around 65 percentage of adjacent reaction cells are positioned within one standard deviation, also describes the microstructure of heterogeneous mixtures. The flexibility of using normal distribution is due to fact that curve may be centered over any number of real lines and it may be flat or peaked to

correspond to amount of dispersion in the values of random variable. The variance of normal distribution corresponds to concentration of point source particles of system when compared to that of periodic system. Different cases of normal distributed systems characterized with different standard deviations are considered for modeling and simulation. The combustion stops are more prominent for higher values of variance and higher ignition temperatures. The induction periods for higher ignition temperatures and higher variance of adjacent reaction cells increases. Burn rates of the systems with normal distribution of adjacent cells are obtained using Eq. (2) and are normalized to burn rates of a periodic system for different ignition temperatures as shown in figure 2.11. By changing the parameters of a distribution, the inter cell spacing can be altered, which is reflected in the probability density function. However, for normal distribution, the burn rates can be varied by changing the parameter (σ). Symbols in figure 2.11 shows the normalized reaction burn rates calculated for different normal distributions. This detail provides us the possibility of tailoring burn rates of a system by suitable normal distribution. The normalized burn rates of a normal distribution are in the wide range (0.3-1). It can be seen that ratio =1 resembles to a periodic system and 0.3 is closer to a high degree of disordered system. As variance of system increases the concentration of sample density decreases and its reaction front propagation corresponds to relay race homogeneous mechanism where as the reaction front propagation for the system with low variance correspond to quasi homogeneous mechanism. Numerical simulations suggest that apart from gamma distribution of reaction cells the normal distribution of reaction cells can also achieve wide ranges of the combustion of actual heterogeneous systems. This shall be made evident by comparing the developed model with available experimental data.

2.3.2.1 Theoretical Analysis for Burn Rates

The present section illustrates the theoretical analysis for dependence of burn rates of a random system, normalized to burn rates of periodic system, on variance of the distribution of neighboring reaction cells. Thus obtained theoretical expression is also compared with numerical results. Burn rates of combustible system (developed model) under consideration are determined by sequential calculation of ignition times of reaction cells.

The correlations (m), between τ and L , are obtained for a disordered system, described by a normal-distribution of neighboring reaction cells (L), as a functional dependence on variance

(σ^2) of distribution of neighboring reaction cells(L) and ignition temperature (ε). As $\sigma^2 \rightarrow 0$ the disordered system described by normal distribution of neighboring reaction cells (L) is similar to periodic system. Correlation analysis is performed on numerical calculations of Eq. (2) for a disordered system over a broad range of parameters $\sigma^2 \in [0.4 \dots 0.05]$ and $\varepsilon \leq 0.48$. The correlation factor (m) thus obtained in terms of power functional dependence of $m(\varepsilon, \sigma^2)$ is as follows:

$$m = 2 + 0.2 \exp\left(3.18\varepsilon^{0.66} + (0.1 + 0.029 \ln \varepsilon)\sigma^2 - (0.0012 + 0.003\varepsilon)\sigma^4\right) \quad (23)$$

As $\sigma^2 \rightarrow 0$ for a disordered system the correlation limit $m \rightarrow 2$ at $\varepsilon \rightarrow 0$. The limiting range considered for normal distribution of neighboring reaction cells (L) is $\sigma^2 \in [0 \dots 0.4 \dots 0.05]$ hence the Eqn.(23) can be further modified to straightforward expression as

$$m = 2.2 - 0.01(1/\sigma^2) + 2.23(1/\sigma^2)^{0.27} \varepsilon \quad (24)$$

The expectation value for L^m with L described by normal distribution in accordance with periodic system Eqn.(12) is given as.

$$\langle L^m \rangle = \int_0^{\infty} L^m P(L) dL$$

The above equation converges for m being integer and the solution obtained is given below as:

$$\omega_r/\omega_p = \frac{1}{\varphi} (1/\sigma^2)^m \frac{\Gamma(1/\sigma^2)}{\Gamma((1/\sigma^2) + m)} \quad (25)$$

In the limit $\sigma^2 \rightarrow 0$ the system becomes periodic; this shows that $\omega_r \rightarrow \omega_p(\varepsilon)$, in accordance to Eqs. (12) $m \rightarrow 2$ in this limit. Subsequently we obtain

$$\lim_{\sigma^2 \rightarrow 0} \frac{(1/\sigma^2)^m \Gamma((1/\sigma^2))}{\Gamma((1/\sigma^2) + m)} = 1; \text{ thus one can conclude that } \varphi \rightarrow 1 \text{ for this limit. Figure 2.11}$$

shows the comparison of burn rates, obtained by direct numerical solution of Eq. (2) , (3) ,represented by markers, and the theoretical dependency, calculated by using Eqs.(24), (25)

,represented by solid lines, with $\varphi = 1$. It is evident that the theoretical dependence Eqs.(24) and (25) with $\varphi = 1$ properly explains the results calculated by numerical simulations using Eq.(2) and (3) for the whole range of parameters σ . Generalized expression for the theoretical dependence of normalized burn rates on variance is obtained and now can be used for direct calculation of burn rate if σ is known.

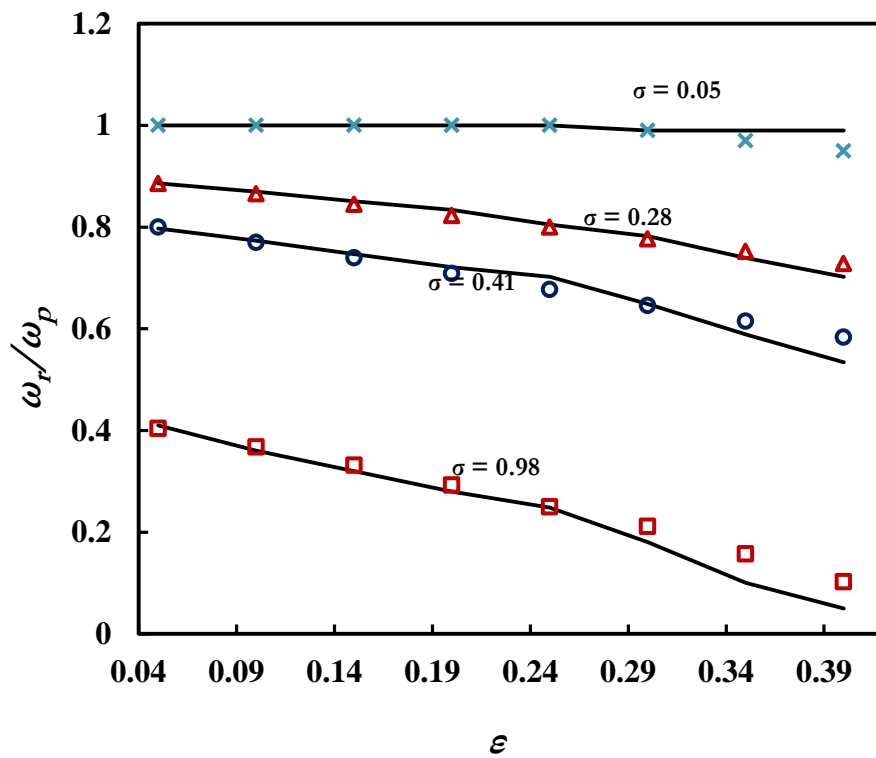


Figure 2.11. Comparison plot for normalized burn rate and non dimensional ignition temperature ε for different values of σ . Markers are the calculated results of Eq. (1),(2); lines are obtained by the theoretical expression Eqs. (24), (25) with $\varphi = 1$.

2.3.3 Comparison With Experimental Data

2.3.3.1 Ti-Si system

Here correlation for the shaping parameter (a (gamma distribution)) and standard deviation (σ (normal distribution)) in the view of one dimensional model, with the stoichiometric coefficient of actual heterogeneous mixtures is obtained. The work [9] for combustion of Ti-Si system is considered, for comparison in the view of developed model, since the amount of gas released is relatively small. The combustion process of Ti-Si mixture is represented as Ti

$+x\text{Si}$, where x is referred as stoichiometric coefficient. The plot for measured mean burn rate r and stoichiometric coefficient x is shown in Figure 2.3 from work [9], along with measured adiabatic temperature T_B . It is investigated that heterogeneous combustion of $\text{Ti} + x\text{Si}$ mixtures occurs in range of $x=[0.3, 1.5]$ as shown in work[9]. Burning rate, changes with change in stoichiometric coefficient. The maximum burning rate (38 mm/s) of mixture coincides at highest value of burn temperature T_B . Burn rate is maximum at $x=0.6$ which corresponds to synthesis $5\text{Ti}+3\text{Si}\rightarrow\text{Si}_3\text{Ti}_5$. Behavior of burn rate in range of $x=[1, 1.4]$ essentially varies by previous trend: rate of burning decreases in the specified range even for the constant burning temperature. Such situation commonly arises in combustion process of heterogeneous mixtures of $\text{Ti}+x\text{Si}$, where combustion process is associated with phase transformations and complex micro structural properties. Currently no such alternate heterogeneous combustion models exist, for quantitative description of change in burn rate of thermite mixtures at constant burn temperature. Developed model, in view of gamma and normal distribution of neighboring reaction cells, has an additional scale of choice for tailoring neighboring reaction cells with variation of shaping and standard deviation parameters respectively. Change of shaping parameter or standard deviation parameter, for describing microstructure of system, results in change of burn rate, even at constant non-dimensional ignition temperature \mathcal{E} . Such a model explains change of burn rate for combustion of $\text{Ti}+x\text{Si}$ mixtures in the range of $x=[1, 1.4]$ where its burning temperature is constant as shown in figure 2.3 from work [9]. From developed model, it is observed that the burning rate decreases with change in shaping, standard deviation parameter. It is sufficient to presume that shaping or standard deviation parameter depends on stoichiometry coefficient x .

According to the developed model, the dimensionless burning rate depends on the dimensionless ignition temperature of reaction cells and the structure of the mixture, which is described by the shaping parameter a . Thus, the shaping parameter a is an additional "degree of freedom" for the burning rate of heterogeneous systems: a change of the shaping parameter can result in changing in the burning rate, even at a constant non-dimensional ignition temperature \mathcal{E} . This allows explaining a change of burning rate of heterogeneous mixtures $\text{Ti}+x\text{Si}$ in the range $x=[1, 1.4]$ where its adiabatic temperature is constant. It is enough to assume that the shaping parameter a depends on the stoichiometry x . Calculations of the burning rate of the mixture $\text{Ti}+x\text{Si}$ were carried out by using dependencies

$$r = r_0 \omega_r(\varepsilon, a) \quad (26)$$

$$\varepsilon = \varepsilon_{cr} \frac{T_{ad(cr)} - T_{in}}{T_B - T_{in}} \quad (27)$$

where T_{ign} , r_0 are the constants; $\omega_r(\varepsilon, a)$ was calculated according to Eqs. (10), (15) with $\varphi = 1$; $\omega_p(\varepsilon)$ was calculated according obtained in [35] for periodic system; $T_B(x)$ was determined by using data [9] (Figure 2.12); $T_{in} = 300$ K. As described above, in the developed model it is impossible to organize a stable combustion process at $\varepsilon > 0.45$ under any initial conditions for the whole range of parameter a . This should be seen as a natural inflammability limit for the combustion model under consideration. In the experiments [9], the inflammability limits $x = 0.3$ and $x = 1.5$ were obtained for heterogeneous mixtures $Ti+xSi$. The developed model allows explaining these inflammability limits, assuming, that $\varepsilon > 0.45$ outside the range $x \in [0.3, 1.5]$. Thus, numerical calculations were assumed that $\varepsilon = 0.45$ on the both inflammability limits, obtained in the experiments; this allowed determined the value of $T_{ign} = 950$ K.

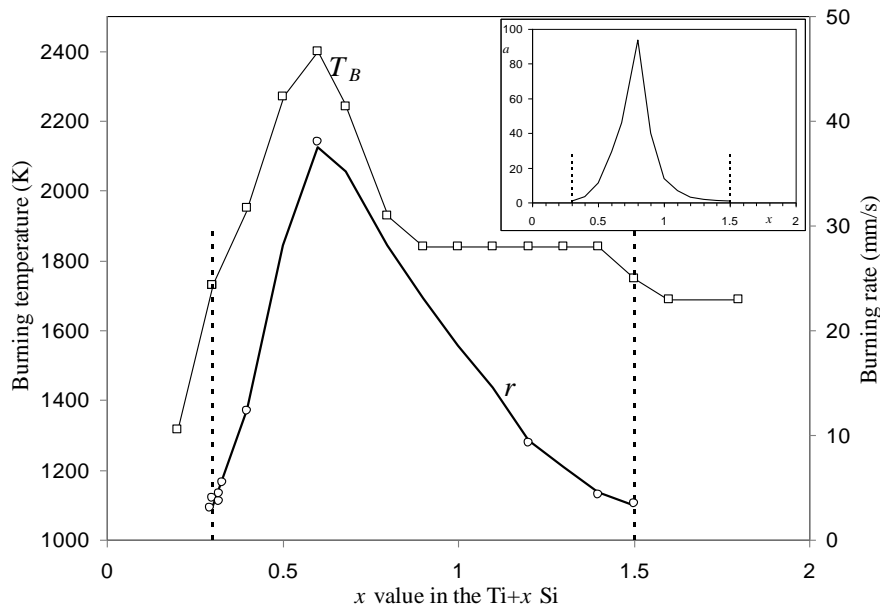


Figure 2.12. Burning temperature T_B (squares: scale in K, on the left) and burning rate r (bullets: scale in mm/s, on the right) as a function of the stoichiometry x of the initial sample. Markers are data of [9], solid line $r(x)$ is the theoretical dependence (26), (27) for gamma distribution. Inserting shows the dependence of shaping parameter a on the stoichiometry x used in calculation; dashed lines are the combustion limits.

Dependence of the shaping parameter on the stoichiometry x , $a(x)$, was matched to obtain the best fit with experimental data on burning rate. For definiteness, it is assumed that $a = 1$

at the inflammability limits. Matched dependence $a(x)$ is shown in the inset of figure 2.12. Calculated dependence of the burning rate on the stoichiometry x for $\text{Ti}+x\text{Si}$ is also shown in figure 2.12 by solid line. Note in calculations $r_0 = 12 \text{ mm / s}$. Thus, the variations in shaping parameter a can completely describe the dependence of the burning rate on the stoichiometry x at constant burning temperature. Analysis of dependence $a(x)$ (Figure 2.12) shows that the shaping parameter a reaches a maximum value $a \approx 94$ at $x = 0.8$. As shown above, the more $a \gg 1$ the more ordered is the system: as $a \rightarrow \infty$ the system tends to be periodic. Obtained dependence $a(x)$ shows that the $\text{Ti}+x\text{Si}$ mixture becomes more ordered at $x \rightarrow 0.8$, while, by contrast, the mixture becomes disordered if it moves away from $x = 0.8$. Such a behavior of structure of the mixture can be connected with peculiarities of packing of Ti and Si particles in the volume of the mixture during the mixing process at different concentrations of the components.

As described in earlier section, in the view of developed model for combustion process it is not possible to systematize a stable combustion process for $\varepsilon > 0.45$ under several primary circumstances in the entire range of standard deviation parameter. $\varepsilon = 0.48$ is interpreted as natural combustion limit for developed combustion model. Equivalent of 1840 k is obtained, in non dimensional ignition temperature by Eqn. (27), as $\varepsilon = 0.44$. The experimental burn rates at different stoichiometric mixtures for constant burning temperature are treated by

$$\omega/\omega_{cr} = (x/x_{cr})(l_0/l_{0cr})$$

Figure 2.13(a) shows for Burn rate v/s stoichiometric coefficient and Burn rate v/s standard deviation σ shows the correlated values of stoichiometric coefficient and standard deviation. The solid line shows the numerical burn rates for different standard deviation parameter at $\varepsilon=0.44$ ($\sim 1840 k$). Symbols represent experimental data. Matched dependence of stoichiometric coefficient x and standard deviation σ for common value of burn rate is obtained. Now the dependence of standard deviation $\sigma(x)$ on stoichiometry coefficient x , is obtained by performing best fit on experimental data of burn rate. Similar to analysis performed for certainty, it is assumed $\sigma=1$ for the lower combustion limits. Matched dependence $\sigma(x)$ is shown in the figure 2.13(b). Thus, variations in standard deviation of neighboring reaction cells completely correlate dependence of burn rate on stoichiometry coefficient x even at constant burning temperatures.

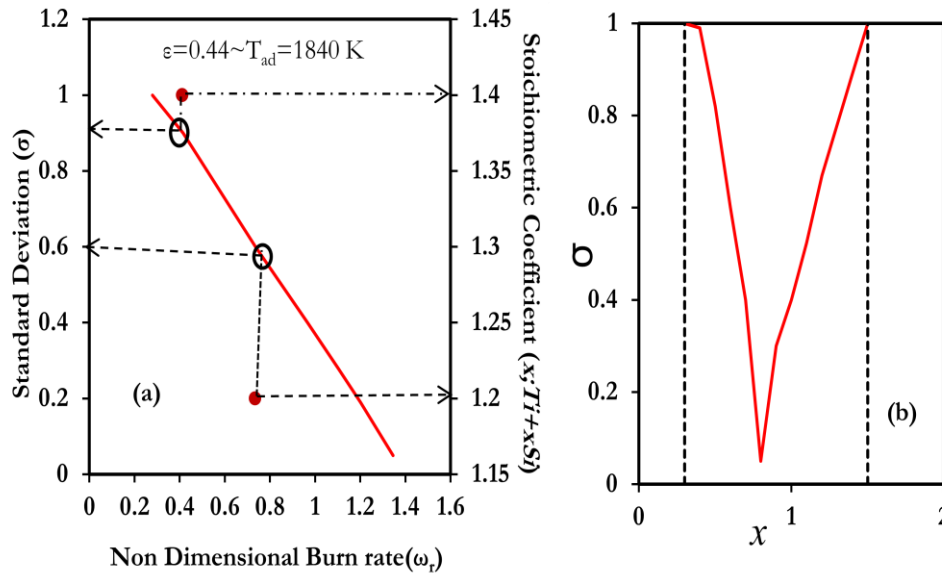


Figure 2.13. (a) Left shows comparison of experimental and theoretical non dimensional burn rates on stoichiometry x [9] and parameter σ . (b) Shows the dependence of shaping parameter σ on the stoichiometry x used in calculation; dashed lines are the combustion limits.

It is evident from figure 2.13(b), analysis for the dependence of $\sigma(x)$, that the standard deviation parameter σ reaches a minimum value $\sigma \approx 0.01$ at $x = 0.6$. As shown above, the less $\sigma \ll 1$ the more ordered is the system. Obtained dependence $\sigma(x)$ (Figure 2.13) shows that the Ti+ x Si mixture becomes more disordered as it moves away from $x = 0.6$. Such an effect of microstructure of the system on combustion process is associated with binding of Ti and Si particles, mixing at different concentrations, over the combustor volume.

2.3.3.2 Relay-race mode vs. quasi-homogeneous mode

For a long time there is a discussion in the literature [1-9,28], on what is the mode in which combustion of disperse (powder) systems, in particular the gasless combustion, occurs: in a quasi-homogeneous mode or in a microheterogeneous (relay-race) mode. This question is of fundamental importance for the simulation of combustion of such systems, because the well-mastered and widely-used quasi-homogeneous combustion model [48,49], which historically goes back to the founders of the combustion theory (Zeldovich, Frank-Kamenetsky, Schwab et al), are based on the assumption about smooth and continuous distribution of temperature and other parameters in the combustion wave, and they need a justification as applied to combustion of microheterogeneous systems. It is easy to introduce a criterion of "homogeneity" of the combustion wave as applied to disperse systems. Let the

characteristic thickness of the thermal layer in the combustion wave be λ . According to the combustion theory of homogeneous systems [40,44], this thickness is connected with burning rate r by expression

$$\lambda = \frac{\kappa}{r} \quad (28)$$

Obviously, the combustion wave in the powder system can be considered as a quasi-homogeneous one, if the condition

$$\lambda \gg d \quad (29)$$

is satisfied or

$$\lambda \gg l_0 \quad (30)$$

where d is the characteristic size of the particles. Criterion Eq. (29) is applicable to the combustion models that take into account the finite size of the particles. In the developed model of point hot-spots one should use the criterion Eq. (30), which with taking into account Eq. (28) takes the form

$$\frac{rl_0}{\kappa} \ll 1 \quad (31)$$

or, by the definition of the non-dimensional burning rate ω :

$$\omega \ll 1 \quad (32)$$

Thus, only if the non-dimensional burning rate is much less than unity, one can consider that the combustion of microheterogeneous system occurs in a quasi-homogeneous mode. In practice, one can speak about quasi-homogeneous mode when at least the condition $\omega < 0.1$ is satisfied. According to the theory under consideration, the less shaping parameter a or more the standard deviation parameter the less burning rate at the same non-dimensional ignition temperature ε .

The commencement of relay-race mechanism and combustion limit is now understood in terms of combustion front propagation. The mechanism for propagation of combustion front is of fundamental importance, now after successful demonstration of correlation between stoichiometry x and standard deviation parameter of developed model, is analyzed with the role of internal microstructure. The developed model explains these combustible limits in the view of ignition time profiles (in the range [0.42, 0.48]), assuming, that $\varepsilon > 0.48$ is not in the range of $x=[0.3,1.5]$. Thus, numerical calculations assumed that $\varepsilon = 0.48$ for both lower combustible limits and this determined value of $T_{ign} = 990$ K. The existence of ignition temperature for heterogeneous systems of particles in suspension

introduces a limit to reaction front propagation, even in the absence of losses and with uniform heat release. The instant at which the heat release of the active cell is just adequate to increase the temperature of the mixture to the pre determined ignition temperature is defined as combustion limit. While performing numerical calculations it is observed that, as time is incremented the temperature of active cell reaches critical temperature which is still lower than the pre determined ignition temperature.

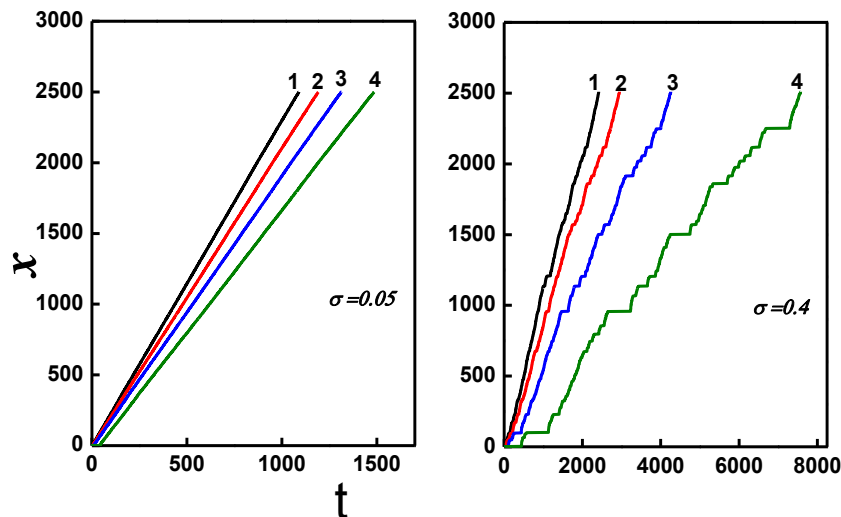


Figure 2.14 Higher Ignition time profile for different Normal distributions. 1=0.42(ϵ), 2=0.44(ϵ), 3=0.46(ϵ), 4=0.48(ϵ).

This instant is determined as numerical combustion limit of developed model. The numerical combustion limit for a periodic system is 0.5459, however for disordered system the combustion limit still further reduces and is observed to be 0.48. The reaction front cannot propagate through the system above the Combustion limit. Figure 2.14 shows the ignition time profiles of different normal disordered systems ($\sigma=0.05$ and $\sigma=0.4$) for higher ignition temperatures ranging from 0.42 -0.48. The periodic system and disordered system with $\sigma=0.05$ has similar characteristics for lower values of ignition temperature <0.42 , however as ignition temperature increases the microstructure of system plays a dominant role in deciding the combustion limit at higher values of ignition temperature.

The reaction front propagated smoothly in a quasi-homogeneous regime when the combined thickness of the two point source particles was much smaller than the reaction front. When the reaction front width was of the order of a inter particle distance, the reaction front

exhibited a relay-race behavior characterized by a region of concentrated heat within the reactive layers.

2.3.3.3 CMDB Propellants

In this section the experimental data for CMDB class of propellants [10] is compared with the model developed. Earlier section establishes that the normal or gamma distributed adjacent cells in combustible systems, have additional degree of freedom and can explain combustion process for wide ranges of heterogeneous mixtures. Systems modeled with normal or gamma distribution of neighboring reaction cells are compared with experimental data [10] to establish accurate model and also account the affects for dynamical combustion properties. During experiments, the samples are comprised of selected components such as DNC (Dinitrocarbanilide) and CL mixed in exact ratio with a binding agent AP(Amonium perchlorate) or without binding agent. When ignited, the propellant burns and generates high temperature and exhaust products that escape at extreme speeds to provide thrust. The burning temperatures and burning rate of such propellants can change over broad range either by adding binding agent (AP) or by changing the compositions of components; the mechanism of heat release during combustion process of such propellant is not altered. In such system, the groups of active cells play the role of reaction cells, while the initial components are capable of reacting chemically. T_{ign} is melting point at which the cells commence reacting. The values of burning temperature and burning rate of CMDB propellants with binding agent or without binding agent are collected from the work [10]. Ignoring the heat losses, calculated burning temperature of propellant mixtures are recognized as adiabatic temperature (T_{ad}) with reference to developed system. Figure 2.15(a) includes the data from the work [10], with burn rate and burning temperature on the axis, for two propellants. The burn rate for CMDB propellants varies with percentage of components and also by adding binding agents. The first propellant comprises of 60% of DNC and 40% of CL without the binding agent and other propellant comprises of 50% of DNC and 40% of CL with AP as binding agent. It is observed that burn rate decreases with addition of binding agent, particularly at 690k.

The treatment for experimental results, as shown in [10], is performed in the coordinates of $\varepsilon-\omega$. In doing so it is considered that critical temperature, noticed in experiments, correspond to the critical values of the theoretical parameters such as ε_{cr} and ω_{cr} . In the view of developed model the critical ignition temperature is established at 0.48; these

parameters are considered as critical parameters for the disordered system. Assuming that minimum burn rate and burning temperatures, determined in the experiments, correspond to the critical regime of combustion for real system. The value $\omega_{cr}=5$ and $\omega_{cr}=5.6$ respectively were used for the mixtures DNC+CL and DNC+CL+AP in these calculations.

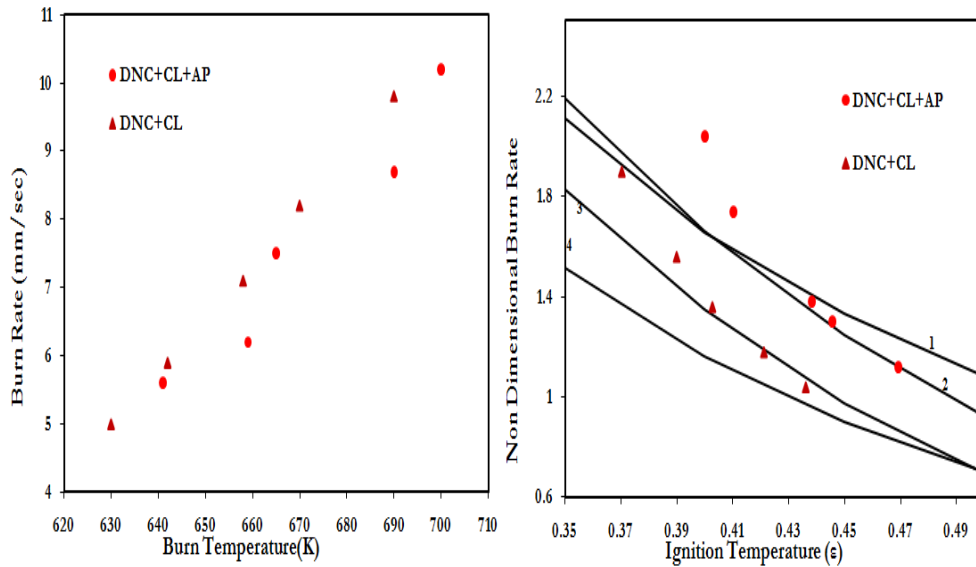


Figure 2.15.(a) Plot for burning rate versus burn temperature for CMDB propellants with and without binding agent, based on data of work [10]. (b) Comparison plot for experimental and theoretical dependencies $\omega(\varepsilon)$. Symbols are treated experimental data [10]; solid lines 1-4 are the theoretical dependence, lines 2&3 represents normal distributed system: 2) $\sigma=0.2886$: 3) $\sigma =0.408$; lines 1&4 represents gamma distributed system:1) $a =12$; 4) $a =6$.

It is enough to assume that the change of burning rate with change in burning temperature for combustion of propellants is associated with change of parameters either σ in case of normal distribution or a for gamma distribution which describes system internal microstructure considering uniform identical reactant consumption. The data [10] is now processed in variables $\varepsilon - \omega$. The numerical results calculated for appropriate parameters of σ, a at different ignition temperatures ε , is now superimposed in figure 2.15(b). Solid lines 1-4 are the theoretical dependences $\omega(\varepsilon)$, calculated by using expressions Eqs. (24), (25) taking into account the matched dependence $\sigma(\varepsilon)$. Line 1 and 4 is obtained by utilizing the gamma distribution (eqn.(10) and (15)) of neighboring reaction cells with parameter $a=12$ and $a=6$ respectively. Line 2 and 3 is obtained by utilizing the normal distribution of neighboring reaction cells with parameter $\sigma=0.2886$ and 0.408 respectively.

Combustion of CMDB propellants releases high amount of energy, which propagates throughout the system, even at low burning temperatures. Thermal reaction below 670k are like streak of lightening and are complex to analyze. However for the burning temperatures above 670k the developed model (Line 2 and 3) show close agreement when compared to that of with Line 1 and 4. The minute aspect of controlling internal micro structure, by normal distribution, allowed for accurate explanation of data [10]. The data [10], processed in variables $\varepsilon - \omega$ in Figure 2.15(b), shows that burn rates for CMDB propellants changes with ignition temperature either by addition or absence of binding agent (AP). This binding agent corresponds to standard deviation parameter, of developed model, employed for describing system's internal microstructure; this is evident from figure 2.15(b). Now it is apparent that present model developed with normal distribution of neighboring reaction cells is accurate for describing the combustion process of heterogeneous mixtures.

2.3.3.4 Thermite systems

The present section illustrates the comparison of experimental data for combustion of thermite systems with theoretical model developed in earlier section. In due process the effect of distribution of heat release on combustion limit of thermite mixtures is established. The work of authors [47] investigate that the burning rate changes with burning temperature for a broad range by altering the inert diluter and percentage of inert diluter; in doing so the phenomenon of heat release in combustion process is not altered.

As established in above sections, by developed model, the noticeable oscillations in those system commence at $\varepsilon_{cr(developed)} = 0.4$; the classification of thermite mixtures from the work of the authors [47] is performed based on their inflammability limits. Thus the thermite systems from the work [47] is referred into two: $\varepsilon_{cr(Work)} < \varepsilon_{cr(developed)}$, $\varepsilon_{cr(developed)} < \varepsilon_{cr(Work)}$. Here the thermite systems with $\varepsilon_{cr(developed)} < \varepsilon_{cr(Work)}$ is considered. Figure 2.16(a) comprise the data of work [47] ($2\text{Fe}_2\text{O}_3 + 3\text{Zr} + n^*\text{ZrO}_2$, $2\text{Cr}_2\text{O}_3 + 3\text{Zr} + n^*\text{ZrO}_2$, $\text{Cr}_2\text{O}_3 + 2\text{Al} + n^*\text{Al}_2\text{O}_3$), processed in co-ordinates of burn rate and burning temperature. Neglecting heat losses and considering uniform heat release of reaction cells, the calculated burning temperature of the mixtures is identified as adiabatic temperature (T_{ad}) of the heterogeneous mixture. The average burn rate, during entire time of combustion process of different heterogeneous mixtures, determined in the work [47]; corresponds to theoretical average burning rate Eq. (25). The arrows in Figure 2.16(a) correspond to commencement of oscillating mode for

combustion process of different thermite mixtures. Treatment of experimental data [47] has been performed in non dimensional co-ordinates $\varepsilon - \omega$ as shown in previous sections. Hence theoretical values of the critical parameters such as ε_{cr} and ω_{cr} are assumed as commencement of oscillating modes of combustion, practical in experiments. As established above, by developed model, the noticeable oscillations in those system commence at $\varepsilon_{cr} = 0.42$; and is considered as critical parameters of developed model. Assuming the critical values of rate of burning r_{cr} and burning temperature $T_{ad_{cr}}$, determined in experiments, correspond to the commencement of oscillating modes of combustion process for a actual system.

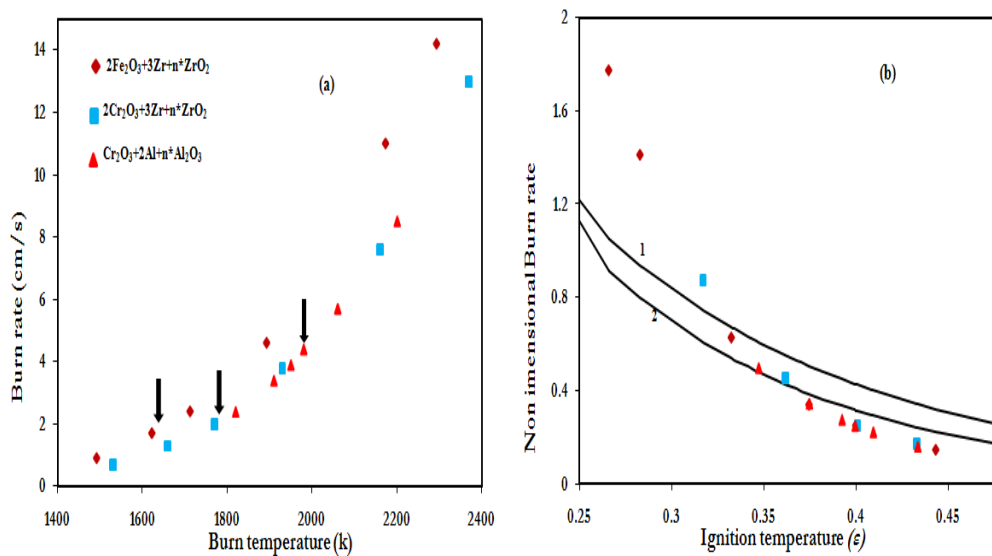


Figure 2.16. (a) Correlation of burning rate and burning temperature for several thermite systems, based on data of work [47]. The arrows shows the critical points, which correspond to beginning of oscillatory combustion modes. (b) Comparing of experimental and theoretical dependencies $\omega(\varepsilon)$. Dots are the treated experimental data [47]: solid lines 1-2 are the theoretical dependence for identical heat release, for normal distribution: lines 2 correspond to calculations for $\sigma=0.98$ and line 1 correspond to gamma $a=0.7$.

Then eqn. (27), in accordance with figure 2.8 and 2.11, critical non-dimensional burning rate $\omega_{cr} = \omega(\varepsilon_{cr})$ depends on the standard deviation of neighboring reaction cells; this implies that ω_{cr} depends on the system microstructure. Experimental data [47] are treated using expressions (26)-(27), similar to method shown in earlier sections, are shown in figure 2.16(b). Line 2 (Figure 2.16(b)) show the theoretical dependence for different values of $\sigma = const$. Line 1 shows the theoretical burn rates obtained for gamma distribution ($a=0.7$) of neighboring reaction cells. It is assumed that the change of non dimensional ignition

temperature (ε) in diluting the system mixture is associated with change of the standard deviation parameter σ or shaping parameter (a), which describe the system microstructure considering uniform heat release at all cells. Furthermore it is considered that the combustion process of thermite mixtures from work [47] can be explained by the respective dependence $\sigma(\varepsilon)$ or $a(\varepsilon)$. The dependence $\sigma(\varepsilon)$ is coordinated for the condition of concurrence of theoretical dependence $\omega(\varepsilon)$ calculated by developed model with the experimental data [47] (Figure 2.16(b)). Such dependence $\sigma(\varepsilon)$ is shown in figure 2.16(b). Theoretical dependence $\omega(\varepsilon)$, is calculated by using expressions Eqs. (24), (25) in the view of matched dependence $\sigma(\varepsilon)$, is shown in figure 2.16(b) (line 2); it describes experimental data [47] accurately for broad class of thermite mixtures. The value $\omega_{cr}=0.25$ was used in these calculations. Solid line 2 is the result of disordered system described with normal distribution of reaction cells and line 1 is from gamma distribution ($a=0.7$). The chi square at higher ignition temperatures ($\varepsilon>0.32$) has been calculated for lines 1 and 2 with respect to experimental data; and we achieve a chi square value of 0.054 for line 2(normal distribution) and 0.523 for line 1(gamma distribution $a=0.7$). The data [47], processed in variables $\varepsilon - \omega$, shows that combustion becomes impossible at $\varepsilon = 0.49...0.5$; this reality correlates well with the theoretical results obtained by developed model for uniform heat release at all reaction cells.

2.3.3.5 Quasi-Arrhenius' macrokinetics

The experimental data for all termite systems considered [47] (Fig. 12) can be approximated (fitted) by the single dependence

$$\omega = 67.6 \exp(-14\varepsilon) \quad (33)$$

although, these systems essentially differ not only from one another by their properties, but also they are different by contents of diluter within a system. Taking into account that, usually, $T_{ad} \gg T_{in}$, the dependence Eq. (33) can be considered as the Arrhenius' one, that is, $\omega \sim e^{-E_{ef}/RT_{ad}}$, with an effective activation energy of macro-process $E_{ef} \approx 9.08R(T_{ign} - T_{in})$, where R is the universal gas constant. A similar dependence of macroscopic burning rate on burning temperature can be obtained theoretically in homogeneous combustion model with Arrhenius' microkinetics [40,44]. Note that the obtained Arrhenius' dependence of macroscopic burning rate of the system on its adiabatic

temperature is not connected with Arrhenius' micro kinetics of chemical reactions in heat sources. The obtained result shows that Arrhenius' macro kinetics which is usually detected in experiments can be connected with an existence of threshold temperature T_{ign} and a heterogeneous nature of the system under consideration and it can have purely a thermal nature.

Section II Disordered Heat release (q_i)

In the work [47], for different thermite mixtures of Fe_2O_3 , it is observed that two thermite mixtures ($Fe_2O_3+2Al+n*Al_2O_3$, $2Fe_2O_3+3Ti+n*TiO_2$) have the inflammability limit less than $\epsilon_{(work)} < 0.4$, and the steady-state mode of combustion is seen for further lower values of ϵ . Above developed model with an assumption of uniform heat release (q_i) at all reaction cells could not explain for the thermite systems that have lower combustion limits. Currently no such combustion models exist that can quantitatively explain the change of combustion limit for thermite mixtures. Unlike the above model, where the heat release is considered identical for all cells, the present section analyzes the effect of randomizing the heat release at all cells on combustion limit. It is established from the above developed model with normal distribution of neighboring reaction cells is far more accurate with experimental data, here in this section the normal distribution for positioning neighboring reaction cells with randomized heat release at each cells is considered. The system modeled with gamma distribution of neighboring reaction cells and randomizing the heat loss, the reaction front does not propagate even at lower ignition temperatures ($\epsilon < 0.05$). Hence the gamma distribution cannot be used in robust modeling of combustion process that considers randomizing heat release. Note the average heat release at each cells is maintained as unit. Heat release in the developed model is also viewed as the consumption of reactant. Randomizing the heat release not only allows us to study the combustion limit but also reveals the nature of distribution of heat releases of neighboring reaction cells.

An identical heat release at all point sources was assumed for the above numerical calculations. However there can be a possibility of unequal heat release or unequal consumption of reactant at different cells. The heat release q_i is randomized and its effects on the combustion are studied in the present section. The heat release distribution, with two extreme cases has been considered. The system with small spread in the distribution of heat release is described by a normal distribution ($q_i \in [0.7-1.2]$) and the more spread by a normal

distribution ($q_i \in [0-7]$), however the average heat release is maintained at one. The modeled systems are calculated numerically and analyzed for their effect on combustion process. It is found that the small spread of distribution of heat release doesn't show considerable effect on combustion process and the combustion process is same as with uniform heat release. However as the degree of randomizing the distribution of heat release increases a considerable change in the process of combustion of such systems is observed. Figure 2.17 shows the ignition time profile for the microstructure of system described by $\sigma=0.05$ and $\sigma=0.4$ and with high disordered heat release.

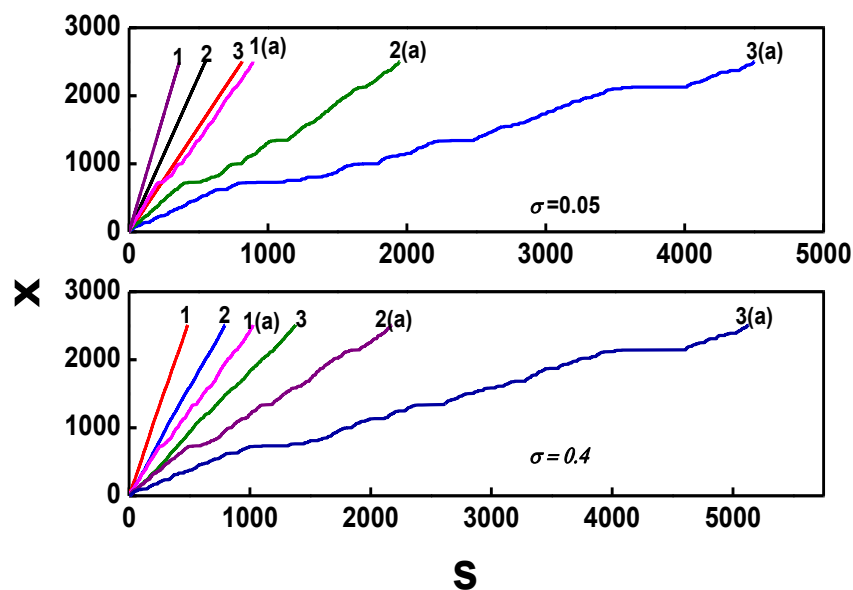


Figure 2.17. Comparison of Ignition time profiles for Identical heat release (1,2,3) and disordered heat release (1(a),2(a),3(a)) (q_i).1=0.15(ϵ),2=0.25(ϵ),3=0.35(ϵ).

It can be seen that the combustion process is affected by the disordered heat release. With the inclusion of the random heat release the burn front moves slower and combustion stops are observed. The affects are more pronounced at higher ignition temperatures and higher disorder of the heat release. Figure 2.18 shows the comparison of the burn rate obtained for a system with high disorder in the heat release with identical heat release. As the randomness in heat release increases the burn rates decreases with increase in ignition temperature. It can be observed that at higher ignition temperatures, the decrease in the burn rate is more when compared to an identical heat release. At any given ignition temperature, a system described by a low degree of randomness in the position of its cells and higher degree of disorderness in nature of heat releases, shows a higher decrease in the burn-rates. The combustion limit

for the present disordered system with randomizing heat release is still further reduced to 0.40 from 0.48.

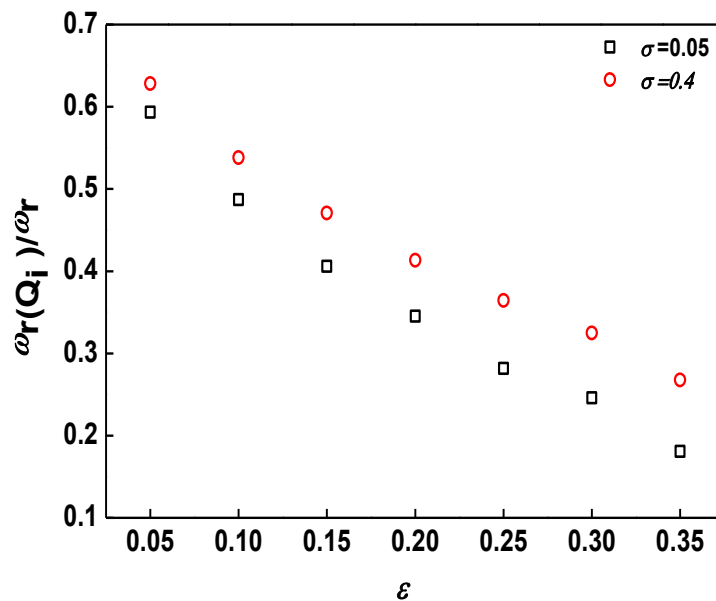


Figure 2.18. Comparison of Percentage of burn rates for identical (Boxes) and disordered (Circles) heat release.

And oscillations of ignition time profiles at $\epsilon=0.35$ is detected. Numerical experiments show that the combustion process of a system is affected by randomizing the heat release that leads to slow heating of system. Thus the distribution of heat release in the system affects the combustion process and hence cannot be neglected while modeling the combustible system. As the clusterization of heat release increases then the combustion process differs to a great extent and this increases with increase in ignition temperature. Heat release study would be helpful for robust modeling of combustible system which not only accounts for microstructure of system but also the different possibilities of heat releases.

2.3.4 Comparison With Thermite systems

Present section compares the experimental data for thermite mixtures [47], that consist of powder components ($\text{Fe}_2\text{O}_3+2\text{Al}+n*\text{Al}_2\text{O}_3$, $2\text{Fe}_2\text{O}_3+3\text{Ti}+n*\text{TiO}_2$) mixed with inert diluter, with theoretical model developed (section 3.2) in the view of randomizing of heat releases. Powdered components are capable of exothermic transformation. The temperature for burning the heterogeneous mixtures and their rate of burning can be altered for a broad range by changing the diluter and also by the amount of inert diluter; in doing so the lower inflammability limit in combustion is changed. The values of burning rate and burning

temperature of heterogeneous mixture that contain different inert diluter and different percentages of inert diluter are collected from the work [47]. Neglecting heat losses and considering randomizing distribution of heat release, the burning temperature of the heterogeneous mixtures is identified as adiabatic temperature (T_{ad}) of the mixture. It is established above, from the developed model, that the detectable oscillations in such mixtures (randomize heat release) begin at $\varepsilon_{cr}=0.35$; the thermite systems from the work of the authors [11] are classified based on their combustion limits. Present section refers to thermite mixtures from the work [11] for which $\varepsilon_{cr(Work)} < \varepsilon_{cr(developed)}$. Figure 2.19(a) contains the data of work [47] ($\text{Fe}_2\text{O}_3+2\text{Al}+n*\text{Al}_2\text{O}_3$, $2\text{Fe}_2\text{O}_3+3\text{Ti}+n*\text{TiO}_2$), performed in the co-ordinates of burn rate and burning temperature. The arrows in figure 2.19(a) correspond to the beginning of oscillating (critical) modes of combustion of thermite mixtures. Treatment of experimental data [47] is performed, similar to method in earlier sections, in non dimensional co-ordinates of $\varepsilon - \omega$. Hence it is considered that commencement of oscillating mode of combustion process, noticeable during experiments, is associated with critical values of theoretical parameters such as ε_{cr} and ω_{cr} .

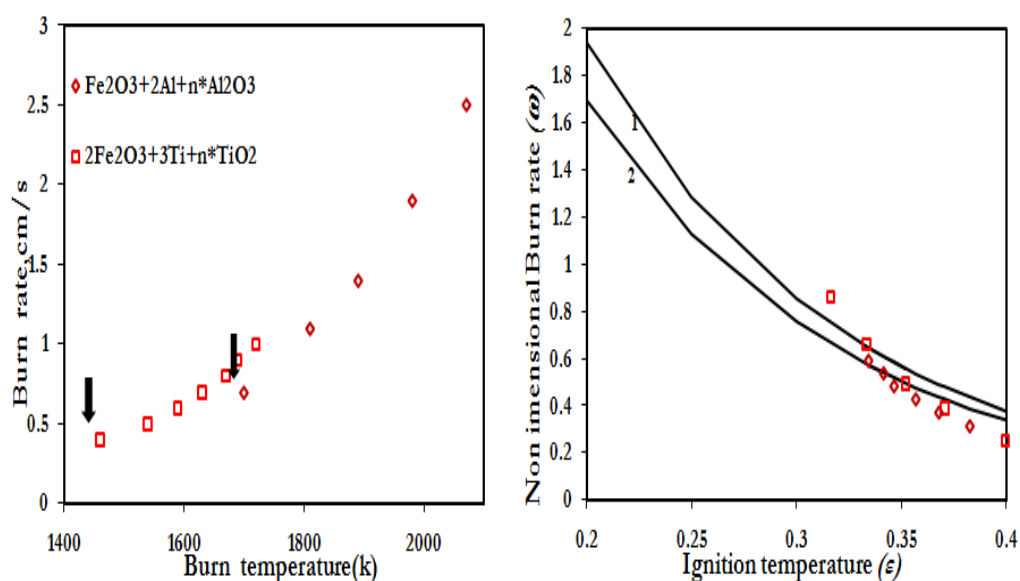


Figure 2.19. (a) Correlation of burning rate and burning temperature for thermite systems having lower combustion limits, based on data of work [47]. The arrows shows the critical points, which correspond to beginning of oscillatory combustion modes. (b) Comparing of experimental and theoretical dependencies $\omega(\varepsilon)$. Symbols are the treated experimental data [47] :solid lines are the theoretical dependence for randomized heat release and normal distribution with microstructure described byline 1 $\sigma=0.05$ and by line 2 $\sigma=0.40$.

As established above the noticeable oscillations of such heterogeneous mixture commence at $\varepsilon_{cr}=0.35$; this parameter is considered as critical value of inflammability limit of developed model. Assuming critical values of rate of burning r_{cr} and burning temperature $T_{ad_{cr}}$, noticeable during experiments, corresponds to commencement of oscillating modes of combustion in an actual system. Experimental data [47] now converted by using equations (26)-(27) is shown in figure 2.19(b). Lines 1-2 (Figure 2.19(b)) show for different values $\sigma = const$ and randomized q_i . It is believed that the changing of non dimensional ignition temperature (ε) in dilution of thermite mixtures is associated with change of standard deviation (σ), which describe the system internal structure. And also assume Change of combustion limit is associated with randomizing of distribution of heat release. Moreover the thermite systems and their combustion limit can be described by the dependence q_i and $\sigma(\varepsilon)$. The value of parameter q_i and $\sigma(\varepsilon)$ is matched from the concurrence of numerical (developed model) burn rates $\omega(\varepsilon)$ with the experimental data [47] (Figure 2.19(b)). Such dependence of $\sigma(\varepsilon)$ and q_i is shown in figure 2.19(b) (line 2). Theoretical dependence $\omega(\varepsilon)$, in view of the matched dependence of parameters $\sigma(\varepsilon)$ and q_i , is shown in figure 2.19(b) (line 2); it appropriately explains the experimental data [47] of thermite mixtures having lower inflammability limits. The value $\omega_{cr}=0.26$ was used for above calculations. Experimental data [47] allows estimating an inflammability limit of ignition temperature (ε) for each mixture, beyond which a stable combustion is not possible. The experimental data [47], now converted in the coordinates of $\varepsilon - \omega$, shows that stable combustion is not possible at values $\varepsilon = 0.35...0.4$; this reality agrees well with numerical results of developed model obtained by randomizing distribution of heat release.

2.4 Conclusion

The results show that the use of the gamma or normal distribution for modeling of microheterogeneous systems allows describing peculiarities of combustion of solid mixtures with wide variations in their internal structure, from periodic, which correspond to $a = \infty$ or $\sigma = 0.05$ to random homogeneous disordered systems, which correspond $a=1$ or $\sigma = 0.50$, and ending with clustered systems which correspond to $0.5 < a < 1$ or $0.5 < \sigma < 1$. An additional "degree of freedom", the shaping parameter a , introduced in the model allowed reproducing theoretically the experimental data for a wide range of pyrotechnic mixtures, as well as explain the previously unexplained from the point of view of the theory

of combustion of homogeneous systems the experimental data on combustion of $Ti+xSi$ mixtures. Only assumption that the burning rate depends on the structure of the mixture and can change with changing of the structure of mixture even at a constant burning temperature allowed describing the dependence of the burning rate on stoichiometry x , including, in the range with a constant burning temperature. Different combustion limit for thermite systems is explained in the view of randomized heat release.

2.5 References

- [1] Merzhanov AG, Mukasyan AS, Rogachev AS, Sytchev AE, Varma A. Microstructure of combustion wave in heterogeneous gasless systems. *Combust Explos Shock Wave* 1996;32(6):334–47.
- [2] A. Varma, A. S. Rogachev, A. S. Mukasyan, and S. Hwang, Complex behavior of self-propagating reaction waves in heterogeneous media. *Proc. Natl. Acad. Sci. U.S.A.* 95, 11053 (1998).
- [3] S. Hwang, A. S. Mukasyan, and A. Varma. Mechanisms of Combustion Wave Propagation in Heterogeneous Reaction Systems. *Combustion and Flame* 115:354–363 (1998).
- [4] Frolov YV, Pivkina AN, Aleshin VV. Structure of HCS and its influence on combustion wave. *Int J Self-Propagat High-Temp Synth.* 10(1):31–54 (2001).
- [5] A. Varma, A. S. Mukasyan, S. Hwang. Dynamics of self-propagating reactions in heterogeneous media: experiments and model. *Chemical Engineering Science* 56, 1459-1466 (2001)
- [6] A. S. Mukasyan, A. S. Rogachev, M. Mercedes, and A. Varma, Microstructural correlations between reaction medium and combustion wave propagation in heterogeneous systems. *Chem. Eng. Sci.* 59, 5099 (2004).
- [7] Zhang JY, Fu ZY, Wang WM, Zhang QJ. A macro-homogenous and micro-heterogeneous model for self-propagating high temperature synthesis. *Mater Sci For* 475(4):475–9 (2005).
- [8] A.S. Mukasyan, A.S. Rogachev, Discrete reaction waves: Gasless combustion of solid powder mixtures. *Progress in Energy and Combustion Science* 34, 377–416 (2008)
- [9] A. S. Rogachev, F. Baras, Dynamical and statistical properties of high-temperature self-propagating fronts: An experimental study. *Physical Review E* 79, 026214 (2009).
- [10]. A.R Kulkarni,K.C Sharma, Burn rate modeling of solid rocket propellants, *Defence Science Journal* 48 (1998) 119-123.

-
- [11]. N. Kubota, Role of Additives in Combustion Waves and Effect on Stable Combustion Limit of Double-Base Propellants, *Propellants Explosives* **3** (6), 163–168 (1978).
- [12]. M. W. Beckstead and K. P. McCarty, Modeling Calculations for HMX Composite Propellants, *AIAA J.* **20** (1), 106–115 (1982).
- [13]. A. P. Denisyuk, V. S. Shabalin, and Yu. G. Shepelev, Combustion of Condensed Systems Consisting of HMX and a Binder Capable of Self-Sustained Combustion, *Combust. Expl., Shock Waves* **34** (5), 534–542 (1998).
- [14]. N. Kubota, *Propellants and Explosives: Thermochemical Aspects of Combustion* (Willey-VCH Verlag GmbH and Co. KGaA, 2002).
- [15] Suzuki A, Yamamoto T, Aoki H, Miura T. Percolation model for simulation of coal combustion process. *Proc Combust Inst* 29:459–66 (2002).
- [16] Miccio F. Modeling percolative fragmentation during conversion of entrained char particles. *Korean J Chem Eng* 21(2):404–11 (2004).
- [17] Sheng C, Azevedo JLT. Modeling biomass devolatilization using the chemical percolation devolatilization model for the main components. *Proc Combust Inst* 29:407–14 (2002).
- [18] Favier C. Percolation model of fire dynamic. *Phys Lett A* 330: 396–401 (2004).
- [19] Viegas DG. *Philos Trans R Soc Lond A* 356:2907 (1998).
- [20] Gardner RH, Romme WH, Turner MG. Predicting forest fire effects at landscape scales. In: Mladenoff DJ, Baker WL, editors. *Spatial modeling of forest landscapes: approaches and applications*. Cambridge: Cambridge University Press; (1999). p. 163–85.
- [21] Scala F, Salatino P, Chirone R. Fluidized bed combustion of biomass char of *Robinia pseudoacacia*. *Energy Fuels* 14(4): 781–90 (2000).
- [22] Molerus O. Appropriately defined dimensionless groups for the description of flow phenomena in dispersed systems. *Chem Eng Sci* 53(4):753–9 (1998).
- [23] Marban G, Pis JJ, Fuertes AB. Characterizing fuels for atmospheric fluidized bed combustion. *Combust Flame* 103(1/2):41–58 (1995).
- [24] Kauffman CW, Nicholls JA. Shock-wave ignition of liquid fuel drops. *AIAA J* 9(5):880–5 (1971).
- [25] Fedorov AV. Mathematical modeling of the ignition of a cloud of microdrops of a hydrocarbon fuel. *Fiz Goren Vzryva* 38(5): 97–100 (2002).

- [26] Umemura A, Takamori S. Percolation theory for flame propagation in non- or less-volatile fuel spray: a conceptual analysis to group combustion excitation mechanism. *Combust Flame* 141(4): 336–49(2005).
- [27] Eckhoff R. K. *Dust explosions in the process industries* 3rd edition, 720 pages, Gulf Professional Publishing/Elsevier, Boston ISBN 0-7506-7602-7 (2003).
- [28]. Merzhanov, A.G. and Mukasyan, A.S., *Tverdoplamennoe gorenie* (Solid-Flame Combustion), Moscow: Torus Press, (2007).
- [29] G. M. Machviladze and B. V. Novozilov, *Prikl. Mekh. Tekh. Fiz.* **5**, 51 (1971).
- [30] K. G. Shkadinskii, B. I. Khaikin, and A. G. Merzhanov, *Combust., Explos. Shock Waves* **7**, 15 (1971).
- [31] G. Nicolis and C. Nicolis, *Foundations of Complex systems: Nonlinear Dynamics, Statistical Physics, Information and Prediction* (World Scientific, Singapore, 2007).
- [32] G. Nicolis, *Introduction of Nonlinear Science* (Cambridge Univ. Press, Cambridge, England, 1995).
- [33] I. R. Epstein and J. A. Pojman, *An Introduction of Nonlinear Chemical Dynamics: Oscillations, Waves, Patterns and Chaos* (Oxford University Press, New York, 1998).
- [34] A.S. Rogachev, Microheterogeneous mechanism of gasless combustion. *Comb. Expl. Shock Waves*, 39, 150–158 (2003).
- [35] S.A. Rashkovskii, Hot-spot combustion of heterogeneous condensed mixtures. Thermal percolation. *Comb. Expl. Shock Waves*, 41, 35–46 (2005).
- [36] P. S. Grinchuk and O. S. Rabinovich. Effect of random internal structure on combustion of binary powder mixtures. *Physical Review E* 71, 026116 (2005).
- [37] F.-D. Tang, A.J. Higgins, S. Goroshin. Effect of discreteness on heterogeneous flames: Propagation limits in regular and random particle arrays. *Combustion Theory and Modelling*. Vol. 13, No. 2, 319–341 (2009).
- [38] S.A. Rashkovskiy, G.M. Kumar, S.P. Tewari, One-dimensional discrete combustion wave in periodic and random systems. *Combustion Science and Technology*, 182: 1009–1028, (2010)
- [39] S.A. Rashkovskiy, Simulation of Gasless Combustion of Mechanically Activated Solid Powder Mixtures. *Advances in Science and Technology*, Vol. 63, P. 213-221 (2010).
- [40] D. A. Frank-Kamenetskii, *Diffusion and Heat Transfer in Chemical Kinetics* (Plenum Press, New York, 1969).

- [41] A. D. Polyanin, *Handbook of Linear Partial Differential Equations for Engineers and Scientists*, (Chapman & Hall/CRC Press, Boca Raton–London, 2002).
- [42] Zel'dovich, Ya.B., Theory of Flame Propagation in Gases, *Zh. Eksp. Teor. Fiz.*, vol. 11, no. 1, pp. 159–168 (1941).
- [43] Spalding, D.B., A Theory of Inflammability Limits and Flame-Quenching, *Proc. Roy. Soc., Ser. A*, vol. 240, no. 1220, pp. 83–100 (1957).
- [44] Zeldovich, Y.B., Barenblatt, G.I., Librovich, V.B., and Makhviladze, G.M. *The Mathematical Theory of Combustion and Explosions*, (Plenum Press, New York and London 1985).
- [45] L. D. Landau and E. M. Lifshitz, *Statistical physics part 1*, (3ed., Pergamon, 1980)
- [46] C.W. Gardiner. *Handbook of Stochastic Methods for Physics, Chemistry and the Natural Sciences*, Springer Series in Synergetics, Volume 13, (2nd, Springer-Verlag, Berlin Heidelberg, New York, Tokyo, 1985)
- [47] Dvoryankin A. V., Strunina A. G., and Merzhanov A. G. Stability of combustion in thermite systems, *Comb. Expl. Shock Waves*, 21, No. 4, 421–424 (1985).
- [48] T. P. Ivleva and A. G. Merzhanov, *Phys. Rev. E* **64**, 036218 (2001).
- [49] T. P. Ivleva and A. G. Merzhanov, *Chaos* **13**, 80 (2003).
- [50] S. A. Rashkovskii, Structure of heterogeneous condensed mixtures, *Combust. Expl. Shock Waves*, 35, No. 5, 523–531 (1999).
- [51] S. A. Rashkovskii, Role of the structure of heterogeneous condensed mixtures in the formation of agglomerates, *Combust. Expl. Shock Waves*, 38, No. 4, 435–445 (2002).
- [52] N. Tarun Bharath, S. A. Rashkovskiy, S. P. Tewari and G .M. Kumar, Dynamical and statistical behavior of discrete combustion waves: A theoretical and numerical study, *Phys. Rev. E* 87,042804 (2013).
- [53] Naine Tarun Bharath, Manoj Kumar Gundawar, Effects of Disordered Microstructure and Heat release on Propagation of Combustion Front, *Cogent engineering* (2016).

CHAPTER 3

Correlation between Discrete Probability and Reaction Front Propagation Rate in Heterogeneous mixtures

Present chapter describes a powerful correlation between the discrete probability of distances of neighbouring cells and thermal wave propagation rate, for system of cells spread on a one dimensional chain. A gamma distribution is employed to model the distances of neighbouring cells. In the absence of an analytical solution and the differences in ignition times of adjacent reaction cells following non-Markovian statistics, invariably the solution for thermal wave propagation rate for one dimensional systems with randomly distributed cells is obtained by numerical simulations. However, such simulations which are based on Monte-Carlo methods require huge computing resources. For several one dimensional systems, differing in the value of shaping parameter of the gamma distribution, it is observed that the average reaction front propagation rates obtained by a discrete probability between two limits, shows excellent agreement with those obtained numerically. With the upper limit at 1.3, the lower limit depends on the non-dimensional ignition temperature. Additionally, this approach also facilitates the prediction of burning limits of heterogeneous thermal mixtures. The proposed method completely eliminates the need for laborious, time intensive numerical calculations where the thermal wave propagation rates can now be calculated based only on macroscopic property entity of discrete probability.

3.1 Introduction

Physics research in heterogeneous combustion [1-13] mainly investigates the effects of change in microscope entities of internal structure of a mixture on reaction kinetics and propagation, stability of thermal wave. Heterogeneous mixtures with voids have wide ranges of ignition behaviour, performance, reaction zone characteristics, internal microstructure and other discontinuities [7, 13-16]. Velocity of reaction front or burn rate of a system is the quantitative and crucial parameter in describing the average behaviour of heterogeneous combustion process. Such experimental study for combustion of heterogeneous mixtures involves huge cost, high speed micro video recorder [5-7] and risk factor. In such situations the mathematical modelling and simulation of combustion of mixtures shown in chapter 2 [13-18] can play a crucial role in understanding the effect of heterogeneities. Also the modelling of heterogeneous combustion has inherent safety and wide operational features that make them attractive choices for a broad range of applications, including combustion of coal, solid propellants, aerosols, thermite mixtures etc. Combustion process of

heterogeneous mixtures shown in chapter 2 is modelled as instantaneous ignition and burning of reaction cells arranged randomly on one dimensional chain [15-16]. Such Monte Carlo simulation [15-16, 19] of heterogeneous combustion process is performed by repetitive random sampling of neighbouring reaction cells. Numerical experiments and theoretical studies on heterogeneous combustion process [8-10, 15-16] had revealed the crucial role of disordered structure in explaining the burning of actual heterogeneous mixtures. Numerical calculation of burn rates is obtained by sequential calculations of ignition times of reaction cells. Heterogeneous mixture performance, role and vulnerability have been successfully modelled at different stages [14-16] in chapter 2. Nevertheless mathematical modelling and numerical simulations of such systems is complicated on account of multiple reasons such as irregular voids, mixing, compressing and packing of mixtures influences and unstable reaction zones. In addition the computational time for simulation and quantifying the reaction front propagation rate of heterogeneous mixtures is tedious process and time consuming. While performing the numerical calculations, the number of cells (particles), wide ranges for distribution of arranging cells and number of realizations of distribution are very crucial. The optimum solution to these parameters is obtained only after rigorous numerical calculation. For example, in chapter 2 the input parameters like ignition temperature (ϵ), number of burnt and unburnt particles and increment of time (dt) are initialized and the combustion process is simulated using governing equation (2) from chapter 2. Burn rates are calculated using equation (2) and (3) from chapter 2 for different random distributions of cells. Each burn rate in the figure 2.8 from chapter 2 (represented by symbols) is a result of repeated calculations for 40 realizations (dependent on degree of randomness) of random distributions of neighbouring cells. This process of obtaining burn rates, is repeated for different values of shaping parameter (a), requires dedicated huge computing resources.

Theoretical analysis performed in chapter 2 gives the relation between burn rates of periodic and disordered system. The normalized burn rate $\left(\frac{w_r(\epsilon)}{w_p(\epsilon)}\right)$ of disordered system with respect to periodic system is established as always less than one by equation (15) from chapter 2. And Eqn. (11) and (15) from chapter 2 can be used for calculation of burn rate of disordered system with knowledge of burn rate of an ordered system. However eqn.(15) from chapter 2 involves the parameter m termed as correlation factor between neighbouring distances and delay in ignition times. Here parameter m can only be obtained after calculation of ignition times. This method of calculating the burn rate is tedious and time taking as

simulation of combustion process involves numerous realizations of disordered micro structures. Numerical experiments of discrete combustion model illustrated in chapter 2 are successfully compared with the actual experimental results [8-10]. Nevertheless, numerical and theoretical methods of obtaining burn rates of a disordered system involve huge computational resources. Hence it is of academic interest to find a numerical technique, based on statistics and the knowledge gained from numerous calculations performed in chapter 2, that can reduce the computational time. Thus invented technique once formulated, tested and validated with established theoretical and experimental results [15-16] can overcome the computational aspects faced by the mathematical modeling of combustion physics. The obtained agreement between the results of developed numerical technique and established mathematical model augurs well, at different values of shaping parameter (a), for numerical technique developed for the heterogeneous flows under consideration. Present chapter shows that the couple of hours of traditional computing can now be reduced to a time for finding cumulative count of effective reaction cells in the range around the mean. Reduction in the huge experimental and computational cost, first on prediction of burn rates for wide ranges of mixtures and providing hands on experience for combustion designers are the advantages of such techniques.

3.2 Motivation

In chapter 2, the statistical and dynamic behaviour of discrete combustion waves in a one dimensional random system are studied. The system was modelled as one dimensional chain of cells with a specific ignition temperature. The position of the cells was assigned by modelling the distances between the neighbouring cells by either uniform, normal or gamma distribution. Further, the cells were connected by thermal bridges characterized by thermal conductivity k , linear mass density ρ and specific heat c . The burn front propagation rate, hence forth referred to as burnrate, was determined numerically by calculating the burn time of all the cells of the system. One of the important results eqn. (15) shown in chapter 2 was that the burnrates of a random system were always less than the burnrate of a periodic system with unit spacing [15-16]. The average spacing of the cells in a random system was also maintained at unity to facilitate a meaningful comparison. However, such numerical simulations demand huge computing powers for couple of hours to days depending on the value of ignition temperature and the time step. As the analytical solution [15-16] for a one dimensional periodic system is well known, it is convenient to discuss the burnrate of a random system w.r.t to a periodic system. It is important to note that the burnrate of random

system w.r.t to periodic system at any ignition temperature is always less than unity and can be expressed as a ratio of the gamma function Eq.(15) of chapter 2. Combining this result, with the fact that burn (ignition) times follow a non markovian statistics, a conjecture is made that the normalized burnrates can be obtained by calculating discrete probability with a careful choice of limits of the integral. In this chapter, the one dimensional random (gamma distribution) system used in chapter 2 [16] is considered. The results obtained by the proposed method are compared with burn rates obtained by the numerical simulations [16].

3.3 Statistics of ignition delay times

In this section the random process τ_i (delay in ignition times) and the difference of actual random process τ_i from markovian one, i.e, when there is a correlation between the ignition delay times τ_i for the different reaction cells is analyzed and demonstrated. Denoting $z_i = \tau_i - \langle \tau \rangle$, it is obtained

$$\sigma_z^2 = \sum_{i=1}^N \sum_{j=1}^N \langle z_i z_j \rangle \quad (1)$$

with

$$\langle z_i z_j \rangle = \sigma_z^2 R_{ij} \quad (2)$$

where $R_{ij} = R_{ji}$ is the correlation function for discrete random process τ_i ; $R_{ii} = 1$; $R_{ij} \rightarrow 0$ at $|i-j| \rightarrow \infty$,

$$\sigma_z^2 = \langle z_i^2 \rangle = \langle \tau^2 \rangle - \langle \tau \rangle^2 \quad (3)$$

Using eqn. (15) from chapter 2 the eqn. (3) is written as

$$\sigma_z^2 = \frac{1}{\omega_p^2 a^{2m} \Gamma^2(a)} \left(\Gamma(a) \Gamma(a+2m) - \Gamma^2(a+m) \right) \quad (4)$$

where the parameter m is determined by the correlation equation $m = 2.2 - 0.01a + 2.23a^{0.27} \varepsilon$ obtained numerically in chapter 2. Because the discrete random process L_i is uniform one, the discrete random process τ_i which induced by them will be uniform one too. This means that $R_{ij} = f(|j-i|)$. Denote $k = j-i$, then one can write

$$R_{i,i+k} = \rho_k \quad (5)$$

where the correlation function ρ_k has the obvious properties

$$\rho_k = \rho_{-k} \quad (6)$$

$$\rho_0 = 1, \quad \lim_{|k| \rightarrow \infty} \rho_k = 0.$$

After simple transformations while taking into account Eqs. (5) and (6), for standard deviation Eq. (1) one obtains

$$\sigma_t^2 = \sigma_z^2 \sum_{k=0}^N (N-k) \rho_k \quad (7)$$

Taking into account eqn. (22) from chapter 2 and eqn. (4), the relative standard deviation of the system's burning time is determined in this case by the expression

$$\frac{\sigma_t}{\langle t_N \rangle} = \frac{\mu(N)}{\sqrt{N}} \sqrt{\frac{\Gamma(a)\Gamma(a+2m)}{\Gamma^2(a+m)} - 1} \quad (8)$$

Where

$$\mu(N) = \sqrt{\sum_{k=0}^N (1-k/N) \rho_k} \quad (9)$$

A case $\rho_k = \delta_{0k}$, where δ_{ik} is the unit matrix, corresponds to Markov random process, for which $\mu(N) = 1$ and Eq. (8) turns into

$$\frac{\sigma_t}{\langle t_N \rangle} = \frac{1}{\sqrt{N}} \sqrt{\frac{\Gamma(a)\Gamma(a+2m)}{\Gamma^2(a+m)} - 1}$$

Function $\mu(N)$ for several values of parameters a (shaping parameter of gamma distribution) and ε is shown in figure 3.1. For the calculations of function $\mu(N)$, the correlation function ρ_k has been determined on the results of numerical solution of eqn (2) from chapter 2. Analysis of correlation function ρ_k shows that even at $|k|=1$ it drops down to ~ 0.05 and at further increasing in $|k|$ it oscillates in the range $-0.05 \leq \rho_k \leq 0.05$. It is necessary to note that analogous correlation function for distance between neighbouring reaction cells oscillates in the same range. This is connected presumably with peculiarities of work of pseudorandom number generator [16]. Detailed analysis has shown that local oscillations of correlation function ρ_k for random process τ_i repeat completely the oscillations of degree of correlation between τ_i and L_i . For $N \rightarrow \infty$ expression equations (8) and (9) can be approximately rewritten in the form

$$\frac{\sigma_t^2}{\langle t_N \rangle^2} = \alpha N^{-1} - \beta N^{-2} \quad (10)$$

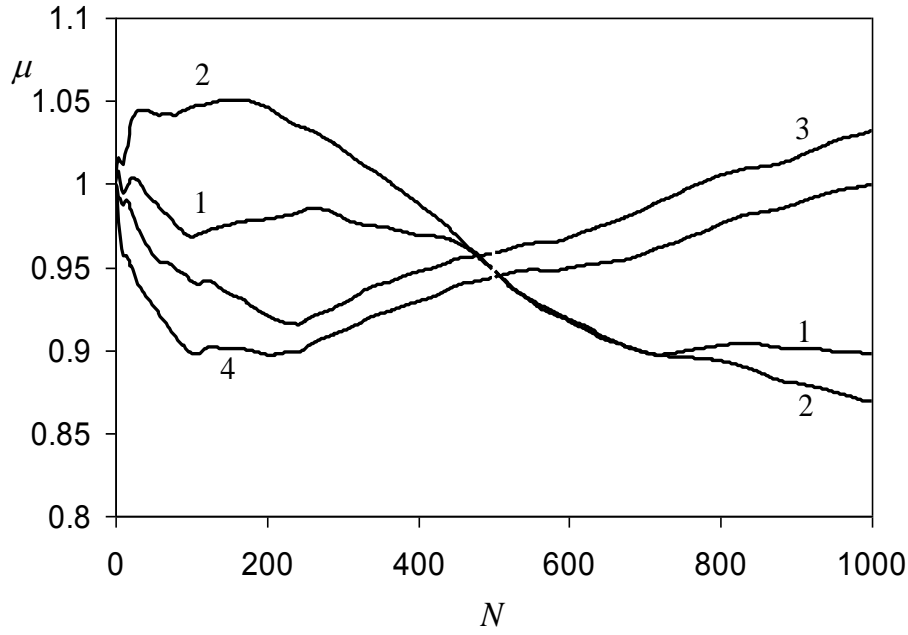


Figure 3.1. Function $\mu(N)$ for different values of parameters a and ε . Lines 1 and 3 - $\varepsilon=0.05$, lines 2 and 4 - $\varepsilon=0.4$; lines 1 and 2 - $a=1$, lines 3 and 4 - $a=15$.

correlation function for random process L_i ; this is connected with high

where the coefficients

$$\alpha = \left(\frac{\Gamma(a)\Gamma(a+2m)}{\Gamma^2(a+m)} - 1 \right) \sum_{k=0}^{\infty} \rho_k, \quad \beta = \left(\frac{\Gamma(a)\Gamma(a+2m)}{\Gamma^2(a+m)} - 1 \right) \sum_{k=0}^{\infty} k \rho_k$$

do not depend on N . Analysis carried out has shown that discrete random process τ_i , $i = \dots, 1, 2, 3, \dots$ is weakly markovian one and approximately it can be considered as non-markovian process. Theoretically, a distinction of the process under consideration from Markov random process one can take into account in a next approximation in solution of

$p(L) = \frac{a^a}{\Gamma(a)} L^{a-1} \exp(-aL)$ in which effect τ_{k-1} on τ_k is taken into account. For

example, in simple case the Eq. (2) from chapter 2 can approximately be rewritten as follows

$$2\sqrt{\pi}\varepsilon = \frac{1}{\sqrt{\tau_k}} \exp\left(-\frac{L_k^2}{4\tau_k}\right) + \frac{1}{\sqrt{\tau_k + \tau_{k-1}}} \exp\left(-\frac{(L_k + L_{k-1})^2}{4(\tau_k + \tau_{k-1})}\right) + \sqrt{\omega_r} \sum_{i=3}^{\infty} \frac{1}{\sqrt{n}} \exp(-\omega_r n/4)$$

$$\frac{1}{\sqrt{\tau_k}} \exp\left(-\frac{L_k^2}{4\tau_k}\right) + \frac{1}{\sqrt{\tau_k + \tau_{k-1}}} \exp\left(-\frac{(L_k + L_{k-1})^2}{4(\tau_k + \tau_{k-1})}\right) = \beta \quad (11)$$

where

$$\beta = 2\sqrt{\pi}(\varepsilon - \varepsilon_p(\omega_r)) + \sqrt{\omega_r} \exp(-\omega_r/4) + \sqrt{\omega_r} \frac{1}{\sqrt{2}} \exp(-\omega_r/2)$$

and burning rate is determined from a transcendental equation with taking into account expression Eq. (11). Obviously, the random process τ_k , described by equation (11), will be a non-markovian, although the random process L_k is itself markovian.

3.4 Results

Gamma distribution among the distances between neighboring reaction cells was employed to assign the position of the particles. A detailed description of the one dimensional system under consideration can be found in chapter 2. The probability density function (pdf) of the gamma distribution is given as

$$p(L) = \frac{a^a}{\Gamma(a)} L^{a-1} \exp(-aL)$$

where a is a shaping parameter and L is the distance between neighboring reaction cells. The shaping parameter ' a ' of the distribution allows for description of wide range of heterogenous systems ranging from random (small a) to periodic systems (large a). The average of the distribution is always maintained as unity to enable a meaningful comparison with a periodic system with unit spacing. Figure 3.2 shows pdf for gamma distribution for two different values of shaping parameter, a . It can be observed that the distances between the neighbouring cells show a smaller spread for higher value of a . Figure 3.2 shows the superimposed vertical lines for the lower (dashed lines) and upper limit (solid line) for two different values of a (shaping parameter) and two values of ignition temperature. In the proposed approach, the normalized burn rates (normalized w.r.t. to a periodic system for same ε) are obtained by calculating a discrete probability between the limits ul the upper limit and ll the lower limit. The cells whose neighbouring distances fall in the ul and ll is referred as '*cells in the range*'.

The proposed prescription for the calculation of the burnrate is

$$p_r(ll(m) < L > ul) = \frac{w_r(\varepsilon)}{w_p(\varepsilon)} \quad (12)$$

where $w_r(\varepsilon)$ and $w_p(\varepsilon)$ are burnrates for a random and periodic systems respectively at ignition temperature ε . Probability, p_r , with zero as lower limit, is a monotonically non-decreasing function and can take values between zero and one. As mentioned earlier, the ratio of burnrates is always less than unity.

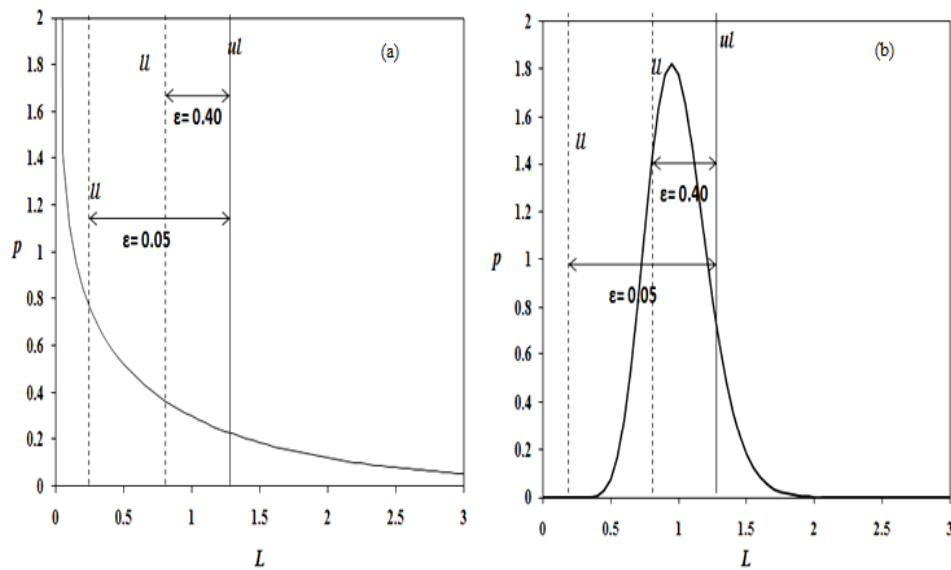


Figure 3.2. Probability distribution function for gamma distribution of the distances between neighboring hot spots (cells) with different values of shaping parameter. Straight lines for lower and upper limits represent the schematic representation of novel method. (a) $a=1$ (b) $a=20$.

Discrete probability with lower and upper limits in the range of 1 (average spacing) is considered for calculation of the normalized burn rate. For higher values of ignition temperature, the lower limit shifts to the right thereby reducing the discrete probability in agreement with the decreasing values of the burnrates. Initially, a coarse search shown in figure 3.3 was performed to locate the intervals for which the probability is same as the normalized burn rates.

After this, the lower limit was fixed and a least square approach was followed to find out the optimum value for the upper limit. This was followed by optimization of the lower limit by fixing the upper limit for all the gamma distributions in the range of one to twenty integral values. Each symbol in figure 3.3 is obtained as chisquare value for 20 different shaping parameter of gamma distribution. The minimum value of chisquare is taken as the optimized lower limit for each ignition temperature. This step is repeated for different ignition temperatures. It is observed from figure 3.3 that the optimized lower limit increases with increase in ignition temperature. Note the value of optimized lower limit for particular ignition temperature is independent of shaping parameter; however it changes with change in ignition temperature.

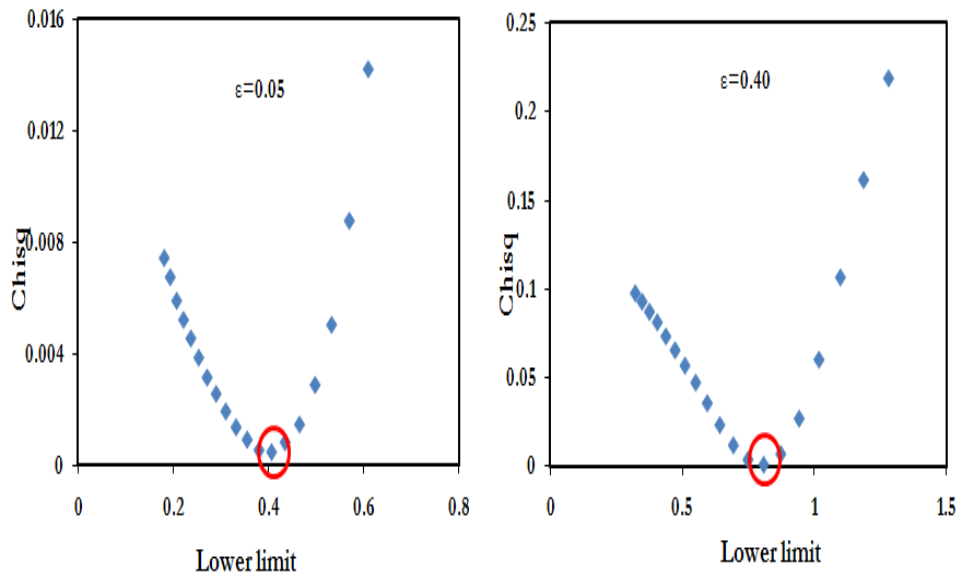


Figure 3.3 Plot for chisquare values at different values of lower limit on ignition temperature.

The optimum values for lower limit was in the range of 0.35 to 0.82 and upper limit was fixed at 1.3. Figure 3.4 shows the dependence of lower limit on the ignition temperature. The dependence of lower limit on ignition temperature is modeled with a exponential function as

$$l(\epsilon) = 0.29 * \exp^{2.56\epsilon} \quad (13)$$

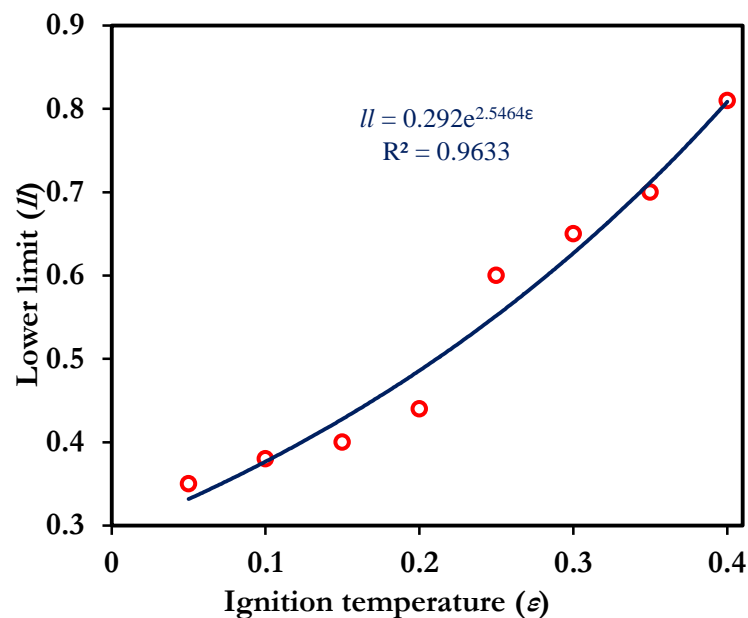


Figure 3.4 Functional dependence of lower limit on ignition temperature. Circles represent the numerical values obtained through methodology and solid line represents the trend line.

Figure 3.5 shows the ratio of burnrates obtained by developed model (represented by circles) using eqn. (13) and (12) superimposed on the results obtained from numerical analysis

(represented by solid line). Excellent agreement can be seen at different values of ignition temperatures and for wide range of systems characterized by the shaping parameter a . This correlation becomes a powerful tool as for an ignition temperature there exists a single lower limit for every gamma distributed system with upper limit fixed at 1.3. A similar agreement is also observed for other ignition temperatures considered.

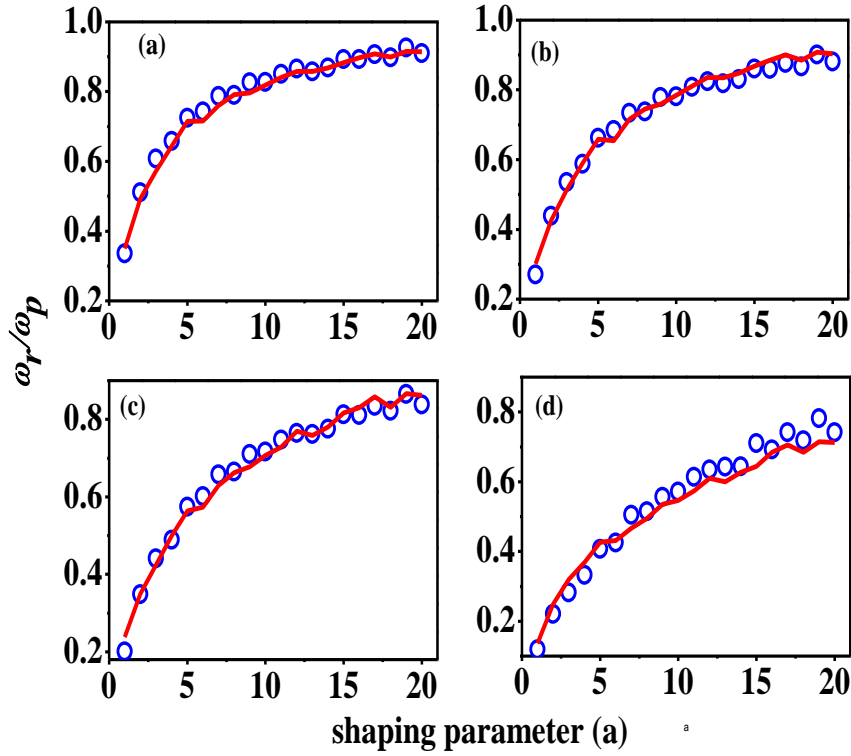


Figure 3.5 Comparison of the burn-rates obtained by the proposed method represented by ‘o’ with the numerically calculated values from chapter 2 represented by solid line. Solid line is compared and validated with experimental results in chapter 2. (a) $\varepsilon=0.10$, (b) $\varepsilon=0.20$ (c) $\varepsilon=0.30$ (d) $\varepsilon=0.40$.

Hence the problem of calculating the burnrates now reduces to three simple steps -

1. Given the ignition temperature, calculate the lower limit ll using Eq. (13).
2. Calculate the discrete probability of the gamma distribution between ll and 1.3.
3. Multiply discrete probability with $w_p(\varepsilon)$ which is a known value.

$$w_r(\varepsilon) = p_r(ll(m) < L > ul) \times w_p(\varepsilon)$$

Eqn. (11) from (chapter 2) [16] provides a relationship between the ignition temperature and the correlation factor, m , between distances and times. This relation is employed to derive

Eq. 13 for the ratio of the burnrates. Using eqn. (13) and substituting in eqn. (11) of chapter 2, a relation between l and m is obtained as -

$$l(m) = 0.29 \exp[1.15(m - 2.2 + 0.01a)a^{-0.27}] \quad (14)$$

where m represents correlation between the differences in the adjacent cell spacing and differences in their corresponding ignition times. The striking similarity between the results obtained by using $l(\varepsilon)$ and $l(m)$ can be observed. It should be noted that m is a result of the knowledge of complete information on positions and times of ignition. And its use to obtain the lower limit for obtaining the reaction front propagation rates shows the robustness of the proposed correlation between burnrates and cumulative probability.

The knowledge of $l(\varepsilon)$ can further be extended to estimate the limiting ignition temperature beyond which the thermal wave cannot be propagated in the system. The existence of an ignition temperature for heterogeneous systems of particles in suspension introduces a limit to reaction front propagation, even in the absence of losses [7,15-16]. This limit is defined as the condition when the heat release of the entire domain of particles is just sufficient to increase the bulk temperature of the mixture to the particle ignition temperature. Equivalently, it amounts to stating that the adiabatic temperature is equal to the ignition temperature [14]. The combustion limit for a periodic system [7, 14-16] is obtained as 0.5459 and 0.48 for a random [16] through numerical calculations. Numerically the combustion limit is calculated as that ignition temperature beyond which the thermal wave does not propagate throughout the system. This method of finding the limit is time consuming as it demands the increment of the ignition temperature in very small steps and check if the thermal wave is capable of passing through the entire system or it ceases to propagate at a particular point on the chain as the temperature cannot attain the required ignition temperature. Again, this leads to complete elimination of the cumbersome time consuming numerical calculations, where ignition temperature must be iterated, in very small steps, to check where the propagation of heat wave is impossible. It is also worth noting here that as the magnitude of the ignition temperature increases, the computation time also increases. The function dependence of l on the ignition temperature can be exploited to calculate the combustion limit of a system. Limit $l \rightarrow 1$, in eqn. (13), enables the estimation of the combustion limit. Accordingly, the combustion limit is 0.48 according to this prescription, which is excellent agreement with the value obtained from numerical calculation.

3.4.1 Theoretical Considerations

In this section the theoretical basis for the methodology that was presented to obtain the burnrates using discrete probability is discussed. As mentioned in earlier section, the calculation of complete time history of the system is very costly computation. The average burnrate is defined as

$$\omega_{ik} = (x_k - x_i)/(t_k - t_i)$$

where $x = x/l_0$ is non-dimensional distance between neighboring cells and $t = t(\kappa/l_0^2)$ is non-dimensional ignition time of cell.

The ratio of burnrates of random system described by gamma distribution, to periodic system is given by eqn. (15) from chapter 2. Considering the eqn. (15) from chapter 2

$$\omega_r/\omega_p = a^m \frac{\Gamma(a)}{\Gamma(a+m)} \quad (15)$$

where ω_r , ω_p are burnrates for a random and periodic systems respectively and a is the shaping parameter. Eq. (15) can be equivalently written as (shown in chapter 2)

$$\omega_r/\omega_p = \frac{1}{\langle L^m \rangle}$$

where $\langle L^m \rangle$ ($= E[L^m]$) is the expectation value of L^m . From the definition of expectation value

$$p(L^m \geq c) \leq \frac{\langle L^m \rangle}{c}$$

For $c=1$ (mean of distributing reaction cells is 1), which reduces to

$$1 \leq \frac{\langle L^m \rangle}{p(L^m \geq 1)}$$

In the context of the proposed approach, the above expression can be written by suitably choosing the limits of the integral as

$$1 \leq \langle L^m \rangle = \left[\int_{l(m)}^{ul} P(L) dl \right]$$

However, the use of m invariably needs the numerical calculation of the ignition times of the all the cells of the system. As mentioned in the earlier section, in the proposed method the lower integral limit has a dependence on ε with the upper limit fixed at 1.3 -

$$\omega_{r(\varepsilon)} / \omega_{p(\varepsilon)} = \int_{l(\varepsilon)}^{ul} P(L) dl \quad (16)$$

In general, the discrete probability is always less than or equal to unity and it is simpler to fix one of the limits and vary the other limit. As seen in the earlier sections, the upper limit is held constant for the ignition temperatures and the lower limit is modelled as a function of ignition temperature.

3.5 Conclusions

A simple and yet powerful correlation has been established between the burnrates and the ignition temperatures. One dimensional heterogeneous system is of interest in various fields and prediction of burnrates involves the tedious numerical calculation of the individual burntimes. The correlation discovered in this work completely eliminates the need for these costly computations and the problem is reduced to finding the discrete probability of pairs of cells that are separated between two limits. The upper limit for finding the discrete probability is fixed and the lower limit is modeled as a function of the ignition temperature. While it should be noted that other correlations leading to a similar answer may not be ruled out but what has been discovered is extremely helpful in reducing the computation time required for calculating the burnrates. Present method also augurs well for the systems with normal distribution of adjacent cells. In the case of normal distribution of adjacent cells the value of constants in lower limit functional dependence change.

3.6 References

- [1] A G Merzhanov, A S Mukasyan, A S Rogachev, A E Sytchev and A Varma, *Combustion Explosion and Shock Waves* **32**(6) 334–47 1996.
- [2] P Kumari, P K Baitha and J Manam, *Indian J Phys* **89**(12) 1297–1306 2015.
- [3] A Varma, A S Rogachev, A S Mukasyan and S Hwang, *Proc. Natl. Acad. Sci. U.S.A* **95** 11053-11058 1998.
- [4] S Hwang, A S Mukasyan and A Varma, *Combustion and Flame* **115** 354–363 1998.
- [5] A Varma, A S Mukasyan and S Hwang, *Chemical Engineering Science* **56** 1459-1466 2001.
- [6] A S Mukasyan, A S Rogachev, M Mercedes and A Varma, *Chemical Engineering Science* **59** 5099-5105 2004.
- [7] A S Mukasyan and A S Rogachev, *Progress in Energy and Combustion Science* **34** 377–416 2008.
- [8] A S Rogachev and F Baras, *Physical Review E* **79** 026214 2009.
- [9] A V Dvoryankin, A G Strunina and A G Merzhanov, *Combustion Explosion and Shock Waves* **21** 421–424 1985.
- [10] A R Kulkarni and K C Sharma, *Defence Science Journal* **48** 119-123 1998.
- [11] N Kubota and H Okuhara, *Chem. Abstr.* **111** 152 117793n 1989.
- [12] M W Beckstead and K P McCarty, *AIAA Journal* **20** 106–115 1982.
- [13] P S Grinchuk and O S Rabinovich, *Physical Review E* **71** 026116 2005.
- [14] S A Rashkovskii, *Combustion Explosion and Shock Waves* **41** 35–46 2005.
- [15] S A Rashkovskiy, G M Kumar and S P Tewari, *Combustion Science and Technology* **182** 1009–1028 2010.
- [16] N T Bharath, S A Rashkovskiy, S P Tewari and G M Kumar, *Physical Review E* **87** 042804 2013.
- [17] P S Bernard and Jun Shen, *Journal of Computational Physics* **199** 41–65 2004.
- [18] H Wang, P P Popov and S B Pope, *Journal of Computational Physics* **229** 1852–1878 2010.
- [19] S Francis , R R van Zyl and W J Perold, *Indian J Phys* **89**(8) 825–828 2015.

CHAPTER 4

Role of Heat Loss on the propagation limits of reaction front of heterogeneous mixtures

*A one dimensional discrete model for heterogeneous mixtures that involve heat loss is developed in present chapter. Theoretical study and numerical experiments are performed using the developed model to analyze the propagation of combustion front. Each reaction cell, characterized by heat parameter (β), is arranged on a one dimensional chain either in periodic or disordered manner. The dynamic behaviour of an internal micro structure of a periodic system at unstable modes of combustion is analyzed with inclusion of heat loss ($\beta > 0$). Reaction cells in disordered system are arranged by probability density function of gamma distribution. Wide ranges of disordered system are obtained by changing the shaping parameter (a) of gamma distribution. Results from numerical experiments suggest that the heat loss in the actual system does not affect the burn rate although plays a vital role in deciding the combustion limit; and is evident in the case of combustion of actual heterogeneous mixtures ($2Cr_2O_3 + 3Zr + n^*ZrO_2$, $Cr_2O_3 + 2Al + n^*Al_2O_3$) [12]. Heat loss in the system leads to decrease in thermal runaway and retards ignition process affecting the combustion limit. Matched combustion limits for heterogeneous mixtures are obtained numerically by developed model.*

4.1 Introduction

Heat energy released from the combustion process either results in enhancing or retarding the burning process [1-4]. Propagation of combustion front in actual combustion process is always accompanied by heat loss [1], due to ambient conditions. Heat loss results in retarding of the combustion process. Heat gain is observed in situations where chemical reactions occur with production of heat and also supplied by external heat around surface walls of the container. Heat gain increases the rate of reaction and promotes external thermal runaway [2-3]. Combustible mixtures undergoing exothermic reaction in the absence of heat loss will always attain the state of thermal explosion.

Instabilities in combustion front are due to temperature perturbation in a combustion chamber, these temperature perturbations lead to heat loss [1-11] in the form of radiation, convection, conduction and evaporation. Heat loss in practical situations is mainly due to radiation. Combustible mixture undergoing exothermic reaction in the presence of heat loss cannot attain the state of thermal explosion and combustion efficiency decreases [6] with increase in heat loss that results in soot formation [6,11].

Combustion process of thermite mixture ($2\text{Cr}_2\text{O}_3+3\text{Zr}+n*\text{ZrO}_2$, $\text{Cr}_2\text{O}_3+2\text{Al}+n*\text{Al}_2\text{O}_3$) [12] is affected with change in inert diluter and its percentage. The behavior of these thermite mixtures is interesting from other mixtures in two ways. 1) The burn rate of thermite mixtures ($2\text{Cr}_2\text{O}_3+3\text{Zr}+n*\text{ZrO}_2$, $\text{Cr}_2\text{O}_3+2\text{Al}+n*\text{Al}_2\text{O}_3$) are identical for identical burning temperatures even there is change of diluter (ZrO_2 , Al_2O_3). 2) The change of diluter for such mixtures only affects the combustion limit. Such a behavior of themite mixture is interesting to understand from an academic point of view. Detailed investigation for such reaction allows us to analyze the characteristic features of thermite mixture. Heterogeneous combustion models developed till today did not concentrate on such minute aspects; instead they have generalized the behavior of all thermite mixtures [13-15]. In addition, earlier literatures have not concentrated to account for heat loss parameter which is apparent during combustion process. Whereas experimental investigations [3-4, 7-11] are only limited for the calibration of the combustion parameters. [3] Reports the effect of change of distribution of point heat sources on burn rate without considering the heat loss of parameter of reaction cells. In real time situations, heat transfer affects internally the combustion performance, efficiency, and emissions.

The heterogeneous combustion models [8, 13-15] developed until now have neglected the heat loss parameter. One dimensional heterogeneous combustion model described in chapter 2 explains the role of disorderness in internal microstructure of a combustible system by assuming there is no heat loss of a reaction cell. Combustion limit or flame extinction in actual combustible systems are the consequences of heat transfer, and this heat transfer may be in the form of loss or gain in the system. Present chapter describes the one dimensional discrete combustion model that accounts for randomness in internal microstructure with inclusion of heat loss in the system. Numerical experiments for different values of heat parameter are performed and results thus obtained are compared with the available experiments on combustion of thermite mixture performed by *Dvoryankin.etal* [12]. The model proposed in this chapter concentrates on the mixing, packing of actual thermite mixtures and their heat loss. The mixing and packing of heterogeneous mixtures is addressed by varying the internal microstructure of the system. Heat loss during combustion of heterogeneous mixture is addressed by the heat parameter.

Heterogeneous combustion process is now simulated in present chapter by assigning discrete positions (similar to chapter 2) and heat loss to the reaction cells. The present chapter reports for behavior of wide ranges of disordered system with inclusion of

heat parameter on reaction front propagation and combustible limits. Detailed analysis for the effect of heat loss parameter on combustion process would facilitate the combustion designer with knowledge of combustible limits.

4.2 Modeling

4.2.1 System definition and assumptions

One dimensional system, consisting chain of reaction cells (the point heat sources particles), distributed along an axis x in periodic and random manner, is considered here. In addition to above specification the heat parameter is adjusted for each reaction cell during reaction front propagation. The medium filling the space between the reaction cells is characterized by thermal conductivity k , density ρ , and heat capacity c . The cells are considered to be immobile and are characterized by an ignition temperature T_{ign} and heat parameter (β). When the temperature of an unburnt cell reaches the value T_{ign} , the ignition and instantaneous burning away of the cell occurs with the release of heat Q_i . The present model is based on the existing theories of flame Propagation [13]. The problem is explained by equation

$$T(t, (x(\beta))) = T_{\text{in}} + \sum_{i(t)} \Delta T_i((t - t_i), (x - x_i)) * ((t - t_i)\beta_i)$$

T_{in} is the initial temperature of the system; t_i is the instant of ignition of the i^{th} cell, located at (x_i) and $\Delta T_i(t, (x))$ is the temperature induced at the point x with β at time moment t by a single-point heat source, located at $x_i=0$ and ignited at time moment $t_i=0$. The summation in expression is over all sources i ignited up to time moment t . For a one-dimensional problem the governing equation for calculating temperature of particle with heat parameter can be obtained as

$$2\sqrt{\pi\varepsilon} = \sum_{i=-\infty}^{k-1} \frac{q_i}{\sqrt{(t_k - t_i)}} \exp \frac{-(x_k - x_i)^2}{4(t_k - t_i)} \exp^{-\beta(t_k - t_i)} \quad (1)$$

Equation (1) is obtained by introducing non-dimensional parameters to the thermal conductivity equation (similar as shown in chapter 2). In practical situations [3-4, 7-12], heat transfer mechanism along with mixing and packing heterogeneous mixture become important during combustion process. The heat parameter β is introduced for each reaction cell to account for heat loss or heat gain in the system. $\beta = \frac{kt}{\rho c}$ is the heat parameter associated with the reaction cell. $\beta=0$ corresponds to the system with neither heat loss nor heat gain and it is same as that of the system considered in chapter 2, $\beta < 0$ is considered as the system with heat gain generally this kind of combustion reactions are practical in case of explosions where as $\beta > 0$ represents the system with heat loss during combustion reactions

and are observed in combustion of thermite mixtures and solid propellants. Situations like larger surface [1] to heat source promote heat loss and retards ignition. In a macro scale combustor, heat loss during the flame propagation is much smaller than the heat produced by the combustion and the heat loss can be effectively ignored in the calculation of the combustion. In a micro scale combustor, the increased heat loss decreases the combustion efficiency and causes quenching when it becomes excessive. Reaction front propagates in radial direction while the dominant heat transfer is towards the top and bottom of combustor walls if the width of the combustor is very small. Heat loss becomes apparent with increasing characteristic time for conduction [3-4]. The present chapter reports for detailed numerical and theoretical analysis for combustion wave propagation with the influence of heat loss ($\beta > 0$).

Consequently flame extinction [7-11] occurs if the heat loss from reaction front becomes excessive. Ignition is directly affected by heat loss, while extinction or combustion limit is affected by reduction in reaction rate [5]. The mean burn rate [13-16] of the system is computed as

$$\omega_{ik} = \frac{(x_k - x_i)}{(t_k - t_i)} \quad (2)$$

Increase in rates of reaction (burn rate) promotes the external thermal runaway whereas increase in heat loss retards thermal runaway and promote the combustion limit. The combustion dynamics depends on relative rates of above two processes. To account for conductive heat loss there must be existence of temperature gradient in a system (model). Flame extinction or combustion limit is achieved in model either by removing a certain amount of branching radicals or by removing certain amount of heat. Reducing branching radicals is achieved by introducing chemical inhabitants into reaction region. Reduction of certain amount of heat is achieved by reducing the reaction rate by blowing it with cold gas or decreasing the reactant concentration. These effects in combustion dynamics are investigated by present one dimensional discrete model that accounts for internal microstructure and heat loss.

4.2.2 Theoretical analysis of Periodic system

Consider briefly the characteristics of combustion of one-dimensional periodical systems with identical point heat sources; that is, in the system under consideration $x_k = kl_0$ and

$Q_k=Q_0$ for any k . The induction period (τ_i) here is introduced as a time interval between ignitions of two neighbor sources

$$\tau_i = t_i - t_{i-1}$$

and then an instant burn rate of periodical system is $\omega_i=1/\tau_i$, then Eq. (1) becomes

$$2\sqrt{\pi\varepsilon} = \sqrt{\omega} \sum_{k=1}^{\infty} \frac{1}{\sqrt{k}} \exp\left[\left(\frac{-\omega}{4} + \frac{\beta}{\omega}\right)k\right] \quad (3)$$

The theoretical dependence $\omega(\varepsilon)$ of non dimensional burn rate on non dimensional ignition temperature (Figure 4.1) is the solution to Eq. (3). Theoretical dependence Eq. (3) thus obtained is utilized for comparison with the numerical results calculated using eq.(1). Figure 4.1 shows that the comparison plot between burning rate (ω) and ignition temperature (ε) for a periodic system for different values of heat loss.

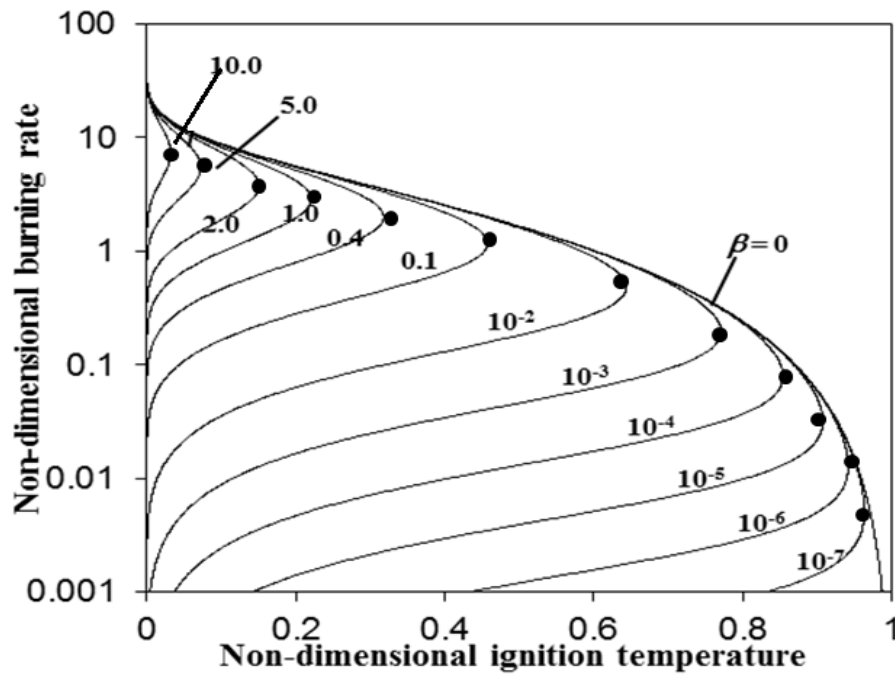


Figure 4.1 Plot between Non-dimensional Ignition temperature and Burn rate calculated using theoretical equation (3) for different values of β . The circles in the figure show the maximal value of ignition temperature that can be obtained using theoretical equation (3).

As the heat loss value is increased the combustion limit or existence of ignition temperature decreases. However the burning rate remains same within the combustion limits at different values of heat loss. For values of $\beta < 10^{-8}$, it is observed that there exists two values of burn rates for a single ignition temperature. The lower curve in figure 4.1 shows that the non-dimensional ignition temperature and burn rate are directly proportional to each other, this situation is not possible in actual situations. The lower curve obtained from eqn. (3) is because of increase in value of β . As the heat loss parameter increases, the combustion limit

decreases. For a given β , a system with $\varepsilon > \varepsilon_{cr}$ steady state combustion is not possible. Hence the upper curve values of burn rate are considered as actual.

The presence of heat loss introduces a limit to survival of ignition temperature [17] even for a periodic system [7-11]. Heat loss in the system causes increase in thermal runaway thus retarding the ignition process. As heat loss increases the theoretical dependence Eq. (3) cannot have solutions at higher ignition temperatures. ε_{cr} (theoretical) at a particular heat loss is obtained as maximal value of existing ignition temperature.

4.3 Results

4.3.1 Numerical Calculation of Burn rates of Periodic system

The numerical dependence ($\omega(\varepsilon)$) using eq.(1) can be explained by simulating the periodic system with concatenation of point heat sources characterized by heat parameter on one dimensional chain. Total point heat sources in the system were divided into two categories - 1000 burnt and 2500 unburnt point heat sources. Initially all the first 1000 particles are considered to be ignited at $\tau_i = 0$. Two cases for distribution of heat parameter of reaction cells are considered one with identical heat loss and the other with random distribution of heat loss. Now the system is left to itself, and the simulation of propagation of reaction front in accordance to eq.(1) is performed at different values of heat loss. The method of distribution (identical or random) of heat loss values did not affect combustion performance. Hence in numerical experiments identical value of heat loss for all reaction cells are considered. The temperature of each unburnt cell is obtained by incrementing the time t_k , and for predetermined ignition temperature the ignition time of the k^{th} particle is noted. The ignition time is calculated for all unburnt cells and the burn rate is now obtained by using eq.(2). The in house C code for numerical simulation of combustion process is compiled and validated for different values of Heat loss parameter (β). Figure 4.2 shows the comparison plot for burn rates of different values of β obtained using Eq.(1) and Eq.(3) which hints C code is simulating combustion process with complete agreement to the theoretical Eq.(3).

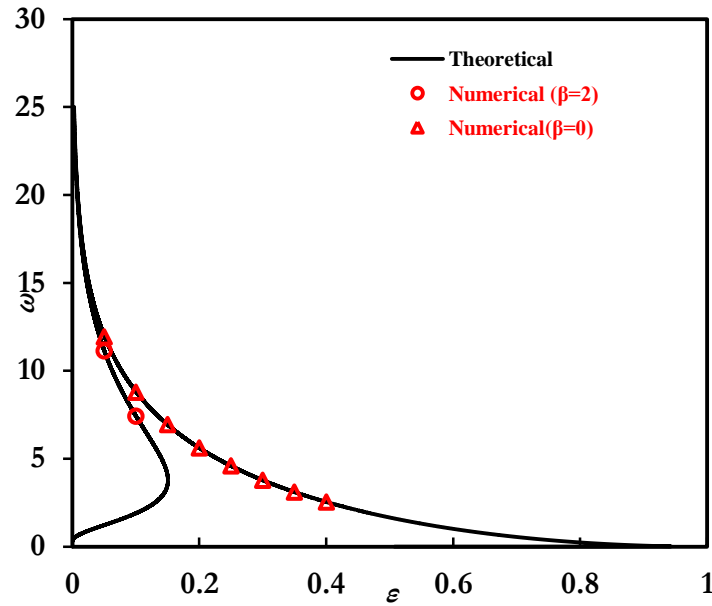


Figure 4.2. Comparison Plot between burn rates (ω) for different values of β . Circles obtained by Eq. (1) and solid lines by Eq.(3).

In spite of the fact that Eq. (3) (solid line in Figure 4.2) has theoretical solutions for all $\varepsilon < 1$, a steady state combustion for a periodic system can exist only in the limited range of parameter ε which can be obtained by numerical calculation of Eq.(1). This can be explained by obtaining the numerical combustion limit of a system using eq.(1).

4.3.2 Combustion limits

This combustion limit [17-20] is defined as the condition when the heat release of the entire domain of particles is just sufficient to increase the bulk temperature of the mixture to the ignition temperature. During the numerical calculation of ignition times of reaction cells at higher ignition temperatures (or at higher values of heat loss) it is observed that the temperature of unburnt particle reaches maximum temperature and then starts decreasing as the time increases as shown in Figure 4.3.

The combustion front doesn't propagate for higher temperatures, this is termed as critical ignition temperature ($\varepsilon_{cr(numerical)}$) of a periodic system. At $\varepsilon < \varepsilon_{cr(numerical)}$ a combustion mode is stable and the combustion process reaches a steady-state mode that proceeds until all heat sources are burnt. It can be observed from table 4.1 that the numerical combustible limit of a periodic system is less than the theoretical combustible limit for each value of heat loss parameter.

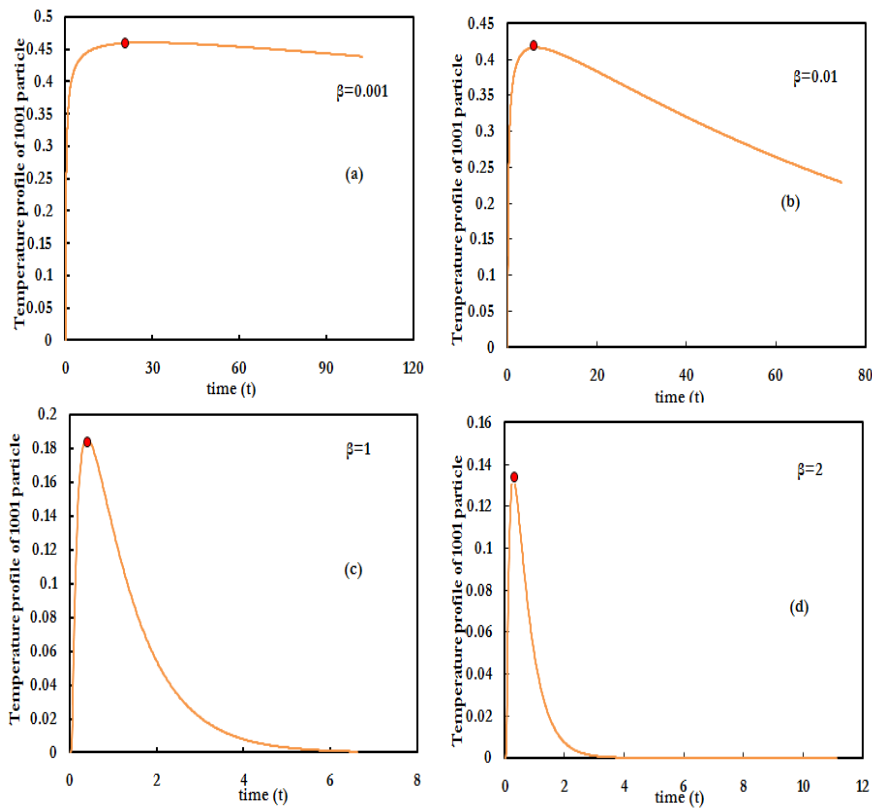


Figure 4.3 Plot between temperature of a unburnt particle and time calculated using numerical equation (1) for different values of β . Dots in figure represent the numerical combustion limit.

Heat loss (β)	$\varepsilon_{cr}(\text{Theoretical})$	$\varepsilon_{cr}(\text{numerical})$
0.0001	0.85	0.47
0.001	0.77	0.46
0.01	0.64	0.4
1	0.25	0.18
2	0.15	0.13

Table 4.1. Theoretical and numerical combustible limits.

The propagation of combustion front is in stable mode for $\varepsilon < \varepsilon_{cr}(\text{numerical})$ at different values of heat loss parameter. The periodic arrangement of neighboring point heat sources is a fundamental property, this means that dynamic behavior of internal microstructure is unaffected by small perturbations at $\varepsilon < \varepsilon_{cr}(\text{numerical})$. Hence it is of academic interest to analyze and justify the structural stability at higher ignition temperatures ($> \varepsilon_{cr}(\text{numerical})$) with affect to change in initial parameters.

The numerical calculations performed till now in this chapter were constrained to a periodic system. The role of randomness in internal microstructure of an actual combustible system is well established in chapter 2. To investigate the dynamic characteristics of actual combustible system with effect of heat loss the change in internal microstructure is

introduced. Unburnt particles in disordered system are distributed utilizing the probability density function of gamma distribution for random system (similar to system described in chapter 2). The probability density function of gamma distribution with different values of shaping parameter ($a=1, 5, 20$) is shown in Figure 4.3 (chapter 2). Numerical simulation and computation of modeled system for different realizations of internal microstructure and heat loss parameter requires high computing speed. This can easily achieved by in house C code with provision of parallel execution.

4.3.3 Disordered System

Present section focuses on the numerical results obtained for disordered system and analyze the same in the view of actual systems. During numerical experiments two issues that arise generally for actual systems like mixing, packing and heat transfer mechanism of thermite mixtures are addressed by varying the internal microstructure and heat parameter. Analysis of extreme reaction conditions during combustion synthesis process requires new methods for controlling the microstructure of the system [21-24] and ambient heat loss. It is therefore important to perform numerical experiments and analyze the results obtained. Heat loss parameter (β) is employed for each reaction cell in a identical fashion. Hence the numerical results of a disordered system modeled with different internal microstructures and identical heat loss parameter are reported. Figure 4.4 and 4.5 displays ignition time profiles for different heat loss parameters ($\beta=0.0001$ and $\beta=0.01$) of different systems. The reaction front for an ordered (periodic) system (represented by (d)) shows linear relation between the non-dimensional ignition time and non-dimensional distance unlike the reaction front for disordered (gamma distribution) system. It is also observed that the reaction front propagates linearly for all systems at lower ignition temperatures (<0.10). As the ignition temperature increases the reaction front starts propagating with stops and this is similar to unstable combustion. Even in actual systems the steady combustion becomes unstable at higher ignition temperatures and is evident when observed with high speed micro video recording [22-23]. Earlier literatures [13-15] where the heat loss is neglected reports the critical combustion or unstable combustion ($\epsilon>0.42$) is similar for all disordered systems. In actual systems this is not the case. During actual combustion process as the temperature increases due to chemical heat release, the rates of reaction and conductive heat loss increases. Because of heat loss there exist a minimum separation between reaction cells beyond which flame cannot propagate. Inherent heat loss mechanisms are associated with combustion front, such as diffusive heat transfer and radicals transfer in presence of steep temperature and

concentrations gradients at the reaction front. Heat loss is also associated with radiation either from high temperature front or formation of soot particles.

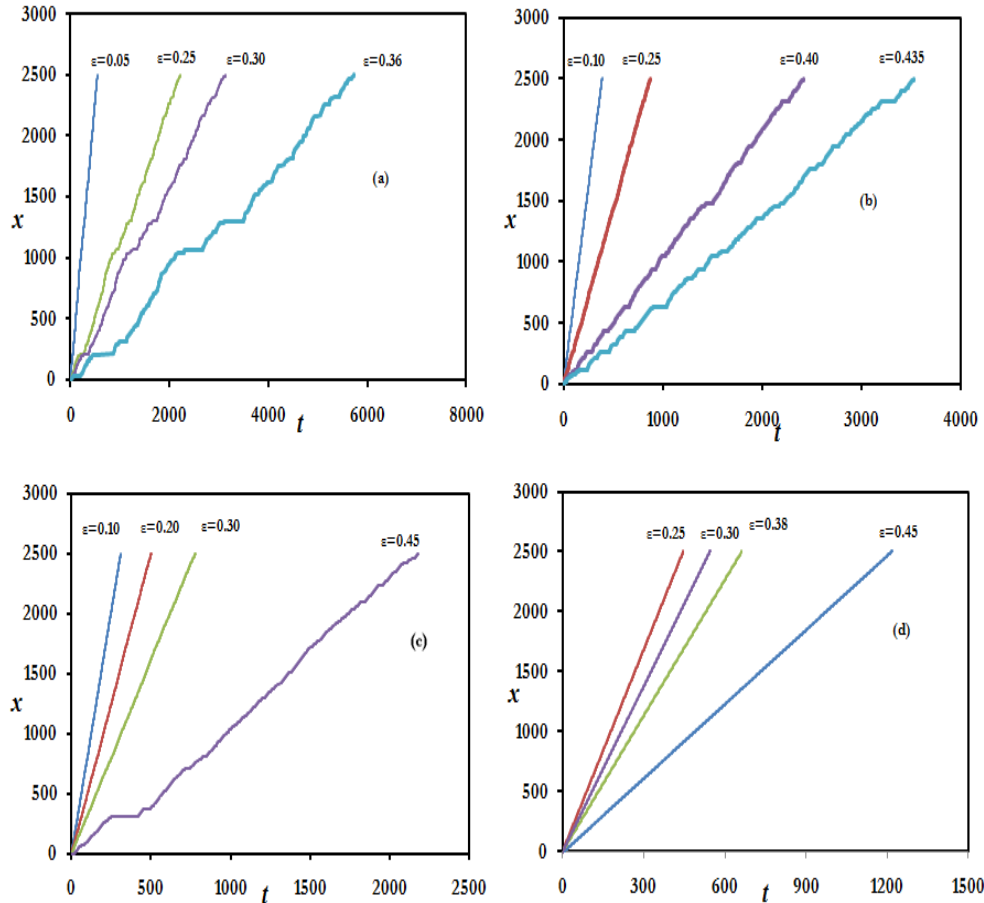


Figure 4.4. Ignition time profiles for $\beta=0.0001$ of a different systems. (a) $a=1$; (b) $a=10$; (c) $a=20$; (d) is periodic.

Numerical results from developed model show that the heat loss in conjunction to internal microstructure plays a crucial role in combustion limit. The critical combustion or non-linear propagation of thermal wave begins at different ignition temperatures for different systems as shown in figure 4.4 and 4.5. Combustion wave propagation is clearly observed to be shifting from stable to unstable for gamma distributed system with shaping parameter (a)=1 as ignition temperature increases. Instabilities in combustion front are due to temperature perturbation in a combustible system. Instability in combustion wave propagation or reaction front stops is more pronounced for the cases of high ignition temperature with randomness in the system. The available heat energy in system has to compensate the heat loss of reaction cells and disordered microstructure of system characterized by different probabilities of inter particle spacing of point heat source particles in system.

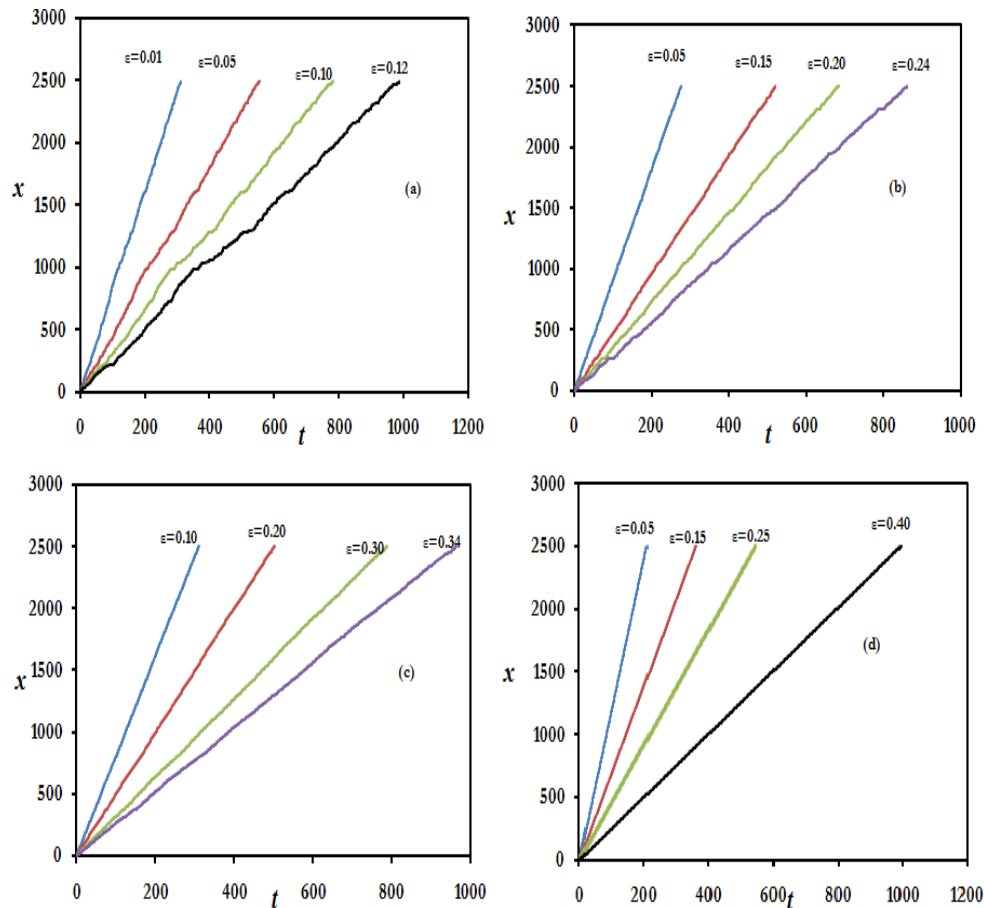


Figure 4.5. Ignition time profiles for $\beta=0.01$ of a systems described by different positioning of reaction cells. (a) $a=1$; (b) $a=10$; (c) $a=20$; (d) is periodic.

As the disorderness (for $a=1$) and heat loss ($\beta=0.01$) increases in the system the critical combustion begins even at lower ignition temperatures ($\epsilon=0.12$). This can be clearly inferred from figure 4.5. The commencement of critical combustion is due to thermal runaway of reaction cells that retards ignition process. Systems with higher heat loss ($\beta=0.01$) and disordered microstructure have higher thermal runaways because of temperature perturbations. Temperature perturbations retard the ignition process in the form of conduction and radiation process. The temperature perturbations are direct consequences of uncertainty in ignition delay times. Figure 4.6 represents the distribution of ignition delay times for reaction cells arranged by gamma distribution ($a=1$ and 20) and cells are characterized by different heat loss values.

It is clearly observed that the distribution of ignition delay times of reaction cells are more clustered for value of $\beta=0.01$. Ignition delay times are more uncertain for higher heat loss values. These characteristics results in more instabilities. The instabilities in reaction front propagation are associated with increased ignition delay times which are directly proportional to the induction periods and ignition temperature of a system. Uncertainty in ignition delay

times of a reaction cells increases with increase in ignition temperature and disordered microstructure of system. These uncertainties in ignition delay times in the system causes for slow self heating. The effect of ignition delay times and temperature gradients plays the crucial role in deciding the stability of reaction front, combustible limits.

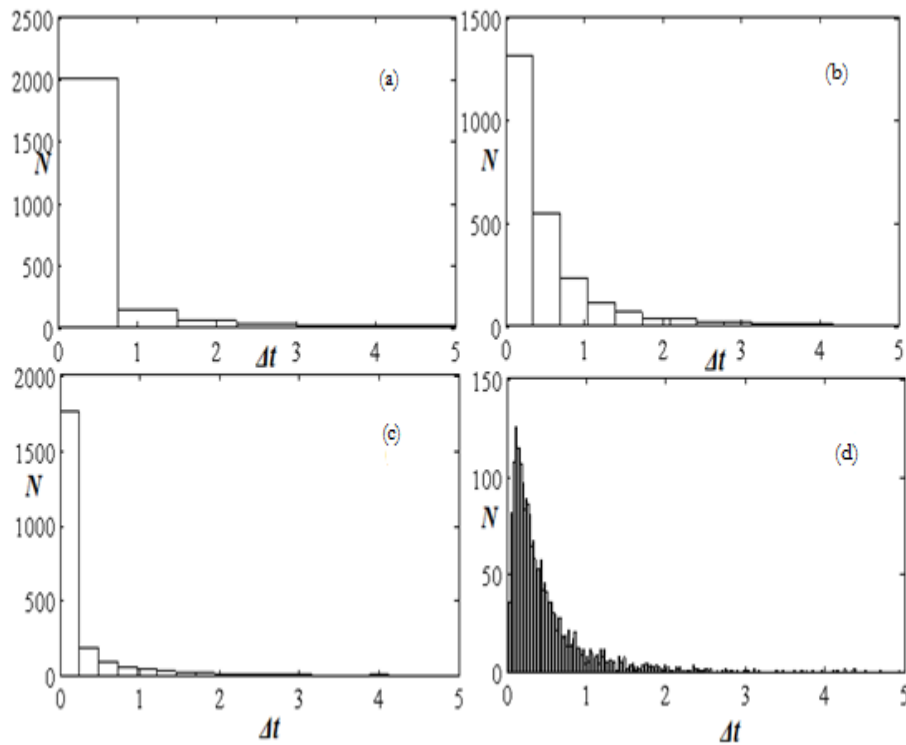


Figure 4.6 Distribution of delay in ignition times for different systems. (a) $a=1$ & $\beta=0.0001$; (b) $a=20$ & $\beta=0.0001$; (c) $a=1$ & $\beta=0.01$ and (d) $a=20$ & $\beta=0.01$.

4.3.4 Combustible limits of Disordered system

Here the combustible limits of disordered system with respect to different heat loss are determined. Combustion limits refer to range of compositions of mixtures, for fixed burning temperature, with in which a chemical reaction is possible when an external ignition source is introduced. Combustion limits are not absolute, but depend on percentage of diluters and strength of ignition source. Experimental studies have shown that the stronger the source of ignition stimulus, the leaner the mixture that can be ignited. Combustion limits for thermite mixture ($2\text{Cr}_2\text{O}_3+3\text{Zr}+n*\text{ZrO}_2$, $\text{Cr}_2\text{O}_3+2\text{Al}+n*\text{Al}_2\text{O}_3$) [9] varies with change in percentage of diluter (ZrO_2 , Al_2O_3). It is established that the propagation of reaction front under actual conditions is always accompanied by heat losses, which can result in combustion break off.

The existence of an ignition temperature for heterogeneous systems of particles in suspension introduces a limit to reaction front propagation [23-24]. This combustion limit is defined as the condition when the heat release of the entire domain of particles is just sufficient to increase the bulk temperature of the mixture to the particle ignition temperature. This condition is equivalent to stating that the adiabatic temperature is equal to the ignition temperature. In actual conditions the heat loss is introduced either by changing the percentage of diluter or by blowing cold nitrogen air over the reacting sample against the reaction front. Numerical combustion limit for one dimensional disordered system is evaluated as point of ignition temperature above which the reaction front doesn't propagate through the system. Numerical combustible limit is obtained using Eq. (1). Figure 4.7 show the temperature profile of a burning particle at different critical ignition temperatures for $\beta=0.0001$ and $\beta=0.01$.

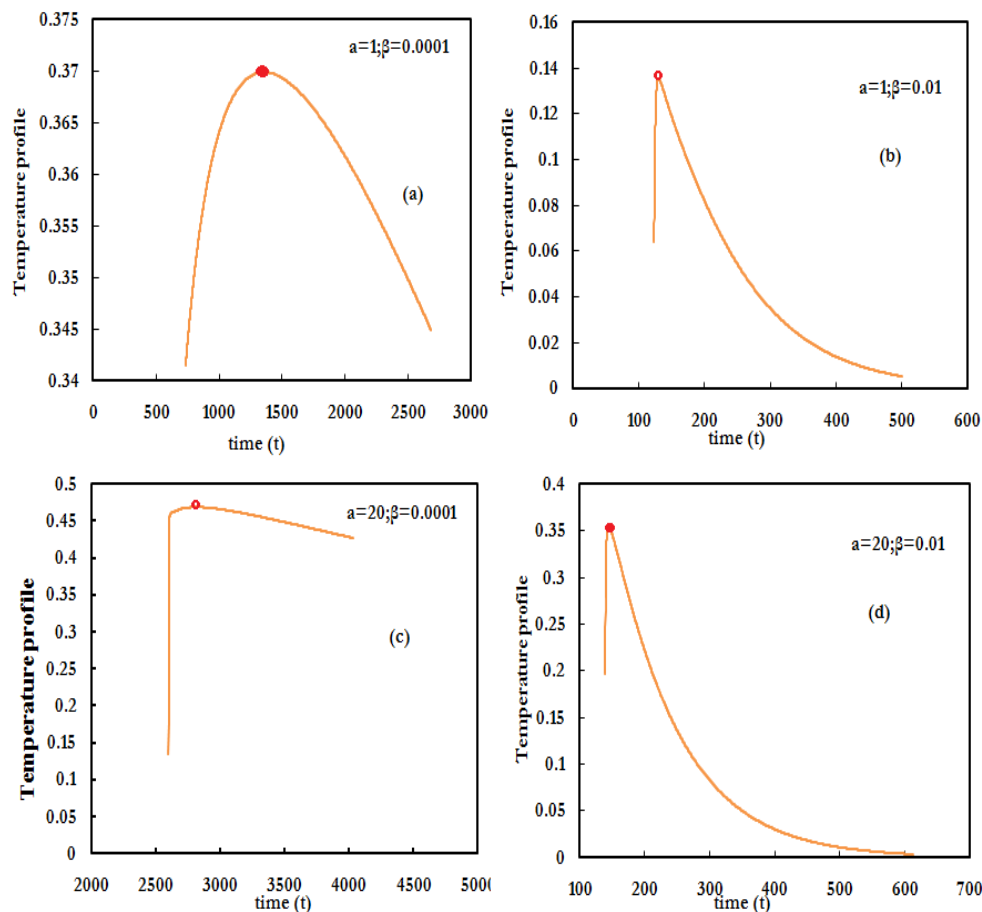


Figure 4.7 Temperature profile for unburnt particle of a disordered system. (a) $\epsilon=0.37$ for 1183 particle (b) $\epsilon=0.14$ for 1184 particle (c) $\epsilon=0.47$ for 3101 particle (d) $\epsilon=0.36$ for 1304 particle.

Note here system whose reaction cells are arranged by gamma distribution with shaping parameter $a=1$ (figure 4.7(a) and (b)) and shaping parameter $a=20$ (figure 4.7(c) and (d)) are considered. The same is repeated for other disordered systems at other values of heat loss

($\beta=0.1, 1, 2..$). It is observed that as time increases the temperature of unburnt particle reaches maximum temperature and then after decreases with increase in ignition time. Thus the numerical combustion limit is obtained numerically and this analysis would provide combustion engineer with information regarding the possible combustion limits. The numerical combustible limit for disordered (gamma distribution) system decreases when compared to periodic combustible limit because of increase in uncertainty in inter particle spacing and heat loss (β).

Table 4.2 illustrates the numerical combustible limits of disordered system with different values of heat loss parameters. It is observed that the combustible limits decreases with increase in randomness of the system structure.

Heat loss(β)	$\varepsilon_{cr(numerical)} (a=1)$	$\varepsilon_{cr(numerical)} (a=10)$	$\varepsilon_{cr(numerical)} (a=20)$
0.0001	0.36	0.44	0.45
0.001	0.255	0.39	0.4
0.01	0.12	0.3	0.34
1	0.000091	0.03	0.07
2	0.0000026	0.013	0.03

Table 4.2. Numerical combustible limits of disordered system.

Combustible system with absence of heat loss ($\beta=0$) the burning temperature is just the adiabatic temperature and the flammability limit for such systems is observed for quite high ignition temperature.

4. 3.5 Burn rate

Burn rate for the developed modelled are calculated numerically using Eq. (1) and Eq. (2). Figure 4.8 shows the burn rates calculated for different gamma distribution ($a=1, 2, 5, 10, 15, 20$) systems and periodic system. It is observed that the burn rate decreases with increase in randomness of the system. Gamma distribution system with $a=1$ is mostly randomized when compared to the gamma distribution system with $a=20$. It is interesting to observe from the numerical results that the burn rates are not affected by the heat loss parameter for a particular system.

The modelled system or heterogeneous mixture with different heat loss or diluter does not affect burn rate at same ignition temperature. This type of combustion can be observed in

burning of thermite mixtures ($2Cr_2O_3+3Zr+n*ZrO_2$, $Cr_2O_3+2Al+n*Al_2O_3$). Burn rates of a random system are essentially less than the burn rate of a periodic system.

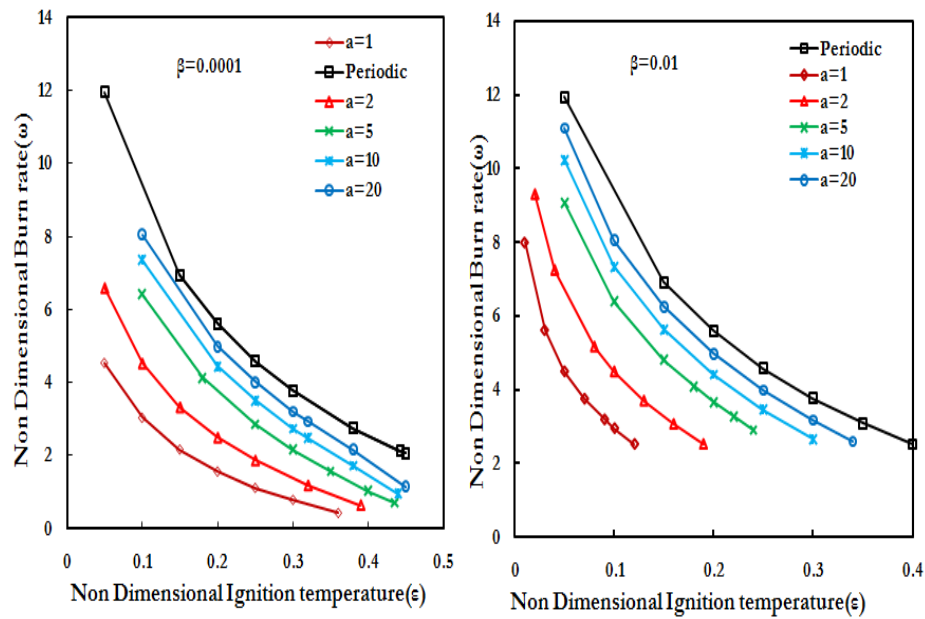


Figure 4.8. Plot for comparison of Burn rates of different systems calculated using Eq.(1) and Eq. (2).

The comparison of experimental data for combustion of thermite systems with theoretical model developed in earlier section. The work of authors [12] investigate that the burning rate changes with burning temperature for a broad range by altering the inert diluter and percentage of inert diluter. Figure 4.9 comprise the data of work [12] ($2Cr_2O_3+3Zr+n*ZrO_2$, $Cr_2O_3+2Al+n*Al_2O_3$), processed in co-ordinates of burn rate and burning temperature. The above mentioned thermite mixtures has different behavior from the other mixtures [12]. It is very interesting to observe that the burn rates for thermite mixture don't vary with change in diluter for particular burning temperature. However the burn rates and inflammability limits changes with change in percentage of diluter. Hence it is of academic interest to find out accurate model parametr and establish the developed model by comparing with available experimental data. The numerical results obtained from model developed in earlier sections are compared with experimental data [12]. The arrows in Figure 4.9 correspond to commencement of oscillating mode for combustion process of different thermite mixtures.

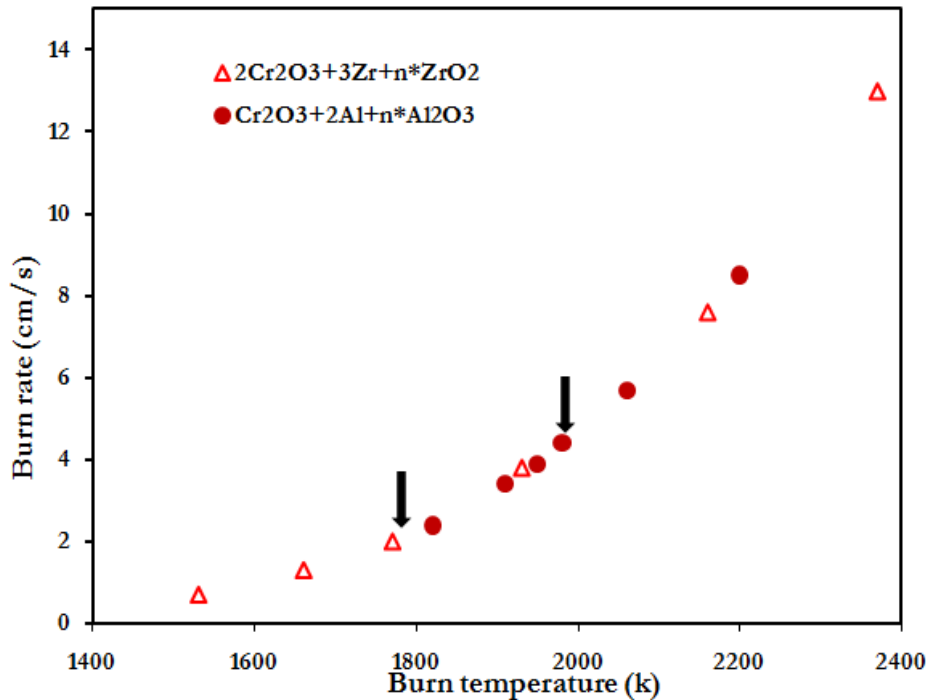


Figure 4.9 Plot for comparison of Burning rates and burning temperature for thermite mixture[12].

Treatment of experimental data [12] have been performed in non dimensional co-ordinates $\varepsilon - \omega$. Theoretical values of the critical parameters such as ε_{cr} and ω_{cr} are assumed as commencement of oscillating modes of combustion, practical in experiments. The percentage and change of inert diluter is correlated with heat loss parameter. Assuming the critical values of rate of burning (r_{cr}) and burning temperature ($T_{ad_{cr}}$), measured in experiments, correspond to commencement of oscillating modes of combustion process for an actual system. Then eqn. (27), from [15], in accordance with Figure 4.9, critical non-dimensional burning rate $\omega_{cr} = \omega(\varepsilon_{cr})$ depends on the shaping parameter of neighboring reaction cells and inflammability limit depends on heat loss parameter (β); this implies that ω_{cr} depends on the system microstructure and heat loss parameter (β).

Experimental data [12] (represented by symbols) are treated using expressions (27)-(29) from [15], similar to method shown in [15] and chapter 2, are shown in Figure 4.10. Treated experimental results are now compared with numerical results obtained from developed model in figure 4.10. It is numerically obtained from developed model that a system with $\beta > (10^{-8})$ has no effect on combustion limit and is similar to system with $\beta = 0$ (neither heat loss nor heat gain). $\beta < (10^{-8})$ is considered as critical heat loss parameter. The

commencement of unstable combustion begins at different ignition temperatures for different values of shaping parameter and heat loss (β).

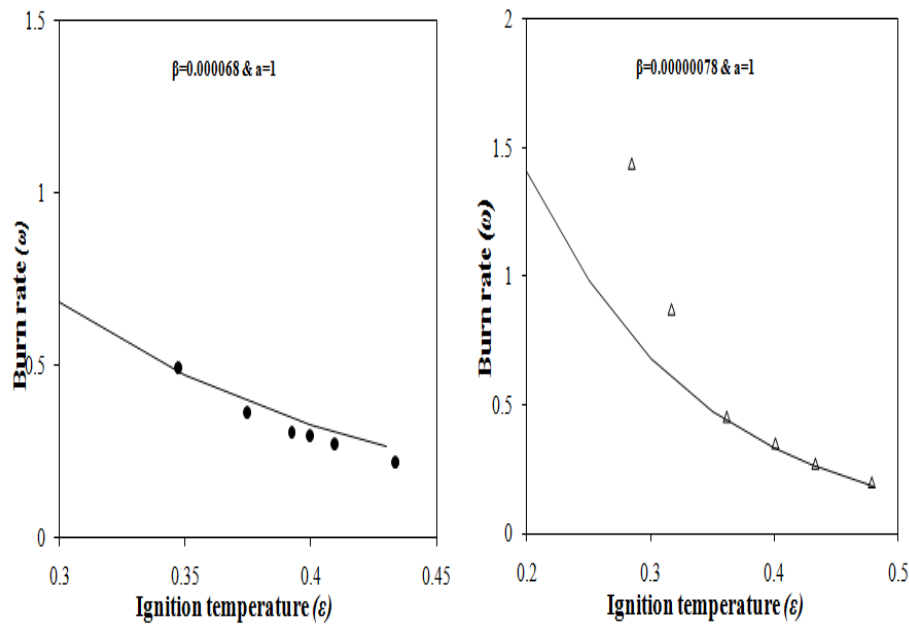


Figure 4.10. Comparison plot between experimental and develop model results for burn rates and combustible limits. Solid lines are obtained from develop model and symbols are representation of experimental [9] .

This is mainly due to the temperature disturbances associated within the system due to heat loss and internal microstructure. As heat loss increases the heat energy released from combustion of particle is lost to surroundings and combustion of succeeding particle. This other way resembles to external cooling of the mixture. The more the heat loss the less is the critical flammability limit and inflammability limit. Suitable heat loss parameter is obtained for agreement of experimental inflammability limit of mixture. These values are found to be $\beta=68 \times 10^{-6}$ with $a=1$ for mixture $\text{Cr}_2\text{O}_3+2\text{Al}+n \cdot \text{Al}_2\text{O}_3$ and $\beta=78 \times 10^{-8}$ with $a=1$ for mixture $2\text{Cr}_2\text{O}_3+3\text{Zr}+n \cdot \text{ZrO}_2$. Experimental burn rates for ignition temperatures above 0.35 are in close agreement with the burn rates calculated by developed model. The inflammability limits for thermite mixtures using diluters ZrO_2 and Al_2O_3 is at temperature 1530K and 1820k respectively and is in close agreement with the limits $\epsilon=0.478$ and $\epsilon=0.433$ obtained by developed model. Thus the developed model (that includes variation in microstructure and heat loss parameters) allowed prediction of the burn rates and inflammability limits of Cr_2O_3 with different diluters. This type of study can now be even extended to analyze the behavior of other thermite mixtures by suitably varying the parameters.

4.4. Conclusion

Modeling of heterogeneous combustion process with inclusion of heat parameter (β) is performed on a one dimensional chain of reaction cells arranged either in ordered or disordered manner. Unstable modes of combustion in periodic system have been investigated for different values of heat loss. Wide ranges of disordered systems are obtained by changing the shaping parameter (a) of gamma distribution. Heat loss parameter ($\beta > 0$) is identical for all cells. Propagation of combustion front and its limits have been investigated numerically. Heat loss (β) is crucial parameter that effects on the combustible limits. As heat loss increases the combustible limit decreases. Burn rates of the system are calculated for different values of β and are affected by the change in microstructure of the system and remain unaffected by the heat loss parameter (β). Results of developed model are compared with experimental result on combustion of thermite mixtures ($2\text{Cr}_2\text{O}_3 + 3\text{Zr} + n*\text{ZrO}_2$, $\text{Cr}_2\text{O}_3 + 2\text{Al} + n*\text{Al}_2\text{O}_3$) in the view of burn rates and inflammability limits. Numerical results from developed model completely agrees with experimental results at higher values of ignition temperature ($\epsilon > 0.3$).

4.5 References

- [1] P. N. Nwosu, *Dimensionless Heat Transfer Correlations for Estimating Edge Heat Loss in a Flat Plate absorber*, Journal of Engineering Thermophysics, 2012, Vol. 21, No. 3, pp. 198–211.
- [2] K. G. Shkadinskii, A. N. Firsov, and N. I. Ozerkovskaya, *Critical Phenomena in the Cellular Mode of Filtration Combustion in the Presence of Heat Loss*, Combustion Explosion and Shock Waves, (2012), Vol. 31, No. 1, pp. 48–53.
- [3] V.I. Ermakov, A.G. Strunina and V.V. Barzykin, *Effect of heat loss on the processes of the ignition of gasless systems by a combustion wave*, Translated from Fizika Goreniya i Vzryva, Vol. 14, No. 6, pp 36-44, Nov-Dec, 1978.
- [4] A. G. Strunina, S. V. Dergachev, L. K. Demidova, and V. V. Barzykin, *Experimental Study Of The Stability and Transient Combustion Regimes for Low-gas Compounds*, Translated from Fizika Goreniya i Vzryva, Vol. 29, No. i, pp. 78-82, January-February, 1993.
- [5] B. L. Kopeliovich, *Gasless Combustion Wave with Extremely High Excess Enthalpy under Heat Loss Conditions*, Russian Journal of Physical Chemistry B, 2011, Vol. 5, No. 1, pp. 110–115.
- [6] Dae Hoon Lee and Sejin Kwon, *Heat transfer and quenching analysis of combustion in a micro combustion vessel*, J. Micromech. Microeng. **12** (2002) 670–676.

- [7] C. B. Vining, A. Zoltan and J. W. Vandersande, *Determination of the Thermal Diffusivity and Specific Heat Using an Exponential Heat Pulse, Including Heat-Loss Effects*, International Journal of Thermophysics, Vol. 10, No. 1, 1989.
- [8] M. Nikian, M. Naghashzadegan and S. K. Arya, *Modeling of Heat Losses Within Combustion Chamber of Diesel Engines*, International Journal of Engineering Science, Vol. 17, No.3-4, 2006, Page 47-52.
- [9] Peter L. Simon, Serafim Kalliadasis, John H. Merkin and Stephen K. Scott, *Quenching of flame propagation with heat loss*, Journal of Mathematical Chemistry Vol. 31, No. 3, April 2002.
- [10] A. G. Strunina, L. K. Demidova, A. N. Firsov, and A. G. Merzhanov, *Stability of Gasless Combustion in the presence of heat loss*, Translated from Fizika Goreniya i Vzryva, Vol. 23, No. 3, pp. 52-58, May-June, 1987.
- [11] Yu. M. Maksimov, A. G. Merzhanov, A. T. Pak, and M. N. Kuchkin, *Unstable Modes of Gasless systems*, Translated from Fizika Goreniya i Vzryva, Vol. 14, No. 6, pp. 36-44, July-August, 1981.
- [12] Dvoryankin A. V., Strunina A. G., and Merzhanov A. G. Stability of combustion in thermite systems, Comb. Expl. Shock Waves, 21, No. 4, 421–424 (1985).
- [13] S.A. Rashkovskiy. *Hot-spot combustion of heterogeneous condensed mixtures. Thermal percolation*. Comb. Expl. Shock Waves 41 (3) 35-46(2005).
- [14] Sergey A. Rashkovskiy, G. Manoj Kumar, Surya P. Tewari . *One-Dimensional Discrete Combustion Waves in Periodical and Random Systems*. Comb. Sci & Tech 182, 1009(2010).
- [15] Naine Tarun Bharath, Sergey A. Rashkovskiy, Surya P. Tewari, and Manoj Kumar Gundawar, *Dynamical and statistical behavior of discrete combustion waves: A theoretical and numerical study*, Phys. Rev. E 87,042804 (2013).
- [16] N. Kubota and H. Okuhara, *Burning Rate Temperature Sensitivity of HMX Propellants*, Chem. Abstr. **111**, 152 (117793n) (1989).
- [17] N. Kubota, *Role of Additives in Combustion Waves and Effect on Stable Combustion Limit of Double-Base Propellants*, Propellants Explosives **3** (6), 163–168 (1978).
- [18] M. W. Beckstead and K.P.McCarty, *Modeling Calculations for HMX Composite Propellants*, AIAA J. **20** (1), 106–115 (1982).
- [19] A.P Denisjuk, V.S. shabalin, Yu. G. Shepelev, *Combustion of Condensed Systems Consisting of HMX and a Binder Capable of Self-Sustained Combustion*. Combustion, Explosion, an shock waves, Vol. **34**, No.5(1998).

- [20] E. I. Maksimov, A. G. Merzhanov and V. M. Shkiro, *Gasless compositions as a simple model for the combustion of nonvolatile condensed systems*, Combustion Explosion and Shock Waves, (1965) pp. 15-18.
- [21] A. S. Rogachev, F. Baras, *Dynamical and statistical properties of high-temperature self-propagating fronts: An experimental study*. Physical Review E **79**, 026214 (2009).
- [22] Sebastien Candel, *Combustion Dynamics and Control: Progress and Challenges*, Proceedings of the Combustion Institute, Volume **29**, pp. 1–28(2002).
- [23] A. Varma*, A. S. Mukasyan, S. Hwang, *Dynamics of self-propagating reactions in heterogeneous media: experiments and model*, Chemical Engineering Science 56 1459-1466(2001).
- [24] S. Goroshin, J.H.S. Lee and Y. Shoshin, *Effect of the discrete nature of heat sources on reaction front propagation in particulate suspensions*, Proc. Combust. Inst. **27** (1998), pp. 743–749.

CHAPTER 5

Two Dimensional Modeling of Heterogeneous Combustion Process by Slice Reconfiguration Scheme

Present chapter explains the indigenous mathematical modeling and numerical simulation of a sheet combustion using the diffusion equation. Combustion of such heterogeneous system is modeled by concatenation of discrete reaction cells in ordered, random distributions on a two dimensional plane. Modeled system is classified into isotropic and anisotropic depending on parameter (θ) along perpendicular direction. θ is related to the amount of voids (oxidizer) between the cells. $\theta=1$ corresponds to the isotropic system and $\theta>1$ represents anisotropic system. Numerical simulation of such a combustible sheet requires high performance computing machine. Progress in high performance computing has allowed fast simulation and diagnosis of heterogeneous combustion sheet. Utilizing the parallel programming from MPI standards in house C code has been built. MPI programming task parallelizes the loop iterations according to number of nodes available in high performance machine (HPC1). HPC1 has 128 nodes with 8 cores each. The programming is designed to provide access to nodes and heterogeneous cores by the mode of Single Program shared Data. Slice reconfiguration scheme is proposed for simulation that instead considers only hot reaction cells. The main idea is to locally reconfigure the reaction cells based on their temperature profile. This method achieves a multi fold improvement in computation time instead of considering total reaction cells, without loss of any accuracy. As θ increases the numerical results show that the ignition time of reaction cells decreases and reaction rate of the combustible system increases. Burn rate sensitively depends on internal microstructure of the system. Various fingering like patterns and splits in fingers that are encountered during actual experiments are reproduced with the developed model.

5.1 Introduction

Chapter 2 discussed about the importance of disordered internal microstructure by one dimensional modeling of heterogeneous combustion [1-13]. However the one dimensional modeling [10-13] of combustion process cannot explain the dynamic issues such as combustion front and fingering instabilities that are apparent during actual situations. These dynamic parameters can be understood by modeling the sheet combustion [14-24]. Present chapter studies two dimensional modeling of heterogeneous combustion by considering the ordered and disordered distribution of point heat sources. In the burning of actual heterogeneous combustible sheet, a propagation of thermal front is complicated by the

internal microstructure, amount of oxidizer and heterogeneity of the mixture [21-24]. Fingering instability patterns shown in the work [25-31] are detected during experiments with help of high speed video recorder. Fingering instabilities are similar to thermal diffusion instability [25-26, 31-30]. Thermal diffusion instability was first reported on Bunsen burner and has been extensively studied ever since. Fingering like patterns, detected in experiments [25-26, 31-30], occur when a solid fuel is forced to burn against the oxidizing wind. As a consequence, the thermal front in the reaction region starts propagating slowly with emission of products. These products do not glow in visible light. These observations suggest that the dynamics of thermal wave are localized to the region of interaction of thermal wave and oxidizer. Such realization of thermal wave leads us to the study of reaction front and to limit thermal wave to a slow burning regime. Analysis of fingering patterns and instabilities are limited to experimental investigations [25-31] till now, however the mathematical modeling [14-24] and dynamical behavior of such fingering patterns are not explored. Mathematical modeling and numerical simulation of such fingering instabilities is of fundamental importance and study in these directions can provide solution to computational aspects of thermal diffusion instabilities. The diagnosis of rate of reaction front (rate of thermal fluctuations) enhances the fundamentals of thermal kinetics and aids in improving the performance of those engineering devices that utilizes it. The flame stability [21-25] is the most important controlling factor in design of combustion chamber. Investigations of stable and unstable flames for different combustion regimes are crucial and they are completely ignored. There were only a few attempts in the earlier literature [14-24] to take into account of the randomness of system. Variation of perpendicular parameter of the system and its effect on the combustion of heterogeneous systems is completely ignored. The systematic study for the effects of variation of perpendicular parameter and change in internal microstructure on reaction rate, flame structure and fingering patterns are being simulated and analyzed on a two dimensional plane in present chapter. The model of discrete combustion waves [1-6,10-13], which has very interesting behavior, similar to the behavior of the combustion of actual heterogeneous systems have been considered here.

Difficulties and uncertainties often associated with experimental determination of flame dynamics [25-27] are overcome by mathematical modeling and numerical simulation. In addition to that, the experimental research is too expensive for observing the factors and conditions affecting the flame propagation. Hence the computer based modeling techniques are considered as an alternative method of estimating burn rates and flame structure over wide ranges of operating conditions. The mathematical models of combustion process that

incorporate detailed reaction kinetics can predict burn rates (reaction rates). Nevertheless the fast and correct prediction of these parameters is a demanding test of the accuracy and completeness of kinetic reaction mechanism.

Arrangement of burnt and unburnt cells on a two dimensional plane is done in periodic and disordered manner in present chapter. Unburnt cells are ignited at different ignition temperatures based on the governing equation obtained using two dimensional diffusion equation. It is difficult and time consuming to track the temperature profile of unburnt cells in a disordered system. Consequently the temperatures of all unburnt cells with effect to burnt cells for different periodic boundary conditions are calculated for each time step. And these unburnt cells are ignited spontaneously at different pre-determined ignition temperatures. This step is repeated until the optimized value of dimensions along axis and periodic boundary conditions for different y parameter are obtained. This method requires dedicated huge computing source for couple of months. In addition, the Computation load increases with increase in size of microstructure, randomness and periodic boundaries of system for present two dimensional model. Consequently simulation of a combustion sheet by two dimensional plane requires high performance parallel computing [32-33]. Desktop systems with single processor takes nearly 1-2 months for numerous loop iterations, the advancements in high performance parallel computing with MPI programming paved a path to access the nodes simultaneously. MPI is abbreviated as message passing interface where the multiple data is shared between the address spaces of all cores through cooperative operations on each cores. MPI provides widely used standards for writing message passing programs. The interface attempts to be practical, portable, efficient and flexible. Interface specifications have been defined for C. The ability to utilize MPI programming to achieve fast and accurate computation of combustion process, allows for efficient and reliable analysis on calculated data. MPI programming is apt for numerical simulations since it provides task parallelism along with data broadcasting and data gathering in synchronization.

The present chapter investigates dynamical behavior of sheet combustion with indigenous mathematical modeling and numerical simulation of combustion process. In this chapter, the affects of dynamical, structural, statistical and linear thermal properties on the combustion of a two-dimensional ordered and random (disordered) heterogeneous system are reported. Implementation of modeling and numerical simulation of combustion process is discussed in the context of optimized computing time, ignition time profile, reaction rates and flame structure.

5.2 Modeling

In the present chapter the combustor chamber is modeled by two dimensional plane. The model is based on the existing theories of flame propagation that assumes the width of the heating and reaction zones are much greater than the size of individual powder particles [1-8, 10-13]. Propagation of combustion front is modeled by distributing combustible point particles (cells) in ordered, random methods. The spontaneous ignition and burning away occurs as soon as the temperature of the unburnt particle reaches a pre-determined ignition temperature (T_{ign}). Experimental data [6, 10-13, 25] show that the chemical reaction between the reactants starts practically immediately after the appearance of the liquid phase in the system and the burn-out time for the active particles is always essentially less (at least order) than the characteristic time of the heating of the particles from the initial temperature up to ignition temperature. This allows us to consider the process of the burn-out of the reaction cells of the system as instantaneous and the instant of reaching of some threshold temperature T_{ign} at which a liquid phase (e.g., molten materials or eutectic) appears in the system, can be considered as an instant of the ignition of the cells. A two dimensional system, consisting of reaction cells (particles) – the point heat sources (reaction cells), distributed along an axis (x, y), with ordered and uniform random distribution have been considered here. Combustion of actual heterogeneous mixture is a exothermic reaction between fuel and oxidizer. Experimental studies have shown that the ignition time decreases with increase in amount of oxidizer [25-28,31]. Burning of engineered mixtures does not vary significantly over the range of temperatures where they are designed to be used. Engineered heterogeneous mixtures are practically impossible to prepare. In actual situations, the burning of reacting mixture apparently varies with change in oxidizers, diluters and its percentage [10]. The amount of oxidizer or thermal capacity between reaction cells in actual system is now related to the expansion of y parameter (θ) in the present model. Hence the variation of the temperature field or expansion coefficient along the transversal(y) direction is considered as θ . Variation of parameter θ is the tendency of matter to change in area in response to change in temperature through heat transfer. Coefficient of expansion describes how fast the amount of heat transfer changes with a change in temperature. The practical calculations' can be based on average or constant value of expansion parameter along y axis. Parameter θ of a mixture is uniform in all directions for an isotropic system, and non uniform along y -direction for an anisotropic system. Consequently it is considered as

isotropic system for $\theta=1$ and anisotropic system with $\theta>1$. The problem is explained by two dimensional equation with delta sources given by

$$T(t, (x, y)) = T_{in} + \sum_{i(t)} \Delta T_i(t - t_i, ((x - x_i), (y - y_i))) \quad (1)$$

T_{in} is the initial temperature of the system; t_i is the instant of ignition of the i^{th} cell, located at (x_i, y_i) and $\Delta T_i(t, (x, y))$ is the temperature induced at the point (x, y) at time moment t by a single-point heat source, located at $(x, y)=0$ and ignited at time moment $t=0$.

The two-dimensional macroscopic equation with expansion parameter can be used for description of the evolution of the temperature of actual combustible system. For a two-dimensional problem the function $\Delta T_i(t, (x, y))$ with boundary conditions is obtained as

$$\Delta T_i(t, (x, y)) = \left(\frac{Q_i}{c\rho} \right) \frac{1}{4\pi\kappa t} \exp\left(\frac{-(x^2 + y^2)}{4\kappa t} \right) \quad (2)$$

The, temperature of heat source (x_k, y_k) at time t is given as

$$T(t, (x_k, y_k)) - T_{in} = \frac{1}{4\pi} \sum_{i=-\infty}^{m(t)} \sum_{j=-\infty}^{\infty} \frac{1}{(t_k - t_{(i,j)})} \exp\left(\frac{-((x_k - x_i)^2 + (y_k - y_i)^2)}{4(t_k - t_{(i,j)})} \right) \quad (3)$$

Here $i = -\infty \rightarrow m(t)$ is referred to as the arrangement of burnt and unburnt cells. Where $m(t)$ in eq.(3) is the number of a last source ignited by time t . And $j = -\infty \rightarrow \infty$ is referred to as the periodic boundary condition as along y-axis. Periodic boundary condition is introduced, so as to exclude the influence of inflammation of the system on the process under consideration. The ignition temperature T_{ign} and specific heat $c\rho$ is considered as identical for all heat sources. In this case particularly laminar flame, the reaction propagates consecutively from source to source, and a source (i,j) can be ignited only after ignition of the source $(i-1, j-1)$. At time t_k of ignition of heat source (x_k, y_k) is defined by solution of the algebraic equation

$$T_{ign} - T_{in} = \frac{1}{4\pi} \sum_{i=-\infty}^{m(t)} \sum_{j=-\infty}^{\infty} \frac{1}{(t_k - t_{(i,j)})} \exp\left(\frac{-((x_k - x_i)^2 + (y_k - y_i)^2)}{4(t_k - t_{(i,j)})} \right) \quad (4)$$

Introducing dimensionless parameters (similar to chapter 2), Eq. (4) is the following:

$$4\Pi\epsilon = \sum_{i=-\infty}^{k-1} \sum_{j=-\infty}^{\infty} \frac{q_{i,j}}{t_{k,j} - t_{i,j}} \exp\left(-\frac{(x_{k,j} - x_{i,j})^2 + (y_{k,j} - y_{i,j})^2}{4(t_{k,j} - t_{i,j})}\right) \quad (5)$$

for given s_i ($i < k$). Equation (5) is utilized for the numerical calculation of ignition times of heat sources. All solutions depend on single parameter (ϵ).

Non dimensional burn rate (reaction rate) of the two dimensional system is introduced. Calculation of burn rates is crucial for the quantification of combustion front. The combustion of such developed system occurs non uniformly in a pulsating mode (shown in results section), and because of this a mean burn rate is considered. Mean burn rate of combustible system is given by

$$\omega = \frac{(N_k - N_i)}{l_y (t_k - t_i)} \quad (6)$$

Where N is number of burnt particles and s is ignition time. Note suffix k and i refer to later and former layer of reaction cells in case of an ordered system. Numerical simulation of combustion sheet is performed by governing equations (5) and (6) in results section.

5.2.1 Theoretical analysis of Periodic system

Considering briefly the characteristics of combustion of two-dimensional periodic (ordered) systems with identical point heat sources; that is, in the system under consideration $x_k = kl_{(o,x)}$; $y_k = kl_{(o,y)}$ and $Q_k = Q_{(x,y)}$ for any k . The ignition delay time (Δt) is ignition time interval between two neighboring reaction cells in case of random distributed system and time interval between two neighboring layers for ordered system.

$$\Delta t = (t_k - t_i)$$

The quantity reciprocal to the dimensionless induction period can be considered as a dimensionless “reaction-propagation velocity” over the length between the sources ($i - 1$) and i . In the steady mode of reaction propagation over a two-dimensional system of point reaction cells, the induction period and, hence, the mean reaction velocities are identical for all layers,

$$\omega = \frac{1}{\Delta t}$$

for all i . In this case, with $s_k = \Delta t * K$ then Eq. (5) becomes

$$\varepsilon = \theta \omega^{n/2} \sum_{i=1}^{\infty} \sum_{j=-\infty}^{\infty} \frac{1}{(4\pi i)^{n/2}} \exp\left(-\frac{\omega}{4i}(i^2 + \theta^2 j^2)\right) \quad (7)$$

θ is isotropic parameter along y direction ω is burn rate (i, j) represents position of front and ε is the ignition temperature. Figure 5.1 shows the comparison plot for theoretical dependence $\omega(\varepsilon)$ for different values of θ using eq. (7). The burn rates increases with increase in parameter (θ). It is observed that the theoretical solution for dependence $\omega(\varepsilon)$ exists for all values of $0 < \varepsilon < 1.2$. These theoretical observations can only be explained and justified by performing the numerical simulation of combustion sheet (periodic) using eq.(5). The mathematical models with periodic internal micro structure (periodic system) are used very often for numerical simulation of the combustion sheet, in doing so the numerical results of combustion sheet thus obtained can be validated with solutions of theoretical equation (7).

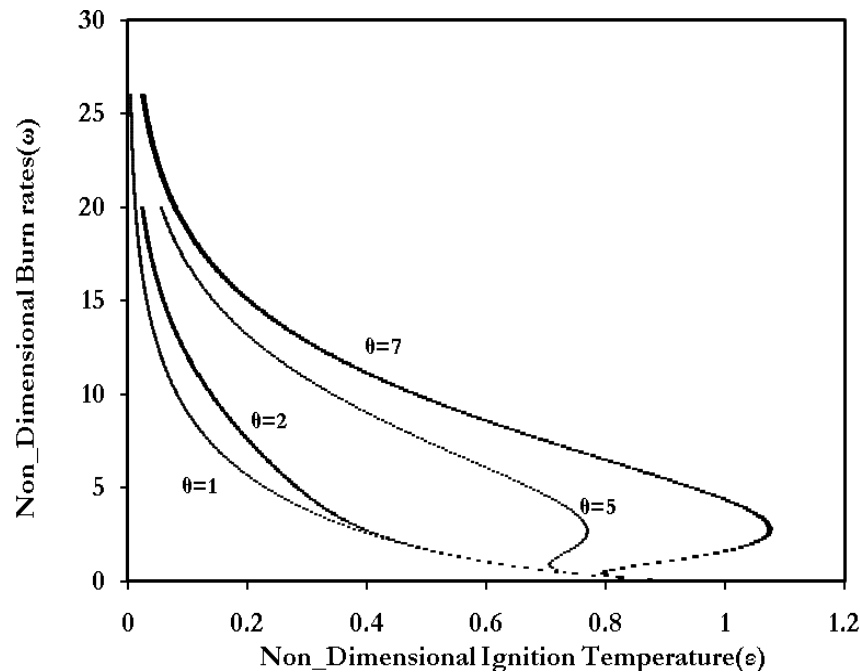


Figure 5.1. Comparison plot for burn rates of an ordered system obtained theoretically using eq.(7) for different values of θ .

In addition this exercise provides the information for optimized dimensions and conditions of a combustion sheet for different values of θ .

5.2.2 Realization of Periodic (Ordered) system

The periodic system concentrates on the parameters such as internal microstructure and parameter θ . Two dimensional periodic system consists of point heat sources distributed orderly along an axis x and y . lx, ly are the dimensions along x and y directions. Total point

heat sources in the system are divided into two categories those are (ly^*burnt) burnt and (lx^*ly) unburnt point heat sources. The internal microstructure of the powdered mixture is achieved by concatenation of the burnt and unburnt point heat sources. Heat transfer between point source particles is carried through the thermal bridge and it is assumed that there are no heat loss i.e., total heat energy released by combustion of preceding particle is utilized for combustion of succeeding unburnt particles.

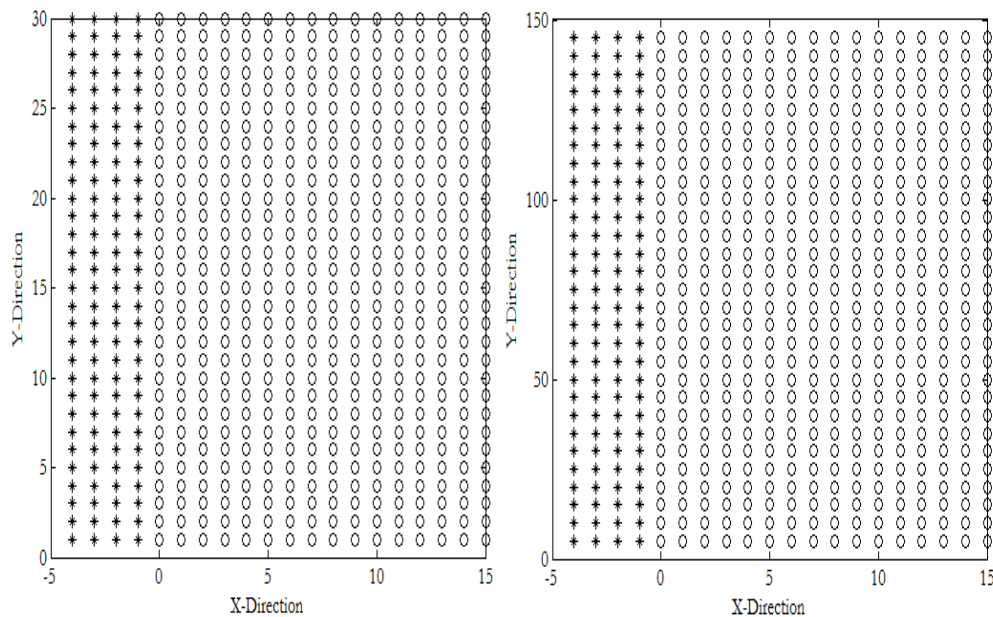


Figure 5.2. Plot for microstructure of the ordered system modeled on a two dimensional plane. '*' represents the burnt particles and 'o' is for unburnt particles. Left represents for $\theta=1$ right $\theta=5$.

A sufficient amount of thermal energy required for propagation of combustion front, is achieved by considering initial combusted (burnt) particles. The ordered microstructure of the two dimensional system with 4×30 burnt and 15×30 unburnt particles is shown in Figure 5.2. Two dimensional system is broadly classified as isotropic 5.2(a) and anisotropic 5.2(b) depending upon the parameter θ along y-axis. The point particles (cells) are considered to be immobile and are characterized by an ignition temperature T_{ign} . When the temperature of an unburnt cell reaches the value T_{ign} , the ignition and instantaneous burning away of the cell occurs with the release of heat Q_i . T_{in} is an initial temperature of the system, t_i is a time moment of ignition, which has a coordinate (x_p, y_j) and $\Delta T_i(t, (x_p, y_j))$ is the temperature induced at the point (x_p, y_j) at time moment t by a single-point heat source, located at (x_p, y_j) and ignited at time moment $t=0$. The simulation of combustion process involves burning away of all the unburnt cells.

5.2.3 Periodic Boundary condition

In the simulations of combustion sheet the temperature changes arising due to inhomogeneity of the system affect the combustion process. Ignoring these temperature changes can cause unphysical dynamics while performing numerical simulation [14-24]. Therefore the size of system must be large enough to prevent unphysical topology. Incorporating periodic boundary can prevent inhomogeneties and account for accurate physical dynamics [18-23]. Figure 5.3 shows the schematic diagram for the periodic system (shown in figure 5.2) incorporating the periodic boundary. The ∞ for the summation of j series in equation (5) indicates the parameter of periodic boundary along y-direction. The fluctuations in temperature gradients increase with increase in parameter θ and ignition temperature of the system. This means for each θ and ε the periodic boundary (j) varies. Consequently a repetitive numerical simulation for system with lx^*ly dimensions have to be performed using eq.(5).

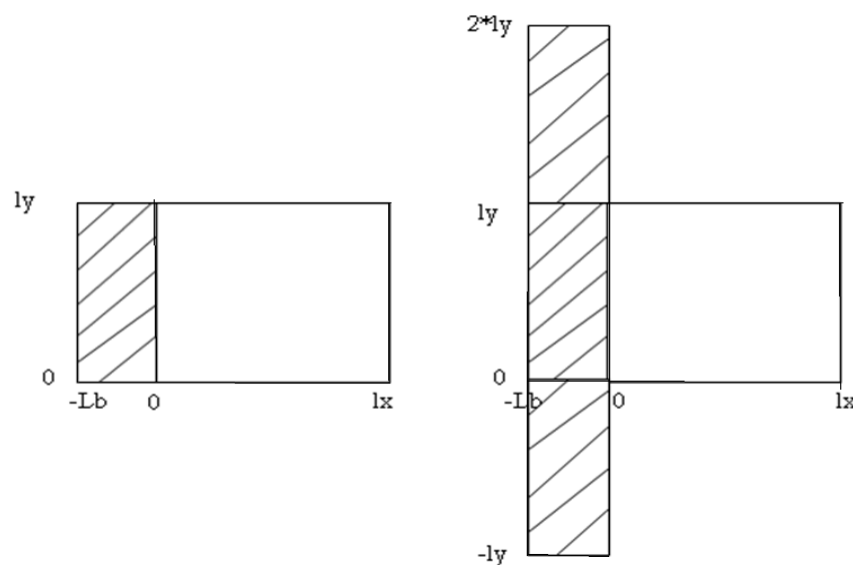


Figure 5.3. Schematic plot for the system incorporating periodic boundary. 1 Periodic boundary ($N_y=0$); 2 Periodic boundary ($N_y=1$).

This method is executed to obtain the optimized periodic boundary condition (j) for different values of θ . During the numerical simulation of periodic system the value of critical (optimized) periodic boundary is considered as a point from where the system's performance does not show significant affect even with further increase in parameter of periodic boundary (j). Note if the periodic boundary is less than the optimized (critical) periodic boundary than the results obtained are inaccurate. The (Algorithm) steps involved in the numerical simulation of combustion sheet for a single ignition temperature are

5.2.4 Algorithm

- 1) Given pre-determined ignition temperature (ϵ) discretize the two dimensional combustible plane with sufficient burnt cells ($ly*(burnt-1)$) and unburnt cells ($lx*ly$). Note initial periodic boundary (Ny) is 0.
- 2) At time $t=0$ all the burnt cells are ignited.
- 3) Time is incremented by dt and the temperature of the all unburnt cells is calculated using equation (5).
- 4) The temperatures of all unburnt cells are compared with the pre determined ignition temperature.
- 5) If the temperature of unburnt cell is $\geq \epsilon$, then it is transferred to burnt cells, else time is again incremented and steps 3-5 are repeated.
- 6) Steps 3-5 are repeated until all the unburnt cells are transferred to burnt cells.
- 7) Using the times of ignition and Eq. (6), the burnt rate is calculated.
- 8) Repeat steps 1-8 for each incremented value of periodic boundary condition until the critical periodic boundary is reached. Critical periodic boundary is referred to as the value of a parameter beyond which it does not affect the burn rate.

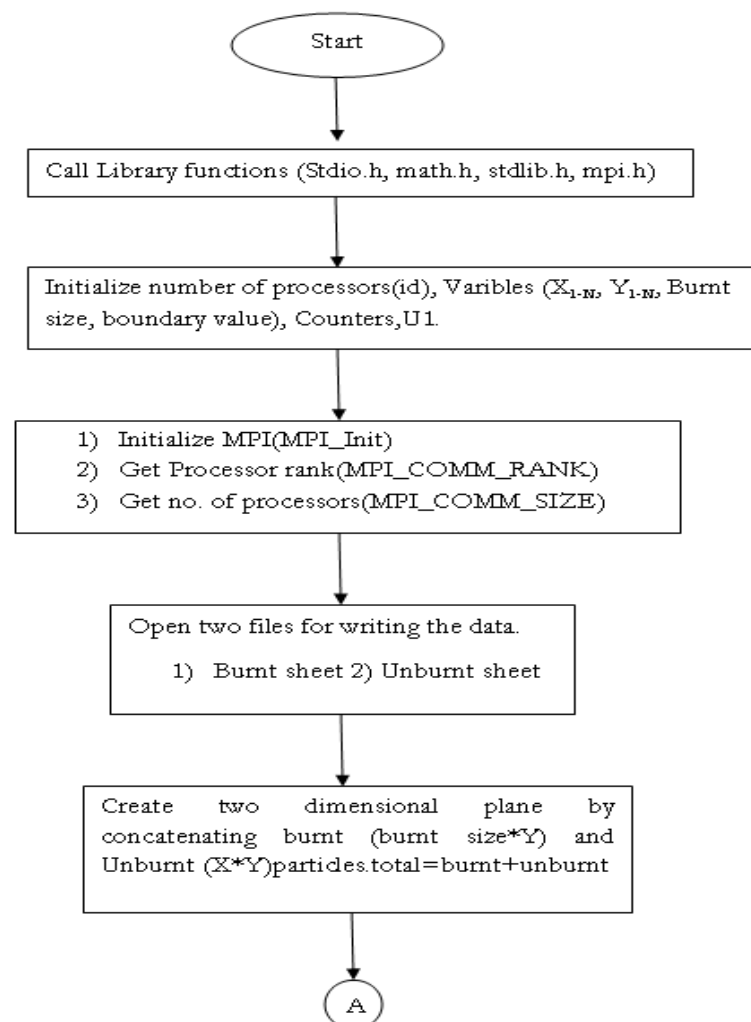
The above steps 1-8 are repeated for each value of pre determined ignition temperature. The Algorithm is programmed by C language and the simulated results (represented by symbol ' Δ ' in figure 5.5) for the ordered combustible system completely agree with established theories and theoretical dependence eq.(7) (represented by solid line in figure 5.5). The numerical results are validated and the C code is referred as standard. Since the execution time using C code by desktop computer is of the order of multiple months for a single ignition temperature (ϵ), this hurdle is overcome by utilizing MPI programming.

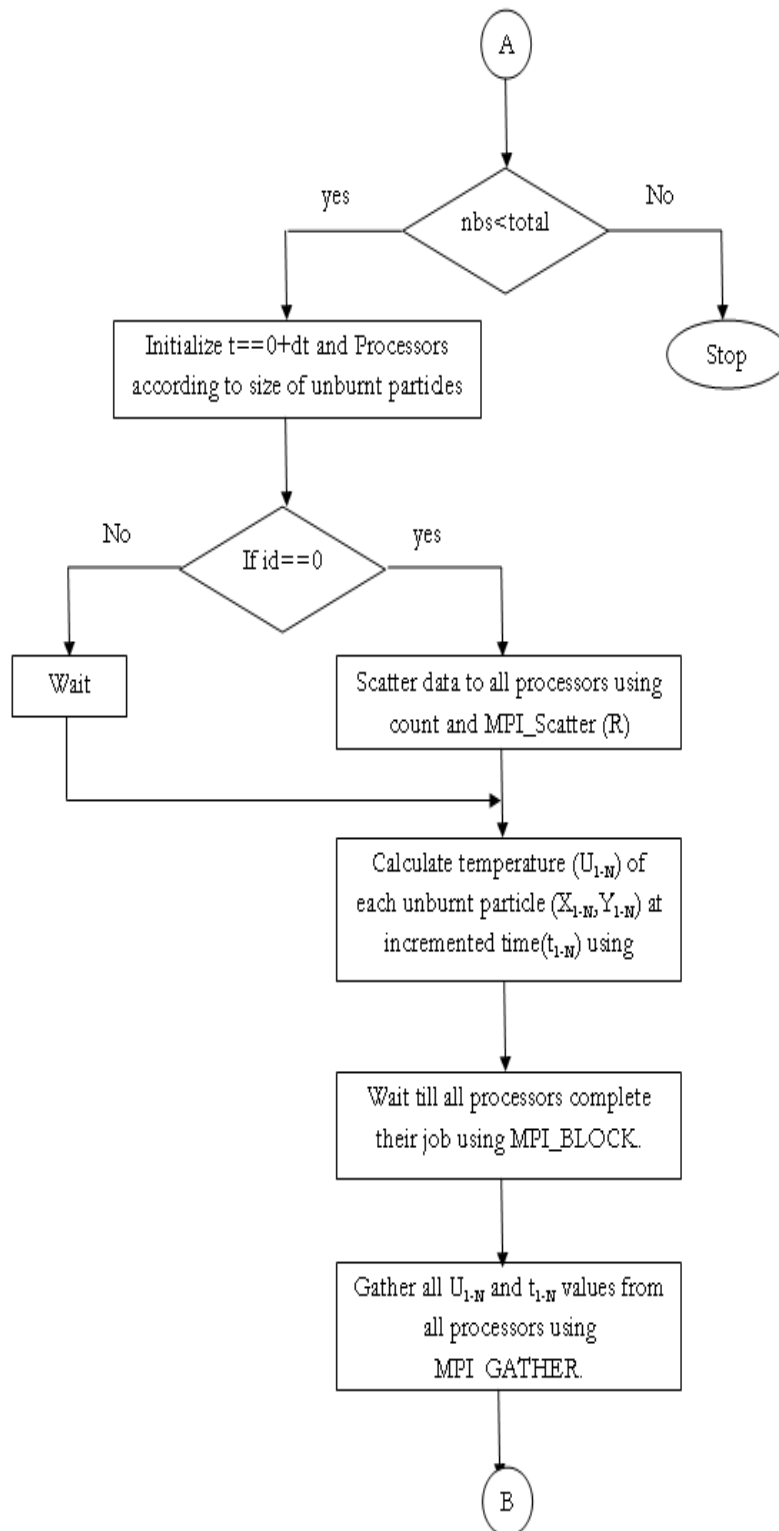
5.2.5 Faster Computation by Using MPI

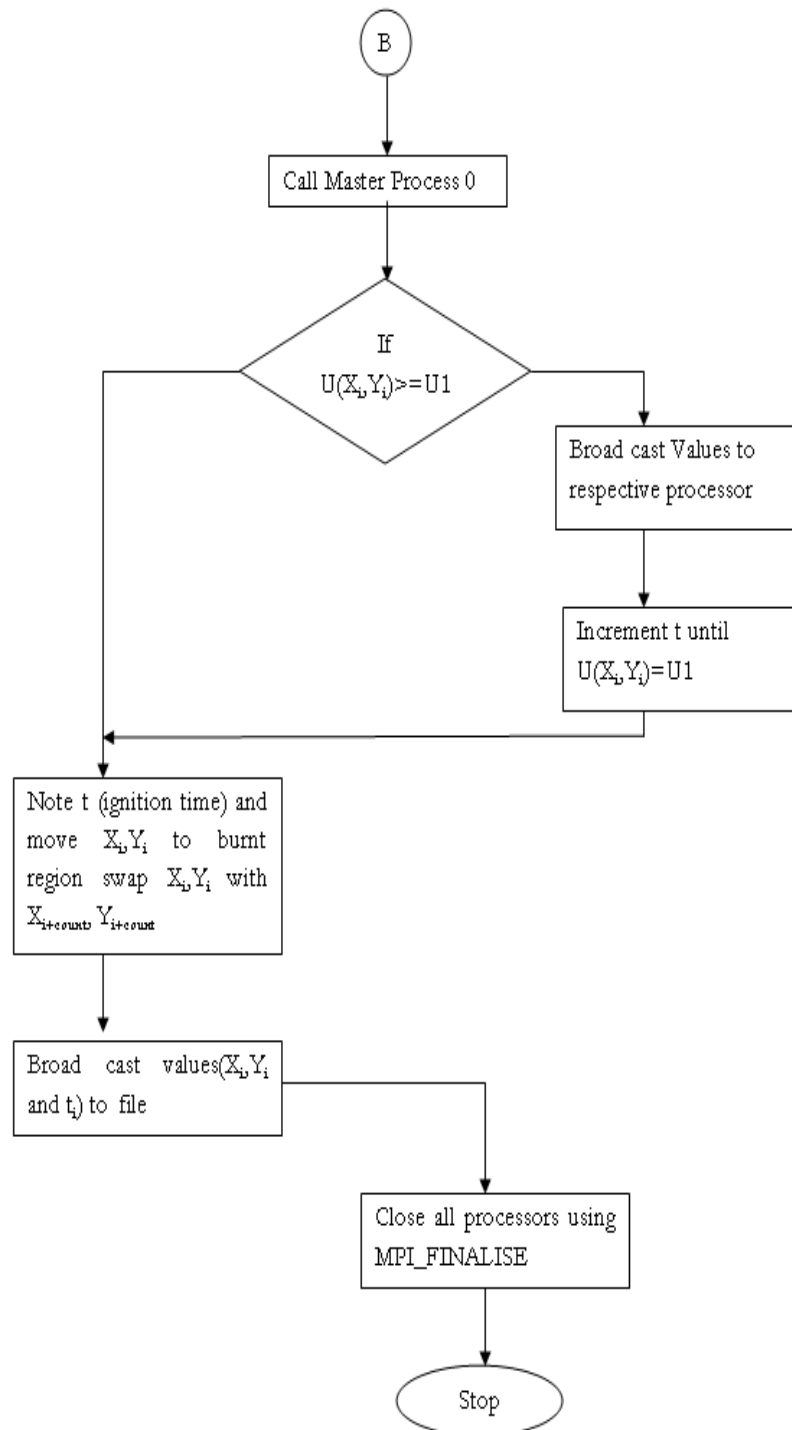
The MPI programming is utilized by distributing the work to different cores and collecting the data in synchronization. Flow chart for the MPI execution of algorithm is shown below. The computation load on each core increases with increase in burnt and unburnt cells and parameter of periodic boundary along y-axis for each ignition time. Since the effect of burnt cells on unburnt cells cannot be ignored, the burnt cells cannot be shared or parallelized among cores. Hence the unburnt cells are task parallelized. The steps involved in MPI programming for simulation of combustion process are same as that of earlier algorithm except for the step 3. Here the total unburnt cells that undergo numerous loop iterations are

distributed (Step (R) in Flowchart) among the slave cores by master core. Slave cores are assigned with the computation of temperature of shared unburnt cells in synchronization. Master core gathers the temperature value of unburnt cells calculated by slave cores and compares the same with pre-determined ignition temperature. Simulation of combustion process using MPI programming cut downs the computation time to a great extent when compared to the computation time of C program.

Note for each nested iteration of periodic boundary (N_y or j), time increment and burnt cells the size of total unburnt reaction cells is of computational concern, hence it is of interest to further reduce the computational time.







5.2.6 Slice reconfiguration scheme

Hence a Slice reconfiguration scheme is proposed based on the monitoring of temperature profiles of unburnt. The vicinity of reaction front distinguishes total unburnt cells into two regions of reaction zone (Hot cells) and cool cells as shown in Figure 5.4. Hot cells (reaction zone) are highly sensible to ignite and release heat instantly even for little increase in heat

energy. The percentage of hot cells with effect to burnt cells is around 20-25% of the total unburnt cells. The cool cells comprise of unburnt cells with low temperature and can be ignored until single hot cell is burnt. Consequently the total unburnt region is now reduced to hot cells (slice) at each nested iterations for j and ignition time.

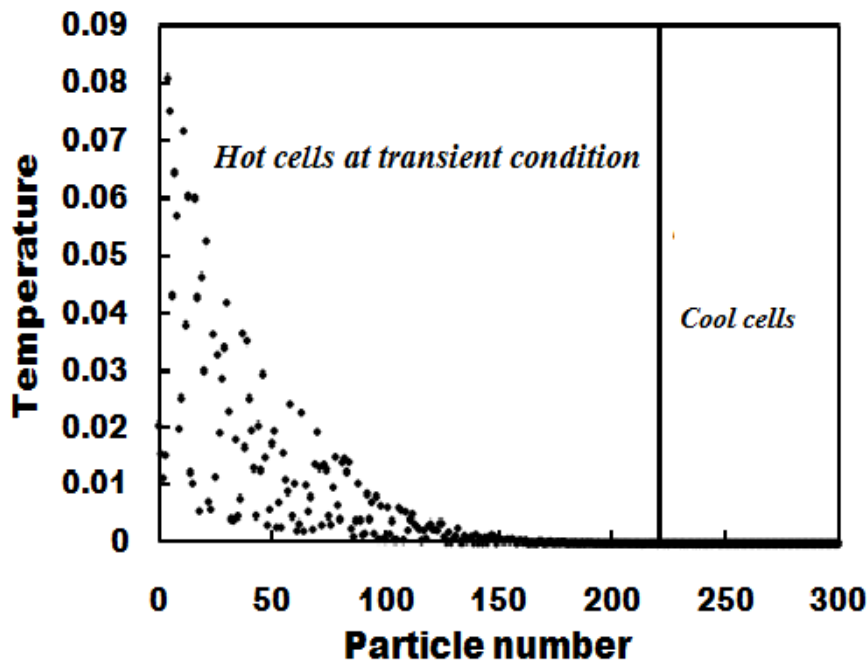


Figure 5.4 Temperature profile for unburnt cells.

The slice is reconfigured time and again only after the temperature of cell has attained the pre-determined ignition temperature. The above step is repeated until all unburnt cells are burnt. Considering the hot cells, the computation load on each core is reduced as the sizes of unburnt cells are reduced to hot cells. The results for different methods of simulation of combustion sheet are shown in results section.

5.3 Results

5.3.1 Periodic system

The mathematical modeling and indigenous numerical simulation of combustion sheet has allowed devising the predictive method for obtaining ignition time profiles, flame structure (can't be obtained using one dimensional modeling), reaction rates and combustion limit at different ignition temperatures. The comparison for the burn rates of periodic combustion sheet computed by MPI program and slice reconfiguration schemes using eqn.(5) are illustrated in this section. The MPI programming for numerical simulation of periodic system is utilized to perform parallel operation of nodes present in HPC1 machine. HPC1 has 128 nodes and each node has 8 cores. In the view of slice reconfiguration scheme the

computational time is improved to multi fold (<15 times). Considering the temperature profile of unburnt cells as shown in figure 5.4, the total number of unburnt cells is now reduced to hot cells (around 20% of total unburnt cells) for the calculation of temperature at each time. This step is performed until all the unburnt cells are burnt. The burn rates calculated from theoretical eqn.(7) for an ordered system shown in figure 5.5 (represented by solid line) is taken as reference for validation of numerical burn rates (calculated by eqn.(5) and eqn.(6)) obtained by considering total (MPI program) combustible system and proposed method(slice reconfiguration). Figure 5.5 shows that the numerical burn rates of an ordered combustible system calculated using MPI program and slice reconfiguration scheme. Numerical burn rates of an optimized combustion sheet calculated using eqn.(5) and (6) completely agrees with the theoretical burn rates. From figure 5.5 it is observed that the burn rates of the periodic system increases with increase in parameter (θ) at particular ignition temperature. Isotropic system with parameter ($\theta=1$) in all directions have lower burn rates when compared to that of the burn rates of anisotropic ($\theta>1$) systems. θ is the extensive property of the combustible system and is related to thermal capacity of the system

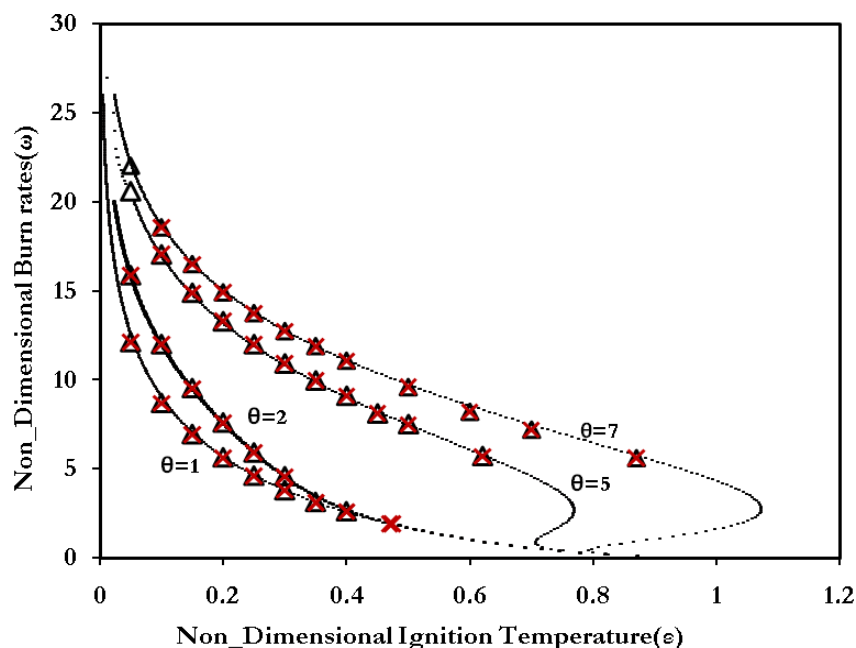


Figure 5.5. Comparison plot for burn rates of an ordered system obtained theoretically and numerically for different values of θ . Solid lines are theoretical burn rates and symbols represent numerical burn rates Δ -MPI and X- MPI and slice reconfiguration scheme.

. As θ increases the thermal capacity of the system increases thus the ignition time decreases. This observation is similar to that of experimental results reported for the role of amount of oxidizer on burning time [25-28]. It is also observed from figure 5.5 that the numerical solution of burn rates using eqn. (5) and (6) exists only in the limited range of ignition

temperature ($\epsilon_{cr(numerical)}$). The combustion front does not propagate above $\epsilon_{cr(numerical)}$ for a periodic system. The value of $\epsilon_{cr(numerical)}$ increases with increase in parameter (θ). The values of $\epsilon_{cr(numerical)}$ for different values of θ are as follows: $\epsilon_{cr(numerical)} = 0.49$ for $\theta=1$, $\epsilon_{cr(numerical)} = 0.51$ for $\theta=2$, $\epsilon_{cr(numerical)} = 0.62$ for $\theta=5$ and $\epsilon_{cr(numerical)} = 0.87$ for $\theta=7$. Ignition time profiles of a periodic systems ($\theta=1$ and $\theta=7$) are shown in figure 5.6. The step by step fashions suggest that the particles in a periodic system burn layer by layer.

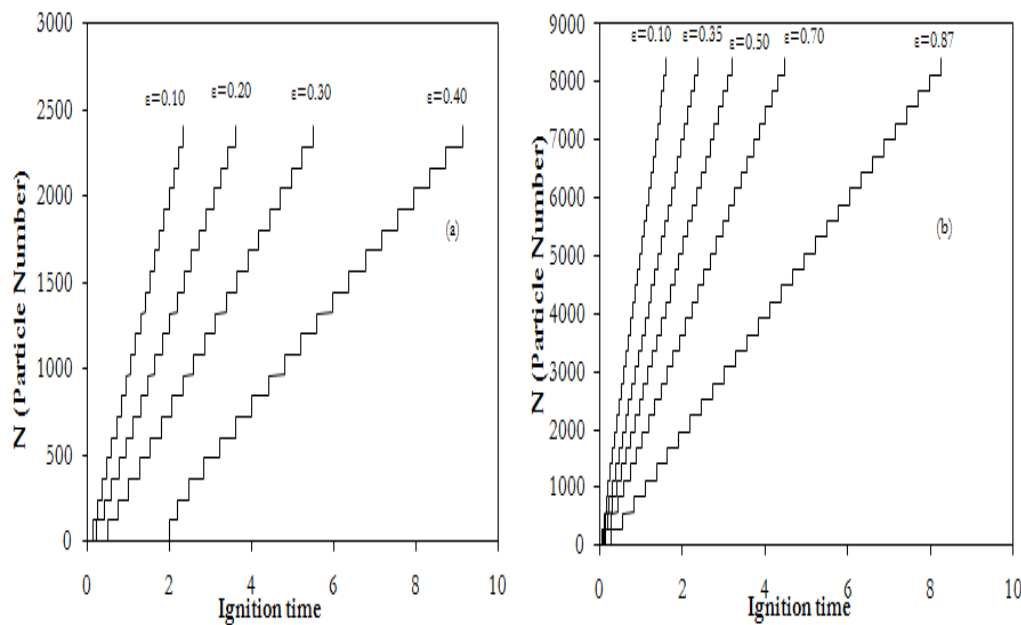


Figure 5.6 Ignition time profiles of a periodic system.(a) $\theta=1$ (isotropic), (b) $\theta=7$ (anisotropic).

The role of randomness in internal microstructure of an actual system is well established from chapter 2 and 4. Numerical experiments for ordered systems performed till now are essential to obtain the optimized dimensions for disordered system and for analyzing the role of disorderness in internal microstructure of actual combustion sheet. The optimized dimension values of combustion sheet obtained from numerical experiments performed for periodic system is taken as operating conditions for disordered system. The optimized dimensions of combustion sheet for different parameters of θ are shown in table 5.1.

θ (Y parameter)	$l_x * l_y$ (Unburnt particles)	Burnt layers (L_b)	Optimized Periodic Boundary (j)
$\theta=1$	30*200	25*200	5
$\theta=2$	30*240	25*240	7
$\theta=5$	30*300	25*300	10

$\theta=7$	30*280	25*280	15
------------	--------	--------	----

Table 5.1 List of Optimized dimensions(x,y) and periodic boundary.

Thus MPI programming with proposed method can now be executed for different random systems. Next section describes about realization of disordered system, role of internal microstructure and numerical simulation of disordered system.

5.3.2 Disordered system

The disordered internal microstructure of combustion sheet (isotropic) is shown in figure 5.7. Unburnt particles are arranged in random distribution. Heat energy released from burning of particles travels in all directions.

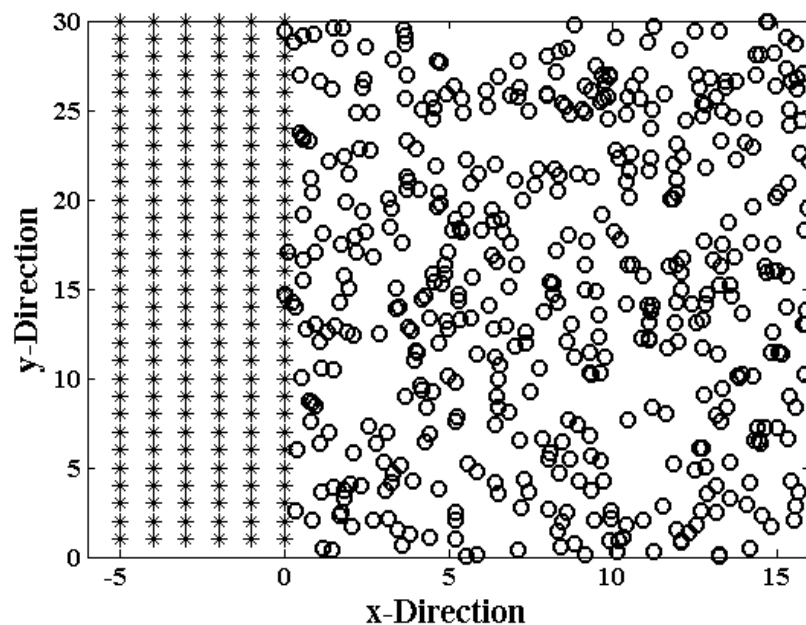


Figure 5.7. Plot for microstructure of the disordered system ($\theta=1$) modeled on a two dimensional plane. '*' represents the burnt particles and 'o' is for unburnt particles.

Whereas in the case of periodic system heat energy released travels in unique direction and hence particles in periodic system burn layer by layer. Disordered system's with different values of θ ($\theta=1, =2, =5$ and $=7$) are simulated numerically by using both methods (MPI and MPI+slice). The comparison of computational time by two methods is shown in next section. The numerical results obtained for disordered system are explained here. Figure 5.8 shows the comparison of ignition time profiles of a disordered system for different values of θ . Ignition time profile for the disordered system is linear at lower ignition temperatures. At higher ignition temperatures burning occurs in form of consequent jumps: relatively long

periods of front stopping (induction periods) are followed by the burning-out of some part of the sample with practically constant burning rate, and followed by a new induction period again. Duration of induction periods and periods of “continuous” combustion are random and it is connected with the random structure of the system [1-7, 10-13]. Transient condition is observed at initial stages of ignition because of the sudden perturbation of reaction kinetics. As the reaction front propagate and reach final stage of burning the accumulation of heat energy decreases and thus leads to self slow heating of the material. Experimental data on combustion of powder mixtures [6, 8] show that the process of reaction front propagation in actual systems is random [10-13] and is accompanied by fluctuations in flame structure and burning rate of system as a whole. Fluctuations observed in calculations are result of both random microstructure and non-linearity of the system.

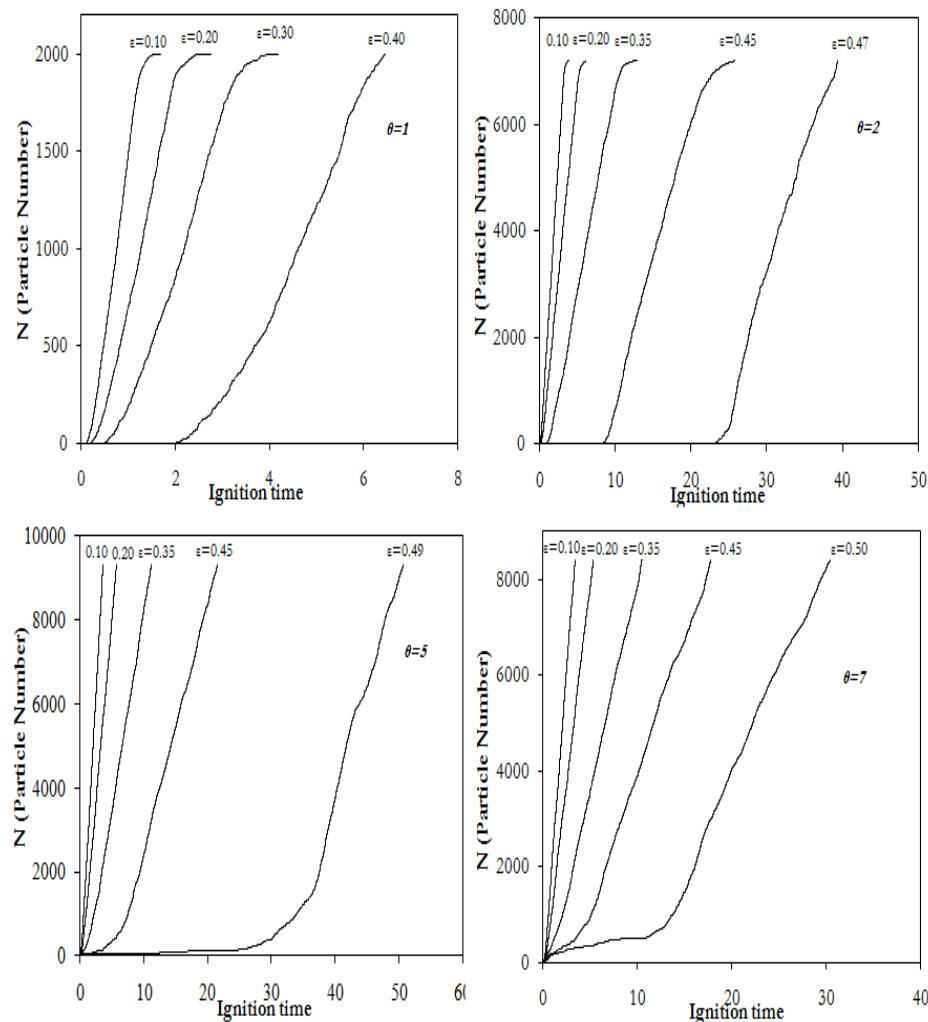


Figure 5.8 Ignition time profile for Isotropic and Anisotropic ($\theta=2$). 1 Ordered 2 random systems.

In experiments [6,8], the change of mixture parameters and concentrations of powder components (e.g. a changing in stoichiometric coefficient x in mixture $Ti + xSi$) results in either regularization or stochastization of combustion process.

A similar behavior of burning front is observed in the model under consideration. In numerical experiments the regularization (at lower ignition temperatures) results in less fluctuations of duration of induction periods and process becomes more stable, and the stochastization (at higher ignition temperatures) results in when combustion becomes more random one with long and random induction periods. The process is more regular at smaller ε and higher values of θ ; the more ε and less θ the more random is the process, the stronger effect of fluctuation of random structure of the system on the burning front propagation.

Thermal wave or combustion front for actual systems [25-31] is observed to be propagating in fingering pattern. These fingers like patterns are observed in a combustion regime with the help of high speed video recorder. Combustion front propagates slowly in non flaming mode where the emitted products do not glow in visible light. The instabilities in the fingering pattern of combustion front are driven by the uncertainty of the reaction zone. Different patterns, of reaction front such as stable, irregular, periodic, fingering pattern with tip splitting and fingering pattern without tip splitting, are observed during experiments [25-31]. Similar behaviour of combustion front is observed in the present two dimensional discrete model. Combustion wave propagation for the disordered system is shown in Figure 5.9, 5.10, 5.11 and 5.12. Structure of combustion wave for different ignition temperature is observed to be different, and propagation of combustion front is effected by ignition temperature. Figure 5.9 shows the structure of combustion (reaction) front at different ignition temperatures ($\varepsilon=0.10, 0.47$) for an isotropic system modeled in the present chapter. Parameter θ for a isotropic system is same in all directions, however the combustion front at different ignition temperatures is observed to be propagating in irregular pattern. It can be detected from figure 5.9 that the irregularity in finger patterns of combustion front increases at ignition temperatures near the critical value ($\varepsilon=0.47$). Here heterogeneity and voids in the internal micro structure of the mixture play a crucial role by creating the uncertainty in the reaction zone and destabilizing the reaction front.

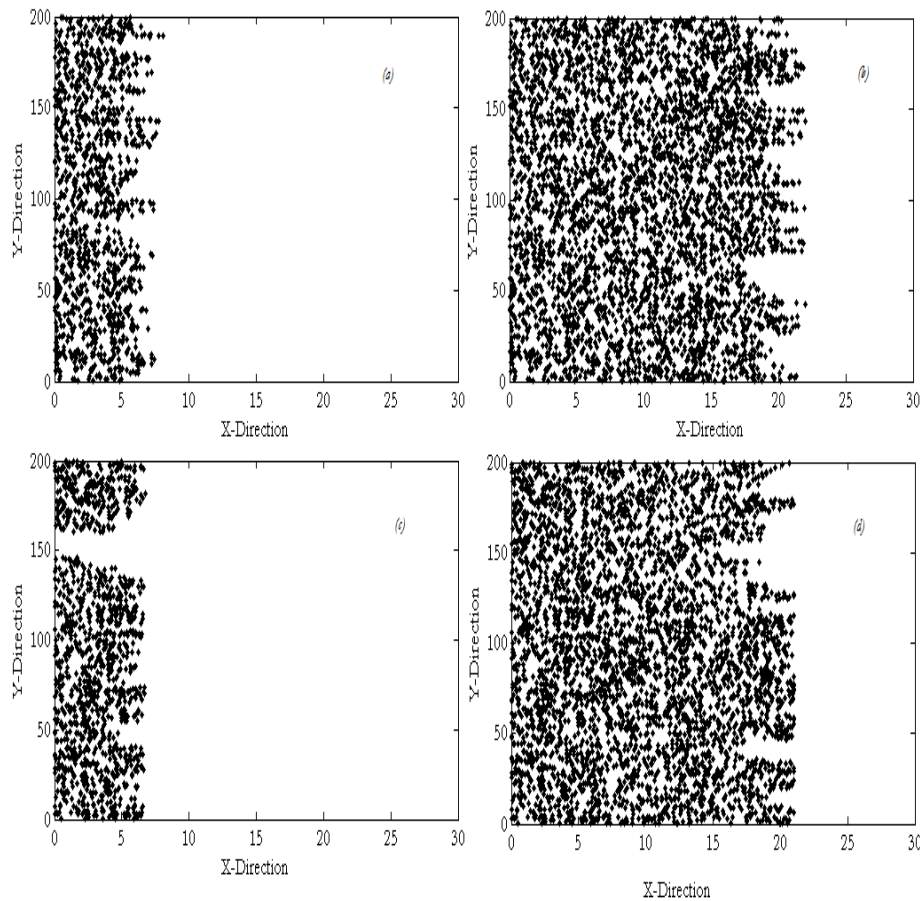


Figure 5.9. Snapshot of burnt region for an Isotropic system at different ignition temperatures (ε). (a) $t = 19$ and $\varepsilon = 0.46$; (b) $t = 25$ and $\varepsilon = 0.46$; (c) $t = 27$ and $\varepsilon = 0.47$; (d) $t = 33$ and $\varepsilon = 0.47$.

Developed model when simulated using eqn. (5) and (6) can reproduce the different fingering like patterns observed for experimental results [19-20]. Unlike in experimental works [25-31], where different combinations of fuel and oxidizer are mixed together and ignited, the combustion front is recorded and analyzed. In the developed model different values of γ parameter (θ) are included so as to study and analyze the role of θ in affecting the burning process. $\theta = 2, 5$ and 7 are considered for numerical simulation. Figure 5.10 shows the structure of thermal wave at different ignition temperatures ($\varepsilon = 0.10, 0.478$) for $\theta = 2$. For lower values of ignition temperature ($\varepsilon = 0.10$) the combustion front moves in irregular pattern. In figure 5.10(a) and (b) irregularities observed are less when compared to that of isotropic system.

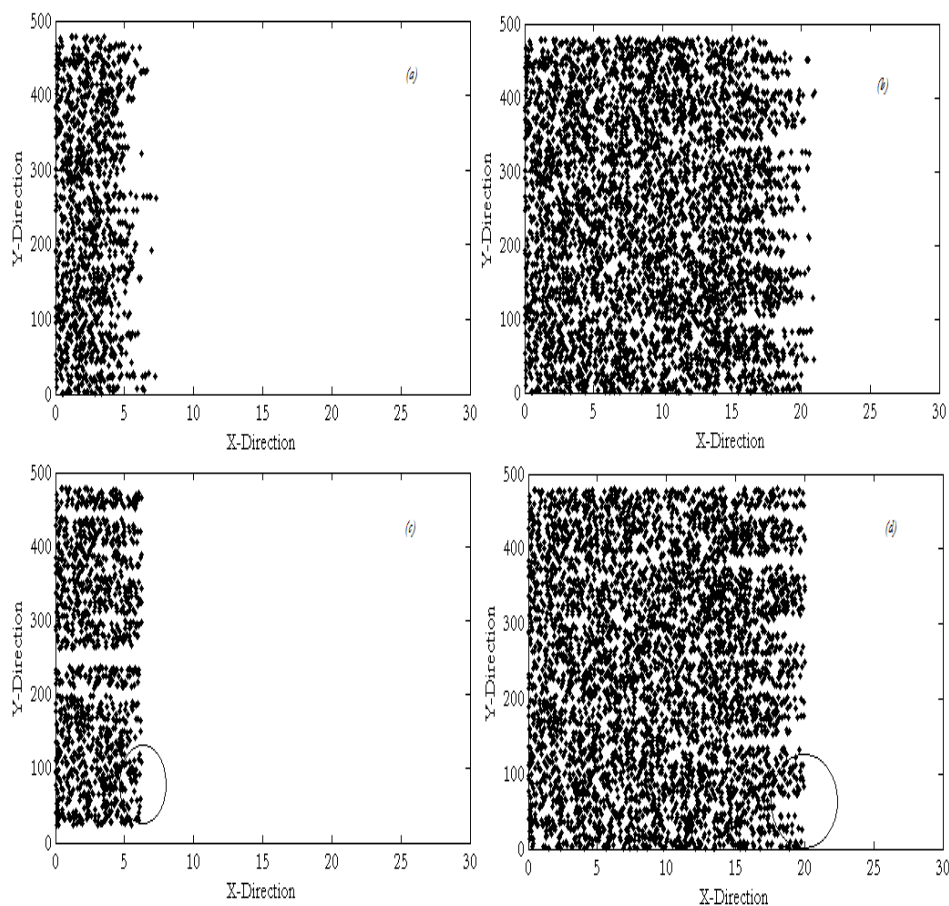


Figure 5.10. Snapshot of burnt region for Non Isotropic ($\theta=2$) system at different ignition temperatures (ε). (a) $t=0.7$ and $\varepsilon=0.10$; (b) $t=2.2$ and $\varepsilon=0.10$; (c) $t=28$ and $\varepsilon=0.478$; (d) $t=34$ and $\varepsilon=0.478$.

However as the ignition temperature increases an interesting feature of combustion front can be observed as shown in figure 5.10(c) and (d). The irregularities in combustion front now take the shape of fingers. Periodic fingering pattern and increase in the width of the fingers are observed for disordered system with $\theta=2$ at $\varepsilon=0.478$ (shown in figure 5.10(c) and (d)). As the combustion front propagates these periodic fingers split. Split in fingers is observed in figure 5.10 (d) (shown by circle). $\varepsilon=0.478$ is the critical ignition temperature for disordered system with $\theta=2$. The heterogeneity and voids in internal microstructure for disordered system with $\theta=2$ have less effect on combustion front when compared to that of isotropic system. And this is the reason for observing periodic finger patterns. It is also observed that the widths of the fingers are increased at higher ignition temperature. The systematic study for the behavior of fingers pattern is also realized for disordered systems with $\theta=5$ and 7. Figure 5.11 shows the structure of combustion front for a disordered system with $\theta=5$ at different ignition temperatures ($\varepsilon=0.10, 0.49$). At lower ignition temperature the combustion front moves in more regular pattern (shown in figure 5.11(a) and (b)). Compared to combustion front observed for disordered system with $\theta=2$ (figure 5.10(c) and (d)) at higher

ignition temperature, the number of periodic fingers, splits in fingers and the width of the fingers are increased for a disordered system with $\theta=5$ (shown in figure 5.11(c) and (d)). In actual systems the finger width is determined by the ability of reaction front to release heat. As θ is increased, heat release for reaction cell increases, the reaction front starts exhibiting the fingering patterns even at lower ignition temperatures. Combustion front with periodic fingers is observed at $\epsilon=0.49$ as shown in figure 5.11 (c). At higher ignition times the fingers split at the tip as shown in figure 5.11(d), this is a slow consequence of heterogeneity and voids in the internal micro structure of mixture.

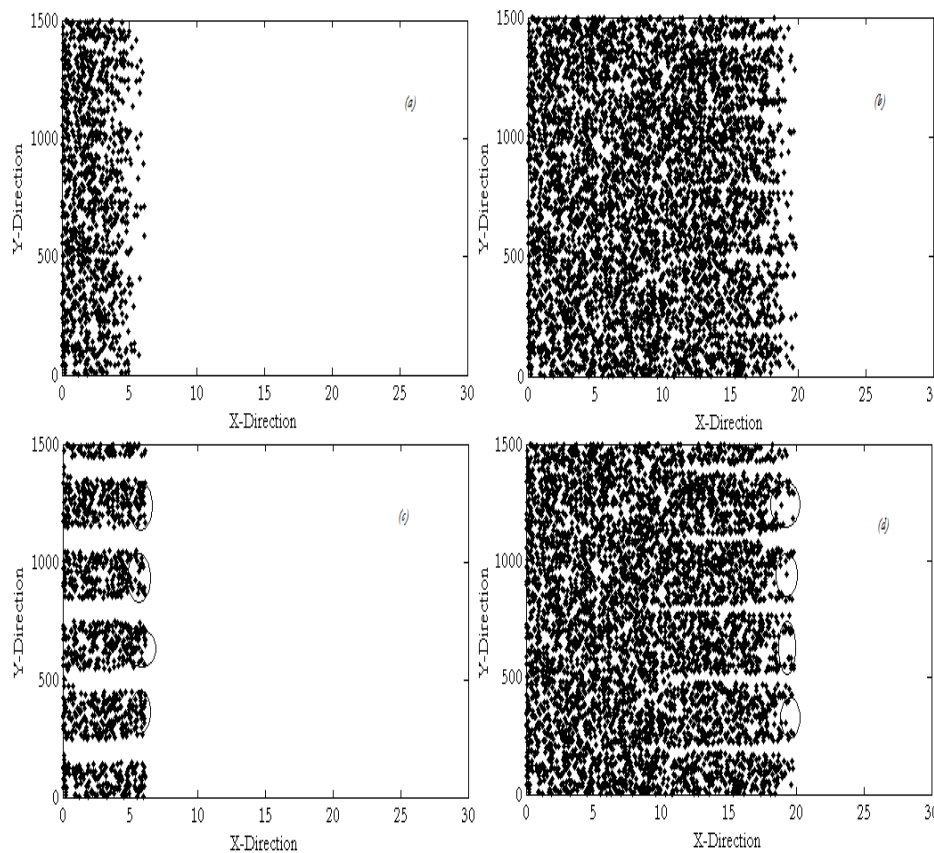


Figure 5.11. Snapshot of burnt region for Non Isotropic ($\theta=5$) system at different ignition temperatures (ϵ). (a) $t=0.7$ and $\epsilon=0.10$; (b) $t=2.1$ and $\epsilon=0.10$; (c) $t=36$ and $\epsilon=0.49$; (d) $t=41$ and $\epsilon=0.49$.

Figure 5.12 shows structure of reaction front for $\theta=7$ at different ignition temperatures ($\epsilon=0.10, 0.50$). Regular patterns without fingers as shown in figure 5.12(a) and (b) is detected at lower ignition temperatures ($\epsilon=0.10$) where the reaction kinetics are very fast. As ignition time increases and reaction front propagates the length of fingers increases, as shown in figure 5.12(c) and (d), because of the system's ($\theta=7$) ability to release more heat when compared to that of the system with lower values of θ . Periodic fingering patterns with

increase in length of fingers as shown in figure 5.12(c) and (d) is observed at higher ignition temperatures ($\theta=0.50$).

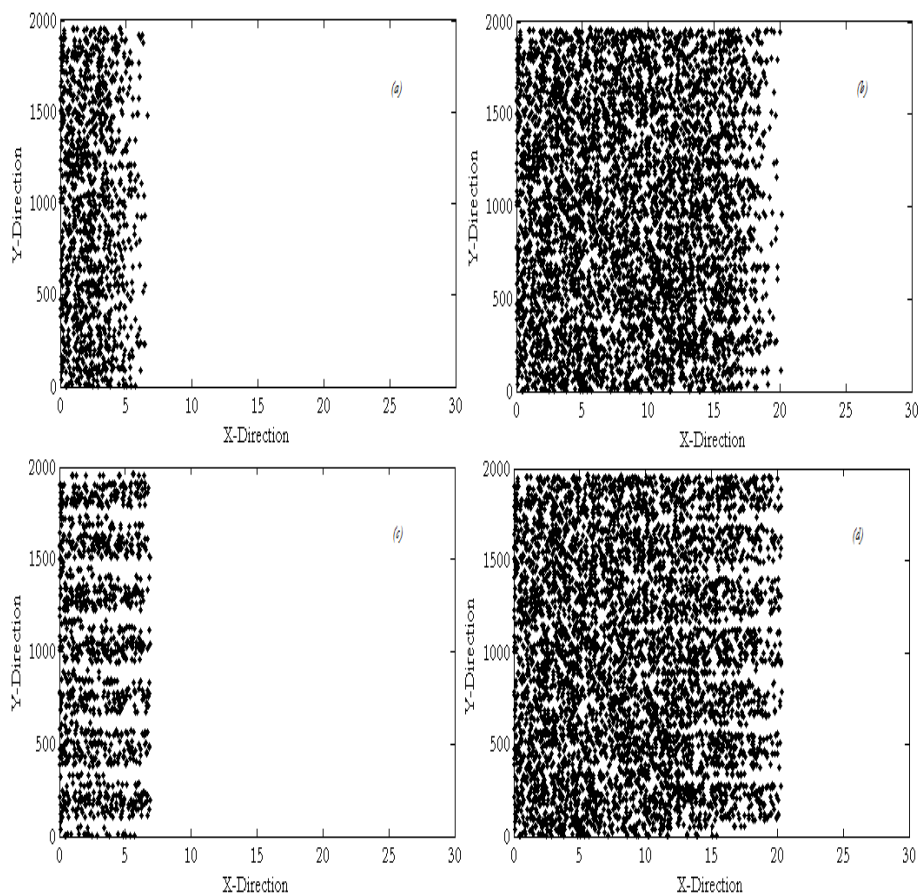


Figure 5.12. Snapshot of burnt region for Non Isotropic ($\theta=7$) system at different ignition temperatures (ε). (a) $t=0.9$ and $\varepsilon=0.10$; (b) $t=2.4$ and $\varepsilon=0.10$; (c) $t=17$ and $\varepsilon=0.50$; (d) $t=25$ and $\varepsilon=0.50$.

Increase in length and distance between fingers as shown in figure 5.12(c) and (d) is detected as reaction front propagates through the medium. As parameter θ is increased, there are enough amounts of voids (oxygen) that enhances the rate of reaction front hence there is increase in distance between fingers. $\varepsilon=0.50$ is combustion limit for $\theta=7$. The analysis of numerical results performed till now in this chapter is obtained by using slice reconfiguration scheme. Nevertheless to figure out the improvement in computational time achieved by slice reconfiguration scheme, the numerical simulation for the combustion of a disordered system with $\theta=2$ at $\varepsilon=0.25$ & 0.35 is performed by using both methods. Comparison of computation time by both methods for disordered microstructure of system is illustrated in table 5.2. The slice reconfiguration scheme allowed seventeen fold and fifteen fold improvement in computation time for ignition temperatures $\varepsilon=0.25$ & 0.35 respectively.

Ignition temperature (ϵ)	Burnt Heat sources ($lx*y$)	Unburnt Heat sources ($lx*y$)	Number of Cores	Computational time (mins) using Methods	
				Total combustible system	Slice reconfiguration
0.25	25 X 240	33 X 240	6 X 8	155	9
0.35	25 X 240	33 X 240	6 X 8	237	15

Table 5.2 Comparison of computational time between both methods for ignition temperatures (ϵ)=0.25 & 0.35.

The numerical simulation of combustion process by proposed slice reconfiguration scheme is now performed with different number of nodes to estimate performance weight for each node. The computation time decreases with increase in available number of cores, for the proposed method as illustrated in table 5.3.

Ignition temperature (ϵ)	Burnt Heat sources ($lx*y$)	Unburnt Heat sources ($lx*y$)	Cores	Computation time (mins)
0.25	25 X 240	33 X 240	1 X 8	57
	25 X 240	33 X 240	3 X 8	19
	25 X 240	33 X 240	5 X 8	12
	25 X 240	33 X 240	6 X 8	9
	25 X 240	33 X 240	7 X 8	9
	25 X 240	33 X 240	8 X 8	9

Table 5.3 Performance weight for number of nodes by slice reconfiguration scheme.

Slice reconfiguration scheme achieves super fast simulation of combustion process at a pre-determined ignition temperature. The proposed scheme has an advantage of analyzing the dynamical properties of combustion process such as ignition time profiles, flame structure and average burn rate which otherwise is difficult to record from experiments.

5.3.3 Burn rates

Burn rates at different ignition temperatures are calculated using Eq.(6) for different periodic and disordered systems. The comparison of burn rates for ordered and random

systems is shown in Figure 5.13. Each single point shown in figure 5.13 is obtained by using slice reconfiguration scheme, which otherwise would be difficult and time consuming to obtain by considering total unburnt particles. Figure 5.13 shows that the burn rates increases with increase in parameter θ at a particular ignition temperature. The burn rates of a disordered system are less than the periodic system. The random internal microstructure and parameter θ of the powder system can play a crucial role in the combustion process and should be taken into account in the modeling of combustion of microheterogeneous systems.

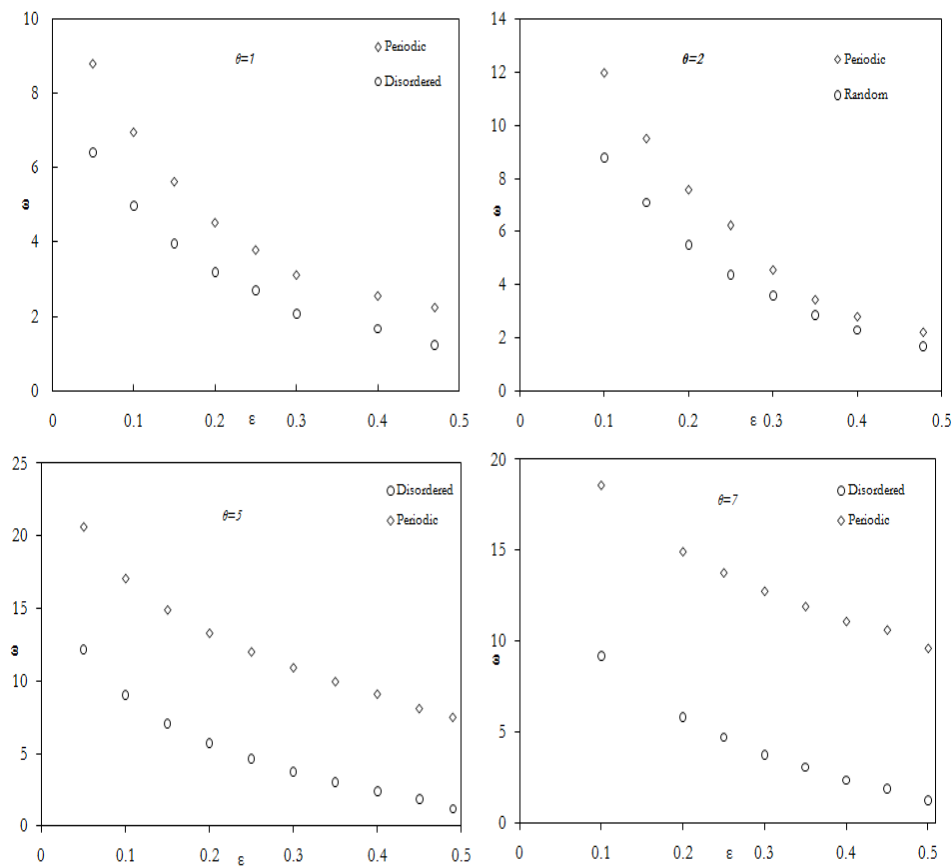


Figure 5.13 Comparison plots of burn rates calculated for Ordered and random systems.

At certain value of higher ignition temperatures it is observed that the combustion front doesn't propagate. Combustion limit is affected by the parameter θ . As parameter θ increases the combustion limit increases.

5.4 Conclusion

The super fast numerical simulation of a gasless combustion process on two dimensional sheet using MPI programming is presented for the first time. Variation in microstructure of the system is achieved by ordered and random spacing of point particles along two

dimensional planes. The change in heat capacity of the mixture is addressed by the parameter θ along y-axis. The parameter θ allowed analysis of reaction front propagation for different mixtures. Ignition time profiles for ordered system is step by step and fluctuates linearly for random systems. It was observed that the propagation of the combustion wave for ordered systems is layer by layer and is determined strongly by the reaction kinetics. In random systems, the rate of combustion is more strongly affected by heat transfer between the cells. Various fingering patterns observed during experiments are reproduced with developed model. The burn rates are affected by θ , and increases with increase in θ at particular ignition temperature.

Multi fold improvement in computation time with accuracy is obtained by using slice reconfiguration scheme. As the number of available nodes increases, the computation load on individual core decreases. MPI programming provided an accurate and high performance parallel computing of Combustion process. The computer based indigenous modeling using MPI programming facilitated faster computation and detailed diagnostics of two dimensional combustion processes

5.5 References

- [1] A.S. Mukasyan, A.S. Rogachev, Discrete reaction waves: Gasless combustion of solid powder mixtures, *Progress in Energy and Combustion Science* 34 (2008) 377–416.
- [2] A. Varma, A. S. Rogachev, A. S. Mukasyan, and S. Hwang, Complex behavior of self-propagating reaction waves in heterogeneous media, *Proc. Natl. Acad. Sci. U.S.A.* 95 (1998) 11053.
- [3] S. Hwang, A. S. Mukasyan, and A. Varma. Mechanisms of Combustion Wave Propagation in Heterogeneous Reaction Systems, *Combustion and Flame* 115 (1998) 354–363.
- [4] A. Varma, A. S. Mukasyan, S. Hwang. Dynamics of self-propagating reactions in heterogeneous media: experiments and model, *Chemical Engineering Science* 56 (2001) 1459-1466.
- [5] A. S. Mukasyan, A. S. Rogachev, M. Mercedes, and A. Varma, Microstructural correlations between reaction medium and combustion wave propagation in heterogeneous systems, *Chem. Eng. Sci.* 59 (2004) 5099.
- [6] A. S. Rogachev, F. Baras, Dynamical and statistical properties of high-temperature self-propagating fronts: An experimental study, *Physical Review E* 79 (2009) 026214.

- [7]. M. W. Beckstead and K. P. McCarty, Modeling Calculations for HMX Composite Propellants, *AIAA J.* 20 (1) (1982) 106–115.
- [8] P. S. Grinchuk and O. S. Rabinovich. Effect of random internal structure on combustion of binary powder mixtures, *Physical Review E* 71 (2005) 026116.
- [9] F.-D. Tang, A.J. Higgins, S. Goroshin. Effect of discreteness on heterogeneous flames: Propagation limits in regular and random particle arrays, *Combustion Theory and Modelling*. Vol. 13 2 (2009) 319–341.
- [10] Naine Tarun Bharath, Sergey A. Rashkovskiy, Surya P. Tewari and Manoj Kumar Gundawar, Dynamical and statistical behavior of discrete combustion waves: A theoretical and numerical study, *Phys. Rev. E* 87 (2013) 042804.
- [11] S.A. Rashkovskiy, G.M. Kumar, S.P. Tewari, One-dimensional discrete combustion wave in periodic and random systems. *Combustion Science and Technology*, 182: (2010) 1009–1028.
- [12] S. A. Rashkovskii, Structure of heterogeneous condensed mixtures, *Combust. Expl. Shock Waves*, 35 5 (1999) 523–531.
- [13] S. A. Rashkovskii, Role of the structure of heterogeneous condensed mixtures in the formation of agglomerates, *Combust. Expl. Shock Waves* 38 4 (2002) 435–445.
- [14] Tanzeer Hasan, Jason I. Gerhard, Rory Hadden, Guillermo Rein, Self-sustaining smouldering combustion of coal tar for the remediation of contaminated sand: Two-dimensional experiments and computational simulations, *Fuel* 150 (2015) 288–297.
- [15] Afsin Gungor, Two-dimensional biomass combustion modeling of CFB, *Fuel* 87 (2008) 1453–1468.
- [16] J. F. Clarke, S. Karni, J. J. Quirk, P. L. Roe, L. G. Simmons, E. F. Toro, Numerical Computation of Two-Dimensional Unsteady Detonation Waves in High Energy Solids, *Journal of Computational Physics* 106, 215-233 (1993).
- [17] Liuyan Lu , Steven R. Lantz , Zhuyin Ren, Stephen B. Pope, Computationally efficient implementation of combustion chemistry in parallel PDF calculations, *Journal of Computational Physics* 228 (2009) 5490–5525.
- [18] Ananias G. Tomboulides, and Steven A. Orszagy, A Quasi-Two-Dimensional Benchmark Problem for Low Mach Number Compressible Codes, *Journal of Computational Physics* 146, 691–706 (1998).
- [19] Li Yuan, Tao Tang, Resolving the shock-induced combustion by an adaptive mesh redistribution method, *Journal of Computational Physics* 224 (2007) 587–600.

- [20] George Ilhwan Park, Parviz Moin, Numerical aspects and implementation of a two-layer zonal wall model for LES of compressible turbulent flows on unstructured meshes, *Journal of Computational Physics* 305 (2016) 589–603.
- [21] Edward J.Kansa, Ralph C.Aldredge, Leevan Ling, Numerical simulation of two-dimensional combustion using mesh-free methods, *Engineering Analysis with Boundary Elements* 33 (2009) 940–950.
- [22] Fedderik van der Bos, Volker Gravemeier, Numerical simulation of premixed combustion using an enriched finite element method, *Journal of Computational Physics* 228 (2009) 3605–3624.
- [23] B. Michaelis, B. Rogg, FEM-simulation of laminar flame propagation. I: Two-dimensional flames, *Journal of Computational Physics* 196 (2004) 417–447.
- [24] Biljana Miljkovic, Ivan Pešenjanski, Marija Vic'evic, Mathematical modelling of straw combustion in a moving bed combustor: A two dimensional approach, *Fuel* 104 (2013) 351–364.
- [25] Ory Zik and Elisha Moses, Fingering Instability in solid fuel combustion: The Characteristic Scales of The Developed State, *The Combustion Institute* (1998) 2815–2820.
- [26] Zhanbin Lu, Yong Dong, Fingering Instability in Forward Smolder Combustion, *Combustion Theory and Modeling* 15 6 (2011) 795–815.
- [27] D.I. Erandi N. Wijeratne, Britt M. Halvorsen, Computational study of fingering phenomenon in heavy oil reservoir with water drive, *Fuel* 158 (2015) 306–314.
- [28] Chuan Lu and Yannis C. Yortsos, Pattern formation in reverse filtration combustion, *Physical Review E* 72, 036201(2005).
- [29] Shakti N. Menon and Georg A. Gottwald, Bifurcations of flame filaments in chaotically mixed combustion reactions, *Physical Review E* 75, 016209(2007).
- [30] Hiroshi Gotoda, Yuta Shinoda, Masaki Kobayashi, and Yuta Okuno, Detection and control of combustion instability based on the concept of dynamical system theory, *Physical Review E* 89, 022910 (2014).
- [31] Ory Zik, Zeev Olami and Elisha Moses, Fingering Instability in Combustion, *Physical Review Letters* 81, 18 (1998).
- [32] Joshua A. Anderson, Eric Jankowski, Thomas L. Grubb, Michael Engel, Sharon C. Glotzer, Massively parallel Monte Carlo for many-particle simulations on GPUs, *Journal of Computational Physics* 254 (2013) 27–38.

[33] E. Martinez, J. Marian, M.H. Kalos, J.M. Perlado, Synchronous parallel kinetic Monte Carlo for Continuum Diffusion-Reaction Systems, *Journal of Computational Physics* 227 (2008) 3804–3823.

CHAPTER 6

Conclusion and Future Scope

In conclusion, the combustion process is simulated and burn rates are calculated numerically for heterogeneous combustion using one and two dimensional mathematical modelling. Numerical calculations performed for simulation of combustion process is single parametric one and depends on ignition temperature (ϵ). Numerical results show that the burn rates sensitively depend on internal microstructure. The internal microstructure of actual heterogeneous mixtures is apriori unknown and changes with mixing, packing and percentage of diluters. The complications and effects of internal microstructure on combustion process are explained by introducing the randomness in positioning the neighbouring cells. Different random distributions are utilized for simulating the combustion process. The systematic study for the effect of nature of heat release on combustion process is also performed by considering two cases of distribution of heat release one with ordered distribution and the other with randomized. Particularly the normal and gamma distribution of spacing neighbouring cells can explain actual combustion process. Normal distribution of adjacent cells explains combustion process at higher ignition temperatures whereas gamma distribution of adjacent cells is more accurate for lower ignition temperatures. The nature of distribution of heat release has impact on both the burn rate and combustion limit.

The obtained agreement of numerical and experimental dependences $\omega(\epsilon)$ augurs well for the discrete combustion model of heterogeneous systems under consideration. The random structure of the powder system can play a crucial role in the combustion process and should be taken into account in the modeling of combustion of microheterogeneous systems. This is a consequence of the nonlinear interaction of the system structure and the thermal wave, which creates the features in propagation of combustion wave. This is an important result of this study. The structure of the system cannot be considered as an unchanged one, and it can vary with changes in the size of the particles of dispersed components or their concentrations, which results in changing in the nature of combustion process and in burning rate, even at a constant burning temperature. This is confirmed by the experimental data. Some features of combustion of actual powder systems can be described by regularization or stochastization of the system when, the structure of the system becomes

more ordered, or, on the contrary, disordered due to the changing of concentration of disperse components. The limiting case of stochastization of the mixture is its clustering, when individual hot-spots are collected into the compact groups (clusters) and act as the larger hot spots in the combustion process. These results are of fundamental importance, because earlier the effect of the structure of system on combustion process either was neglected, or assumed that the structure of the system does not change with changing in the concentration and dispersion of the components. The analysis in chapter 2 shows that the combustion process becomes very sensitive to the structure of the system at high ignition temperatures: the higher ignition temperature, the higher the sensitivity. Thus, the presence of random heterogeneities in the system can have a weak affect on the combustion process at low ignition temperatures, but can result in significant fluctuations of burning rate and even long periods of stopping of burning front (big ignition delays) at high ignition temperatures. The heterogeneities of the system are the precisely that obstacle, on which a termination of combustion occurs at suprathreshold ignition temperatures.

Numerical calculation of burn rate is obtained after simulation of 40 realizations of random distributions of adjacent cells. This numerical exercise of calculating burn rate is time consuming and needs dedicated computing resource. A numerical technique is proposed for the calculation of burn rate of a random system based on the knowledge gained from statistical analysis performed in chapter 2. Burn rate of a random system can be calculated from the discrete probability between two limits. It is interesting to note that the width of limits remains same for different shaping parameter, however changes for ignition temperature. This numerical technique is also extended to find the combustion limit. This numerical technique can become a hand on tool to predict the burn rate of heterogeneous mixture if the internal microstructure is known. The present technique can be extended to problems that involve quantification of average physical parameters (flow rate, propagation of reaction front and combustion limit) in monte carlo simulations.

The effect of heat loss on propagation of combustion front is also studied, and it is observed from numerical experiments performed in chapter 4 that the heat loss affects the combustion limit but not the burn rate. As heat loss increases in the system the combustion limit decreases because of the increase in thermal runaway.

Structure of combustion front or burnt region is obtained by mathematical modelling and numerical simulation of combustible sheet. An indigenous slice reconfiguration scheme with

parallel computing is proposed to reduce the computation time. Numerical results show that burn rate depends on internal microstructure and parameter θ of the system. The super fast numerical simulation of two dimensional combustion processes is achieved by slice reconfiguration scheme through MPI programming. The computation time required to obtain a burn rate numerically using C program is of the order of multiple months and is reduced to 150 minutes using MPI programming and further improved to 9 minutes using slice reconfiguration scheme through MPI. The super fast simulation of combustion process allowed with detailed analysis of dynamical combustion process. Snapshots of burnt region shown in chapter 5 resembles finger like patterns.

The actual powder systems are the three-dimensional ones, the particles in them have the finite sizes, and the internal structure of the mixtures is automatically formed in the process of their preparation, depending on the sizes and concentrations of the components. Accordingly, if regularization or a clusterization of the system occurs, it must be a result of the system composition, but not specified as an input data. For this reason, a more natural way is the direct simulation of the structure of the system, based on one of the method of packing of particles, and the subsequent direct calculation of the combustion process, which automatically takes into account the actual structure of the system, including its possible regularization or clustering. As applied to actual powder mixtures this work is planned in the next stage of this research. The numerical exercises performed in chapters 2, 4, and 5 are the intermediate steps in simulating the three dimensional combustion process.

The in house C code for simulation of three dimensional combustion process is built, however the optimized dimensions of parameter are yet to be obtained. Numerical simulation of three dimensional combustion process requires huge computing sources and dedicated work station for multiple months. It would be very interesting to see that burn rates of three dimensional system can be obtained by utilizing the numerical technique shown in chapter 3.

List of Publications related to Thesis:

- [1] **Naine Tarun Bharath**, Sergey A. Rashkovskiy, Surya P. Tewari, and Manoj Kumar Gundawar, Dynamical and statistical behavior of discrete combustion waves: A theoretical and numerical study, **Phys. Rev. E** 87,042804 (2013).
- [2] **Naine Tarun Bharath**, Manoj Kumar Gundawar, Effects of Disordered Microstructure and Heat release on Propagation of Combustion Front, **Cogent Engineering**.
- [3] **Naine Tarun Bharath**, Sergey A. Rashkovskiy, Surya P. Tewari, G. Manoj Kumar, Role of Nature of Discreteness on the Burn-rates of Heterogeneous Energetic Materials, **8th international High Energy Materials Conference & Exhibit HEMCE(2011)**.
- [4] **Naine Tarun Bharath**, Surya P. Tewari, and Manoj Kumar, One Dimensional Discrete Combustion of Random system with a Gamma Distribution, **Proceedings of the 22nd National Conference on IC Engines and Combustion, 3-024(2011)**.
- [5] **Naine Tarun Bharath**, Sergey A. Rashkovskiy, Surya P. Tewari, Manoj Kumar Gundawar, New Insights into the effects of Randomness on Combustion of Discrete Gasless Systems, **9th Asia-Pacific Conference on Combustion(2013)**.
- [6] **Naine Tarun Bharath**, Sergey A. Rashkovskiy, Manoj Kumar Gundawar, Effect of Heat loss in propagation of reaction front for combustion of heterogeneous systems, **23rd National Conference on I. C. Engine and Combustion (NCICEC 2013)**.
- [7] **Naine Tarun Bharath**, Manoj Kumar, Propagation of Reaction front in Heterogeneous Combustion of High energy materials, **9th international High Energy Materials Conference & Exhibit HEMCE (2014)**.

Manuscripts Under Review:

- [1] **Naine Tarun Bharath**, Manoj Kumar Gundawar, Correlation between Discrete Probability and Reaction Front Propagation Rate in Heterogeneous mixtures, **Indian Journal of physics**.

Manuscripts Under Preparation:

- [1] **Naine Tarun Bharath**, Sergey A. Rashkovskiy, Manoj Kumar Gundawar, Effect of Heat loss in propagation of reaction front for combustion of heterogeneous systems.
- [2] **Naine Tarun Bharath**, Manoj Kumar, Propagation of Reaction front in Heterogeneous Combustion of High energy materials.

Achievements:

- Best Poster Awarded at **8th international High Energy Materials Conference & Exhibit HEMCE (2011)**.
- Best Poster Awarded at **Frontiers in physics (2012)**.

ORAL presentations delivered:

- [1] **Naine Tarun Bharath**, Surya P. Tewari, and Manoj Kumar, One Dimensional Discrete Combustion of Random system with a Gamma Distribution, **Proceedings of the 22nd National Conference on IC Engines and Combustion, 3-024(2011)**.
- [2] **Naine Tarun Bharath**, Sergey A. Rashkovskiy, Manoj Kumar Gundawar , Effect of Heat loss in propagation of reaction front for combustion of heterogeneous systems, **23rd National Conference on I. C. Engine and Combustion (NCICEC 2013)**.
- [3] **Naine Tarun Bharath**, Manoj Kumar, Propagation of Reaction front in Heterogeneous Combustion of High energy materials, **9th international High Energy Materials Conference & Exhibit HEMCE (2014)**.

NUMERICAL PREDICTION OF BURN RATES OF PERIODIC

ORIGINALITY REPORT

46%

SIMILARITY INDEX

2%

INTERNET SOURCES

27%

PUBLICATIONS

27%

STUDENT PAPERS

PRIMARY SOURCES

1

Bharath, Naine Tarun, Sergey A. Rashkovskiy, Surya P. Tewari, and Manoj Kumar Gundawar. "Dynamical and statistical behavior of discrete combustion waves: A theoretical and numerical study", Physical Review E, 2013.

Publication

20%

2

Submitted to University of Hyderabad, Hyderabad

Student Paper

19%

3

Submitted to Sardar Vallabhbhai National Inst. of Tech.Surat

Student Paper

4%

4

Sergey Rashkovskiy. "One-Dimensional Discrete Combustion Waves in Periodical and Random Systems", Combustion Science and Technology, 08/2010

Publication

1%

5

www.science.gov

Internet Source

<1%

6

S. A. Rashkovskii. "Hot-spot combustion of heterogeneous condensed mixtures. Thermal

<1%